MSc. thesis in Geomatics

Extraction of Exterior Building Envelopes from Building Information Models

Lan Yan

2023

MSc thesis in Geomatics

Extraction of Exterior Building Envelopes from Building Information Models

Lan Yan

June 2023

A thesis submitted to the Delft University of Technology in partial fulfillment of the requirements for the degree of Master of Science in Geomatics

The work in this thesis was carried out in the:

3D geoinformation group
Delft University of Technology

Supervisors: Dr. Ken Arroyo Ohori
Jasper van der Vaart
Co-reader: Dr. Roderik Lindenbergh

Abstract

With the development of technologies and people's raising standards for both indoor and outdoor environments, buildings have expanded their functionalities of merely being human's everyday sheltering place. Common modern building applications include but are not limited to Building Energy Modelling (BEM), solar potential estimation, wind simulations, shadow analysis, noise propagation, and digital building permit checking. Among all the common building applications, many of them only need to use the building's envelope (A building's envelope is composed of all building elements that are exposed to the outdoor environment). It is apparent that building envelope extraction can be beneficial to these applications. Currently, building envelopes are mainly constructed from point cloud data or satellite image data. With the increased usage of Building Information Model (BIM) models within the Architecture, Engineering and Construction (AEC) industry, more attempts have been done on extracting building envelopes from BIM models as well. In addition, the BIM-based building envelope tool can be used throughout the building's life cycle. However, previously developed BIM-based building envelope extraction tools all have different types of flaws. The main problem with the existing methods is separating the building envelope elements is difficult and time-consuming. Considering the benefits extracting building envelopes from BIM models can bring and the limitations of the developed methods, it is beneficial to develop a different BIM-based building envelope extraction approach that can produce high-quality building envelopes efficiently.

Therefore, in this study, to avoid the difficult problem of separating building interiors and building exteriors, we first extract the point cloud from BIM models and then extract this point cloud's exterior boundary using the 3D alpha shape algorithm, and therefore obtain the building envelope. The quality of the extracted building envelopes is evaluated by their geometric accuracy, simplicity, and time efficiency. Among them, the geometric accuracy is evaluated by the deviations between the extracted surfaces and the original surfaces. The simplicity is measured by the number of vertices and faces, and the time efficiency is measured by the building envelope extraction speed.

The results show that despite the developed method has some limitations, it can extract building envelopes with high geometric accuracy from various types of small-scale BIM models. The main limitations include its inability to process big BIM models, the extracted building envelope merely contains its geometry without the enrichment of topological and semantic information. For all the tested BIM models, the average geometric accuracy is within 2.00cm. Walls and roofs are very accurately extracted, with errors of less than 0.01cm. Windows, doors, and other types of small-scale objects are extracted with a bigger error of 0.1m to 0.3m. The extracted building envelope also simplifies the input models significantly regarding the number of vertices and the number of faces. Lastly, for small-scale models, the developed building envelope extraction tool is able to process them within 150s.

Acknowledgements

In this acknowledgment section, I would like to express my sincere gratitude to all the people that have guided and helped me throughout this thesis project. I could not have been able to achieve this without all your help and support, and I am simply so grateful.

First and foremost, I want to say thank you to my two supervisors: Dr. Ken Arroyo Ohori and Jasper van der Vaart. I want to thank my first mentor Dr. Ken Arroyo Ohori for his constant help and guidance for this thesis project, for giving me valuable advice when I encounter difficulties, for providing suggestions throughout my research and writing process, and for giving me constructive feedback on my thesis draft. In addition to the academic help, I am also extremely grateful for the kindness, belief, encouragement, and patience he has for me throughout the thesis process.

I also want to thank my second supervisor Jasper van der Vaart, also for his help, advice, feedback, and encouragement, and especially for taking the time to give me advice on how to deal with IFC files and to have additional meetings to look into problems together.

In addition, I would like to thank Dr. Roderik Lindenbergh to be my co-reader. I want to thank him for taking the time to read my thesis draft thoroughly, attending my P4 in person even though not required to, giving me constructive feedback, and giving me the opportunity to revise and analyze my work from different angles. I also highly appreciate Dr. Azarakhsh Rafiee for taking the time to be my delegate and organizing everything perfectly so my thesis project progresses smoothly.

Apart from the above people that are directly involved in this thesis project, I want to also thank the developers of IfcOpenShell and CGAL for developing software packages that make the implementations of this project possible. Last but equally important, I want to thank my family, my friends Xinyu, Tiantian, Yunyun, Thanh, Nağme, and Àlex for always being able to see the best in me, for all the joy they bring, and for all the everyday unconditional love and support they provide me.

Contents

List of Figures

List of Tables

Acronyms

1. Introduction

1.1. Background and motivation

It is difficult to imagine a city's skyline without buildings. Buildings provide our human's everyday sheltering place, and their designs affect the comfort and safety of people's everyday activities. During the past decades, technologies advanced in various ways, and people also have higher standards for indoor and outdoor environments. These two factors have led to a growing variety of building applications. For instance, people have realized that buildings play crucial roles in the energy transition process. Currently, the building sector contributes to 36% of final global energy consumption (Hamilton et al. 2021). In order to understand, analyze and then further reduce buildings' energy use, there are more and more studies and projects on Building Energy Modelling (BEM), both on the individual building level and on the urban level (Li et al. 2020; Gao et al. 2019; Allegrini et al. 2015). Besides cutting energy consumption, estimating buildings' solar potential can help to supply buildings with clean and renewable energy (Freitas et al. 2015; Choi et al. 2019). Aside from the huge effects buildings have on a city's energy consumption and production, buildings can also affect the urban scene, and their surrounding wind, light, and sound environment greatly. Therefore, it is important to carry out wind simulations, shadow analysis, and noise propagation analysis, and investigate how buildings change and influence the urban environment.

When examining the aforementioned applications, one fact becomes apparent: many important applications and analyses on buildings only use building envelopes. The building envelope refers to all the components that are exposed to the outdoor environment. As the interface between the outside world and the built environment, building envelopes heavily influences the building's thermal performance (Sadineni et al. 2011), and its impacts on buildings' energy demand are analyzed widely in BEM. Since the solar panels can only be equipped on the building exteriors, the solar potential estimation also only uses the building envelopes. Furthermore, as buildings are the predominant objects in cities, buildings envelopes affect the quality of the urban scene significantly. When visualizing an urban scene in the digital twin, estimating noise propagation for a neighborhood, or simulating the wind dispersion of a district, also only the building envelopes should suffice. Last but not least, building envelopes can help with digital building permit checking as well. When checking for whether the maximum height of the designed building fits with the land use plan (Prusti 2022), the examiner also only needs to use the building envelope.

It is natural to imagine building envelope extraction benefits all the aforementioned applications. Even though detailed building energy demand estimation needs more information than building envelopes, extracting building envelopes can be highly beneficial in analyzing the envelope's effects on the building's energy performance. By extracting the building envelopes, we can calculate the envelope's energy demands and analyze its contribution to the building's total energy demand. Furthermore, despite the fact that the building envelope

is not enough for building-level detailed energy simulations using software like EnergyPlus(Crawley et al. 2001), it will suffice for urban-level simulation software, for instance, SimStadt and CitySim, and can be used as input for urban energy analysis. Furthermore, as aforementioned, extracted building envelopes can be used in buildings' solar potential estimation, shadow analysis, wind simulations, and noise propagation, and help us create better urban living spaces.

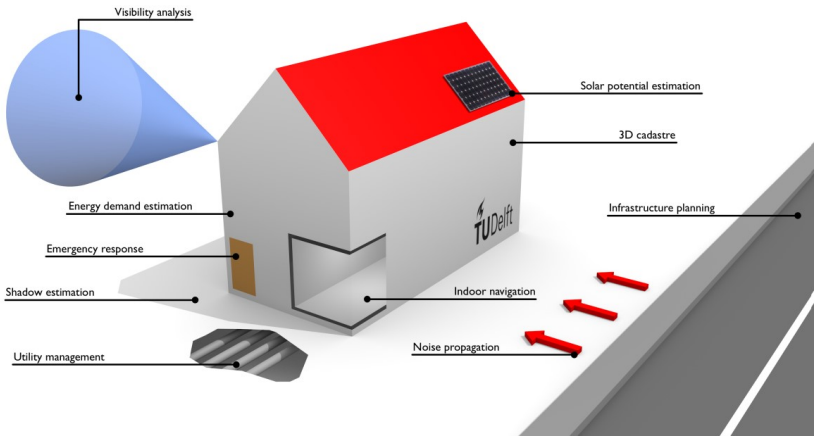

Figure 1.1.: Possible applications of building models(Biljecki et al. 2015)

Currently, building envelopes are mainly extracted from point cloud data and satellite images (Singh et al. 2013). Currently, the BIM, the building's digital representation throughout its life cycle, is increasingly used in the Architecture, Engineering and Construction (AEC) industries. BIM models can also be another great information source for extracting building envelopes since they already contain buildings' highly detailed geometric and semantic information (André Borrmann 2018). Another advantage of using BIM models instead of remote-sensing data is: the building envelope extraction tool can be used throughout the building's whole life cycle. For instance, architects can extract building envelopes, place them in digital twins, estimate their solar potential, and analyze their potential effects on the surrounding environment during the design and construction stages. In addition, the resulting building envelopes' geometries can be used to convert into 3D city models, a format widely used in the modern Geographical Information Science (GIS) industry. Therefore, this work can also potentially strengthen the tie between the AEC and GIS industries.

There are previous attempts to extract the building's envelope from BIM models (Donkers et al. 2015; Noardo et al. 2020; Deng et al. 2016), but limitations with efficiency and reliability among these methods are present. For instance, some methods have slow processing speeds (Karydakis 2018), some methods can only successfully extract envelopes from certain types of buildings (Fan et al. 2009), and some methods introduce holes and gaps on the building envelopes' surfaces (Deng et al. 2016). In many studies, the researchers attempt to separate the building envelope elements and then directly output these elements to be the eventual envelope. But this creates many problems and limitations because it is difficult to develop widely-applicable exterior separation criteria, considering the complexity and variability of building shapes.

Considering the clear benefits that extracting building envelopes from BIM models can bring to areas such as BEM and urban wind simulations, and the limitations of the present extraction methods, it is not only beneficial but also necessary to develop another approach that can extract building envelopes accurately and efficiently from various types of buildings.

1.2. Research Objectives

The goal of this research project is to develop a method that can extract building envelopes from input BIM models. The method should be able to process different types of buildings. The output building envelope should preserve the geometries of the building envelopes accurately. Furthermore, the developed extraction tool should be able to extract building envelopes quickly and efficiently. In order to achieve all the aforementioned goals, the following research questions need to be addressed:

- How can we extract building envelopes from different types of BIM models both accurately and efficiently?

1.3. Research Scope

The research project focuses on extracting building envelopes from BIM models. The research scope for this research covers two main sections: the extraction of point clouds from BIM models, and the reconstruction of building envelopes from the extracted point clouds. These sections will be covered by answering the following questions:

- How to extract a point cloud from a BIM model that is suitable for building envelope reconstruction?
- How can we develop a building envelope extraction method, that can reconstruct the building envelope both accurately and efficiently?
- How to measure the quality of the extracted building envelope?
- What are the factors that influence the reconstructed building envelope's quality?

The extraction of building envelopes from other data resources, for instance, aerial image data, is out of our research scope. Furthermore, our main focus is to produce accurate geometries of building envelopes, and the output will be stored in OBJ format. Even though the extracted building envelopes' geometries can be potentially converted to 3D city models, the format conversions of the extracted building envelopes, for instance from OBJ format to CityGML format, are also not included in this research.

1.4. Thesis Structure

- Chapter 2 introduces the theoretical backgrounds and related works. In the theoretical background part, we present important concepts related to this study: building information models (BIM), Industrial Foundation Classes (IFC), the OBJ format, and 3D city models. In the related work part, we cover related studies regarding this thesis study.
- Chapter 3 presents our developed methodologies for BIM-model-based building envelope extraction. Point cloud extraction, point cloud simplification, building envelope extraction, and building envelope simplification are covered sequentially.
- Chapter 4 covers the implementation details of this study. This includes used data sets, used programming language and software tools, and specific implementation details of the developed data processing pipeline.
- Chapter 5 presents the results and discussions of this research. Firstly intermediate and final results along the data processing pipeline are presented. Secondly, we analyze the quality of the extracted building envelopes from different perspectives. Thirdly, the effects of different parameters on the geometric accuracy of the extracted building envelopes are discussed. Finally, we present the main limitations observed through the testing process.
- Chapter 6 presents the main conclusions of this research, and answers the research questions. This chapter also suggests relevant future work based on our research.

2. Theoretical backgrounds and related works

This chapter presents important concepts and previous studies related to this research. In the theoretical backgrounds section, firstly, the concept, benefits, applications, and data formats of Building Information Model (BIM) are introduced(subsection 2.1.1). Secondly, we introduce the concept of the building envelope (subsection 2.1.2). Lastly, subsection 2.1.3 introduces how to evaluate the quality of reconstructed geometries from different aspects, for instance, accuracy and simplicity. In the related work section, firstly the previous research on BIM model-based building envelope extraction will be covered (subsection 2.2.1). Secondly, as we plan to firstly extract point clouds from BIM models and secondly reconstruct the building envelope geometry based on the extracted point cloud, subsection 2.2.2 covers different kinds of point cloud-based geometry reconstruction techniques. In addition, their applicability to building envelope reconstruction is investigated.

2.1. Theoretical backgrounds

2.1.1. Building Information Model (BIM) and Industrial Foundation Classes (IFC)

Building Information Model (BIM) is a building's digital representation. It describes the buildings' physical and functional characteristics, throughout the building's whole life cycle, including planning, design, construction, and operations (Epstein 2012). The theoretical concepts of BIM can be traced back to the 1970s. However, it was not implemented until the 21st century (Azhar et al. 2012). BIM brings many benefits to various stakeholders in the

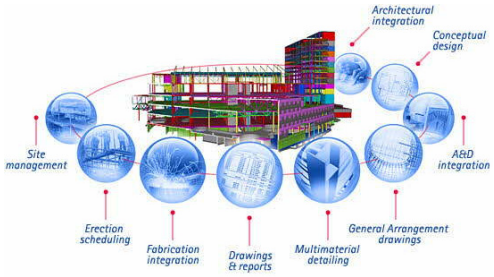

Figure 2.1.: Schematic diagram for BIM modeling (Gharehbaghi 2016)

AEC industry. In the pre-construction stage, BIM helps various stakeholders better specify and evaluate the requirements and estimate costs. In the design stage, using BIM models make early-stage 3D visualization and energy analysis possible, and thus potentially leads

to less design errors and more sustainable design. BIM models can also improve the process of actual construction by eliminating mistakes that may be caused by 2D drawings. After the asset is built, BIM can be used for better asset management (Eastman et al. 2011). Currently, BIM has widely been used in the AEC industries, in different stages of construction projects. Real-world use projects that utilized BIM technologies include but are not limited to: Aviva Stadium, Maryland General Hospital, Crusell Bridge, and Helsinki Music Center (Eastman et al. 2011).

Since BIM models are still majorly used within the commercial context, many BIM models are stored in software-specific formats, for instance, Autodesk Revit. The lack of open BIM standards hindered the BIM models' re-usability and interoperability. To resolve this issue, BuildingSMART, an international non-profit organization involving various AEC companies proposed Industrial Foundation Classes (IFC), a vendor-neutral BIM standard. The IFC schema stores the building's physical and abstract components and defines relationships between different components. One key characteristic of the IFC format is that it is composed of many different types of objects. Among them, there are physical building elements, for instance, walls, roofs, floors, windows, and doors. There are also non-physical objects, for instance, IfcSpace, an object that refers to a bounded area or volume within buildings, and IfcProject which describes the overall construction project. These objects are organized in a hierarchical way. More low-level classes, for instance, IfcDoors or IfcWindows, get properties and behaviors from more general classes like IfcProduct. Each object has different properties that describe its characteristics, for instance, geometrical information, or semantic information. Objects can also have relationships with other objects, for instance, an IfcBuilding object is in a composition relationship with IfcBuildingStorey objects.

For physical elements stored in the IFC format, their geometries need to be modeled. In the IFC schema, the physical objects are modeled as volume-filling physical objects, and their geometries can be modeled in the following ways (Jaud et al. 2020):

- Primitive instancing: Some simple objects are defined using pre-defined parameters. IFC format uses primitive instancing to define 2D profiles as well as simple 3D objects, for instance, spheres.

- Constructive Solid Geometry (CSG) and Boolean operations: Objects can be defined as a tree composed of different Boolean operations of a set of volumetric objects.

- Sweep volumes: Objects can be defined using a 2D profile and a height curve along the 2D surface. The extrusion of the 2D profile along the height curve is the defined object.

- B-rep: Objects are defined by their boundary surfaces. The faces can be triangle meshes, polygon meshes, and topological arrangements of free-form surfaces.

The creation of IFC schema provides a common and open standard for exchanging BIM data, and it allows exchanges of BIM models between various stakeholders, even when they use different BIM software. Figure Figure 2.2 shows more specific benefits IFC can bring. The IFC format is applied in real-world projects, for instance, the Oslo airport project, the Naples central station project, and the third Nanjing Yangtze bridge project.

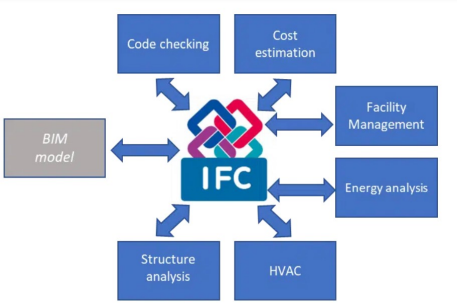

Figure 2.2.: Benefits of using IFC schema, source: buildingSMART

2.1.2. Building envelope

The building envelope is an important concept in many different fields within the AEC and GIS industries. However, it is worth noting that the exact definition of the building envelope is sometimes unclear and varies under different contexts. Therefore, in this section, we first provide an overview of building envelope definitions across various studies. Then we clarify the definition of the building envelope in this research project.

In the field of AEC industry, building envelopes are usually defined as the barrier between the indoor and outdoor environment. Brock (2005) defines a building envelope as the skin of a building supported by the skeleton of the structure. Since the building envelope plays an important role in a building's energy performance, the building envelope is sometimes defined as the building parts which have thermal energy exchanges between the indoor space and outdoor environment (Doty, Steve and Turner, Wayne C 2004). Syed (2012) defines the building envelope as the separator between the indoor and outdoor environment and controls the air, water, heat, light, and noise transfer. Okba (2005) states that a building's envelope is usually composed of its roof, walls, doors, windows, and ground surfaces, and its design controls the energy transfer between the indoor and outdoor environment. Even though the terminologies vary, the key principle of deciding whether a building component belongs to the building envelope is consistent: a building envelope component must be exposed to both the indoor space and the outdoor environment.

In the GIS field, building envelopes are also vastly studied, but sometimes an exact definition of the building envelope is not present in these studies. Therefore, the building envelope definition in the GIS is inferred from related studies. In the GIS field, most studies done on building envelopes are extracting building envelopes from various data sources, for instance, BIM models and Light Detection and Ranging (LiDAR) point cloud data. subsection 2.2.1 and subsection 2.2.2 present these studies in more detail. In these studies, usually, a building's envelope equals the building's exteriors which can be observed from viewpoints of outdoor environments. In other words, the key principle of deciding whether a building component belongs to the building envelope is: a building envelope component must be exposed to the outdoor environment.

For some buildings, the different building envelope definitions in the AEC and GIS fields lead to the same results. For example, for the building shown in Figure 2.4, all the building elements that are exposed to the outdoor environment (roofs, exterior walls, doors, win-

Figure 2.3.: Extracted building envelope in the GIS field (Karydakis 2018)

dows, and ground surfaces) are also exposed to the indoor environment. However, for some buildings that contain building elements that are only exposed to the outdoor environment but not the indoor environment, for instance, the pillars in Figure 2.3 and the exterior stairs in Figure 2.5.

In this research, we use the building envelope definition in the GIS field: a building's

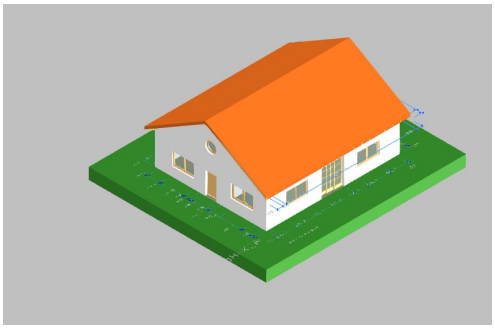

Figure 2.4.: FZK-Haus model

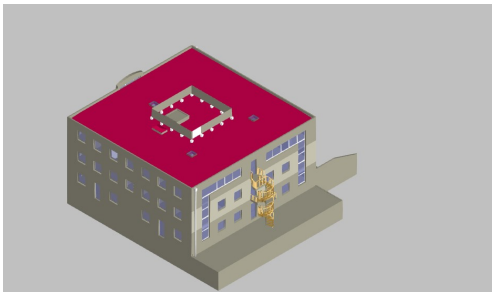

Figure 2.5.: BUREAUX model

envelope contains all the building elements (for example, roofs, walls, doors, and windows) that are exposed to the outdoor environment. To better clarify our definition, we compare our defined building envelope with two similar concepts: bounding box and convex hull. A building's bounding box defines the minimal cubical space that contains the building. On

the contrary, our defined building envelope contains detailed geometries of all the building exterior elements. A building's convex hull defines the smallest convex envelope that bounds the building. Our defined building envelope keeps all the original building's exterior geometries, therefore the concave parts are also included. We define the building envelopes to contain all exterior building elements because even when the exterior elements are not exposed to the indoor environment, they still influence the urban scene and many urban applications, for instance, wind and noise simulations. In addition, if these exterior elements add to the vertical heights of the building, it also affects the validity of the maximum building height checking when processing building permits (Prusti 2022).

2.1.3. Evaluation metrics for geometry reconstruction

Since this study aims to reconstruct building models using suitable reconstruction methods, it is necessary to provide guidelines for evaluating different reconstruction methods and therefore choosing the suitable method. This section covers common evaluation metrics for geometry reconstruction methods, for instance, the result's geometric accuracy, topological accuracy (Berger et al. 2016), simplicity, and the method's reproducibility and time efficiency.

Geometric accuracy

The geometric accuracy of reconstruction results is one of the most important indicators. It is usually indicated by the deviations between the reconstructed and original surfaces (Berger et al. 2016; Du 2019). Mainly the deviations can be measured in the following four ways (Berger et al. 2016):

- Hausdorff distance: The Hausdorff distance measures the closeness between two spaces. By definition, given two space set A and B, the Hausdorff's distance from A to B is calculated as follows. For every point in A, the distance between this point and all points in B is calculated and the shortest distance is kept. Among all the obtained shortest distances, the maximum value is the Hausdorff distance. An example of using Hausdorff distance to measure the geometric accuracy can be found in Aspert et al. (2002).
- Average distance: Similar to the Hausdorff distance, given two space set A and B, for every point in A, the distance between this point and all points in B is calculated and the shortest distance is kept. But instead of choosing the maximum value, the mean value of all the obtained shortest distances is calculated. An example of using mean distance to measure the geometric accuracy can be found in Du (2019).
- Distance distribution: In some studies, given two space set A and B, for every point in A, the distance between this point and its closest point in B is calculated. Instead of calculating a single indicator for geometric accuracies like mean value or maximum value, the whole distance distribution is visualized. An example of using the distance distribution for geometric accuracy analysis can be found in Elberink and Vosselman (2011).
- Error in normal: Apart from the distances, the deviations between the original and reconstructed surfaces can also be measured by calculating and comparing the difference between face normal (Berger et al. 2016).

Topological accuracy

Apart from the geometric accuracy, the reconstruction results' topological accuracy is also an important indicator of the reconstruction quality. Different reconstruction methods focus on different aspects of recovering topology. Some studies focus on generating the correct genus in the output, and others focus on recovering the geometries underlying the skeletal structures and their important branches and junctions (Berger et al. 2016). For buildings, the Building Topology Ontology (BOT) defines the explicit relationships between building elements (Rasmussen et al. 2020), more specifically, how different types of building elements connect, intersect, and form enclosed spaces.

Other indicators

There are other indicators to consider when evaluating the reconstruction methods. For instance, the reproducibility of the method is also important (Berger et al. 2016). This can include how strict the input data requirements are, whether the method has open-source implementation available, or the method's implementation complexity. The simplicity of the resulting geometries (number of vertices, number of faces) is also worth considering because a complex and big geometry file takes up storage space and is difficult to be operated on. Last but not least, the time efficiency of the reconstruction method is very important. If a reconstruction method is very slow or needs high computational power, its usage can also be very limited. Watertightness is also important in some cases, because small gaps between walls and roofs may lead to false results in wind or energy simulations.

2.2. Related works

2.2.1. BIM-based building envelope extraction

There is limited research regarding extracting building envelopes explicitly from BIM models. Therefore, we cover building envelope extraction methods developed based on other types of building models as well.

One common technique for extracting building envelopes is to generate building footprints and classify building objects that intersect with the building footprint as exterior building objects. For instance, Benner, J and Geiger, A and Leinemann, K (2005) developed a method that can convert IFC models to the QUASY model (a data format that is similar to the CityGML format). One key step of this mapping process is to extract the building model's building envelope. Firstly, using the semantic information of the IFC model, they group the building elements that belong to each building story. After the grouping process, for each building story, they vertically and horizontally project all of the building elements, merging the projections and keeping the inner and outer contours, thus producing two footprints (vertical and horizontal footprints for each story). After obtaining the footprints for each story, all building elements that touch the building footprints are classified as belonging to the building envelope.

Figure 2.6 shows the resulting building envelope using this method. This method has several advantages. It can detect most exterior building objects. In addition, since it keeps both the

inner and outer contours of the building footprints, this method is applicable to buildings with courtyards as well. Finally, if the input IFC models have separate IfcSlab elements as roof components, the building footprint generation process can help reduce the geometry of roofs and other slabs by merging them together. However, it has multiple flaws as well: since gaps between IFC elements are common, this method sometimes yields building envelopes with gaps between walls and roofs, and as aforementioned in subsection 2.1.3, these gaps can lead to wrong wind or energy simulation result. In addition, since this method performs a direct mapping between IFC elements and QUASY model elements, the output model is still composed of elements modeled with volumes instead of surfaces.

In the work of Fan et al. (2009) for building generalization, they proposed a method that

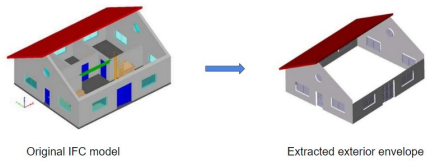

Figure 2.6.: Extraction of building envelope using the footprints testing method (Benner, J and Geiger, A and Leinemann, K 2005)

can extract a building's envelope from CityGML models. The main strategy for extracting the building's exterior shell in this study is to determine whether a building element belongs to the exterior shell by evaluating its distance to the building centroid. To put it in more detail, the method proposed is divided into the following steps. Firstly, the walls and roofs in the CityGML models are converted to point clouds. After the conversion, the centroid and the adjusting plane for each wall are computed, and the average point of all walls' centroids is viewed as the building center. Then, the distance between each wall or roof and the building's centroid is calculated, and the walls with maximum distances are labeled as belonging to the exterior shell. The windows and doors are also projected onto the exterior shell to preserve the details.

The following figure 2.7 shows one example of results from this method. The main advantages of this method are: firstly it makes use of the digital building's semantic information. secondly, the method of separating the building model's interior and exterior elements is relatively simple and straightforward. Thirdly, even though the input of this method is in CityGML format, this method can be used on IFC models, because the key strategy is about testing the relative position of building elements. However, its applicability is limited: it only produces viable results with buildings that have convex shapes, as buildings with concave shapes may have exterior walls that are closer to the building center than some other interior walls, and the concave building parts can not be extracted.

Donkers et al. (2015) developed a method that can automatically convert IFC models to CityGML models. During this process, they need to extract buildings' exterior envelopes. Before extracting the building envelope, a series of pre-processing is performed on the input IFC model. Firstly, they filter out IfcObject that is not meaningful to the CityGML models. In the filtered dataset of the IfcObjects, for each object's surfaces, they map the semantics from IFC models to the CityGML model based on a set of rules.

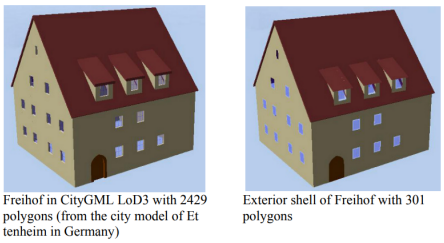

Figure 2.7.: Extraction of exterior shell from CityGML model using distance function (Fan et al. 2009)

After performing the aforementioned data conversion and processing, they obtain a set of solids, and all the boundary surfaces of this solid have been assigned with CityGML semantics. The core strategy of this building envelope extraction method is space partitioning. As shown in figure 2.8. Firstly, this space partitioning method divides the 3D Euclidean space into non-overlapping volumes. Then it performs the Boolean union operation on all solid pairs that have adjacent faces. Finally, it removes all the geometries inside the outer boundary of the resulting geometry.

This method often fails in practice due to the geometrical or topographical errors present

Figure 2.8.: Extracting building envelope by using space partitioning (Donkers et al. 2015)

in the IFC files. For instance, the utilities that penetrate building exteriors, and small gaps between geometries (Donkers et al. 2015). It prevents holes in the resulting 3D city models, but it introduces artifacts, and the semantic data is lost, thus semantic-recovering methods needed to be applied, making the method complex (Ohori et al. 2018).

Deng et al. (2016) developed a set of mapping strategies between BIM models and CityGML models. During this process, they need to extract the building's exterior envelopes. To make extracting building envelopes from complex-shape buildings possible, they proposed a ray-scanning method. The ray-scanning method extracts the building's exterior surface by testing every surface with rays. The core strategy of the ray-scanning method is that it identifies a building's exterior envelope by testing building surfaces with multiple viewpoints: from each viewpoint, a ray is cast onto the building, and the first surface it encounters will be classified as an exterior surface.

In the study of Karydakis (2018), the building envelope is also extracted using the ray-casting method, and the data processing pipeline is documented in greater detail, as shown in figure 2.9. In this study, firstly the researcher constructs a building bounding box and populates the bounding box with evenly-distributed viewpoints. Then as shown in figure

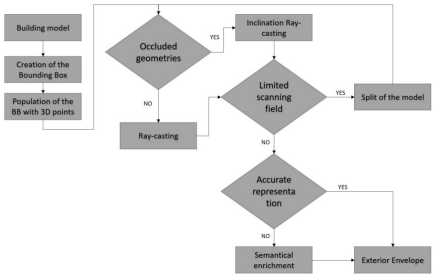

Figure 2.9.: Workflow of extracting building envelopes using the ray-casting method (Karydakis 2018)

2.10, from each viewpoint, a ray will be cast onto the target BIM model to another viewpoint on the opposite side of the bounding box. The first and last surfaces that the ray encountered will be identified as parts of the exterior shell. In addition, in order to access the exterior building parts that are occluded by other building parts, this study uses not only vertical and horizontal rays but also rays with inclinations.

The resulting building envelopes from the ray-casting process are shown in figure 2.11

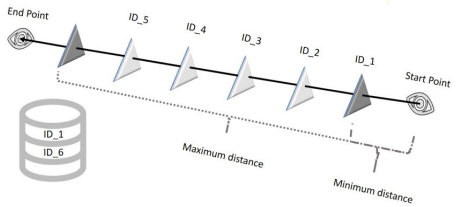

Figure 2.10.: Illustrations of the ray casting algorithm (Karydakis 2018)

and 2.12 below. Compared to previous methods, this ray-casting method has the ability to process buildings with complex and non-convex shapes. However, this method can produce buildings with small holes and gaps when not all exterior surfaces are successfully identified. In addition, the processes of casting a large number of rays from various viewpoints, and calculating the distances between the beginning viewpoint and each intersection point are very computationally expensive. Therefore this method may not be able to extract the building envelopes with a reasonable processing speed.

In conclusion, most of the aforementioned BIM-based building envelope extraction methods aim at extracting the exterior IFC objects and output them as the final building envelopes. However, determining whether a building object is exposed to the exterior environment is difficult. This is because different buildings can have a great variety of shapes and levels of complexity, and the designed criteria that suit some buildings may not work with other types of buildings. Checking whether every building's elements belong to the building envelope is also computationally expensive. This is because one IFC model can have hundreds and thousands of models. Therefore, it is necessary to develop a new BIM-based building envelope extraction approach.

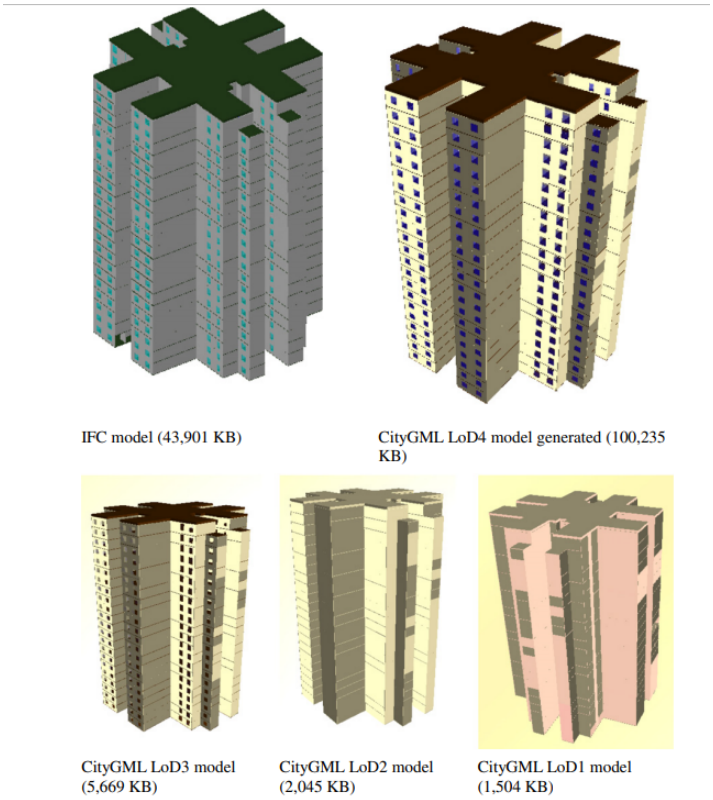

Figure 2.11.: Extracted building envelopes using ray-casting method (Deng et al. 2016)

2.2.2. Point cloud-based geometry reconstruction

As concluded in subsection 2.2.1, extracting building envelopes by isolating and outputting exterior building elements is not ideal. Therefore, in this study, instead of isolating the exterior objects, we propose a method that first generates a point cloud from IFC models. Then point cloud-based geometry reconstruction is performed to extract building envelopes. This section presents an overview of point cloud-based geometry reconstruction methods, and evaluate their applicability to the building envelope reconstruction problem.

Voxel-based method

Voxelisation is a common method used in point cloud processing. As the name indicates, voxelisation transforms a point cloud into a set of voxels. A voxel is the 3D equivalent of a 2D pixel. Figure 2.13 shows one example output of voxelization. There are four main steps in the voxelisation process (Xu et al. 2021):

- Calculation of the bounding box: the bounding box of the input point cloud is calculated.
- Construction of the 3D grid: based on the calculated bounding box, a 3D grid is constructed, and dividing the bounding box into voxels.

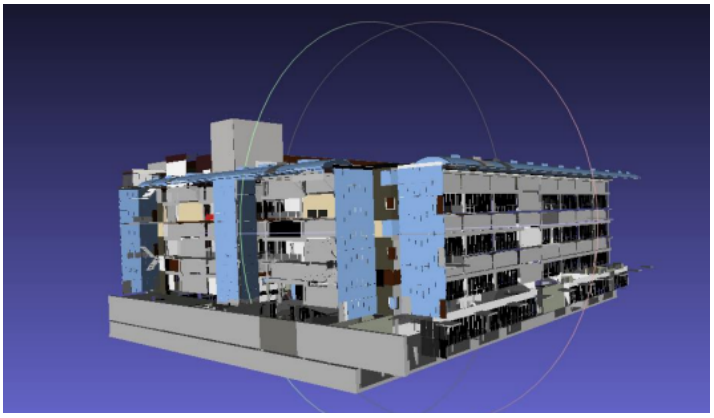

Figure 2.12.: Extracted building envelopes using ray-casting method (Karydakis 2018)

- Segmentation of the point cloud: the input point cloud is segmented by the unit of voxel, using the constructed 3D grid in the second step.
- In the last step, voxels that contain points in the original point cloud are kept. The voxel's attributes can be calculated using the point clouds' attributes.

Figure 2.13.: Results of point cloud-based voxelisation(Wang et al. 2015)

After voxelization, surfaces can be extracted from the voxels. This is usually done by using the Marching cube algorithm (Lorensen and Cline 1987). The marching cube algorithm uses many surfaces to iterate and slice through voxels. Then it generates surfaces within the cube based on the results of these slices. The main steps of the marching cube algorithm are described as follows:

- Using two surfaces to slice the target cube, as shown in figure 2.14. For each vertex of the cube, if the vertex is inside or on the surface, then it is marked with 1. If the vertex is outside the surface, then it is marked with 0. For each edge, if one vertex is marked with 1 and its other vertex is marked with 0, then the edge intersects with the current slicing surface. For each cube, this creates 256 types of possible surface intersections. In order to make the triangulating process easier, the authors simplify the 256 cases to 14 patterns using symmetries, and the 14 patterns are shown in figure 2.15.
- After determining the intersection condition, the surfaces can be interpolated using linear interpolation along the edges.
- Lastly, to help with better visualization, the normal of each triangle's vertices is calculated.

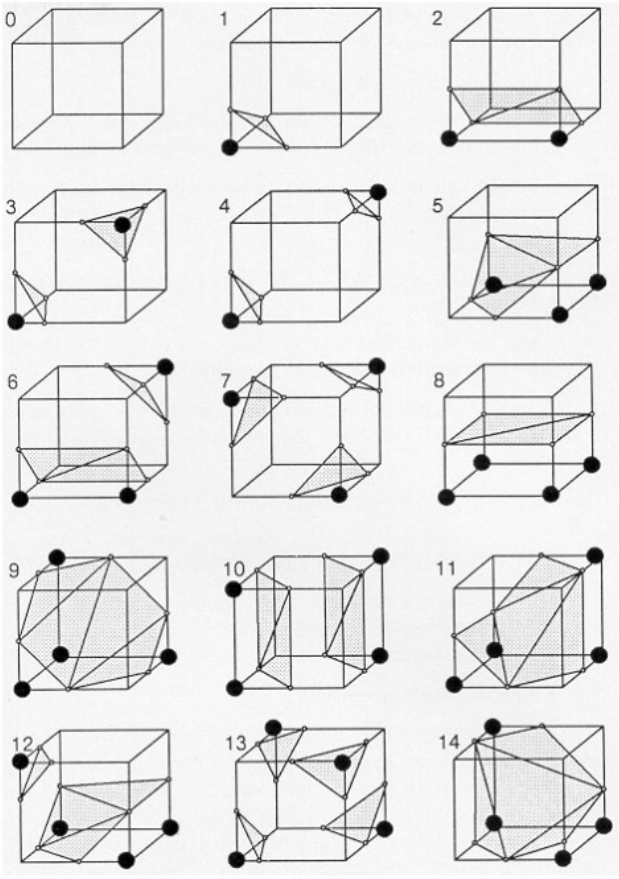

Figure 2.14.: The slicing process of the marching cube algorithm (Lorensen and Cline 1987)

The voxel-based method is not suitable for our study for the following reasons. Firstly, as aforementioned in subsection 2.2.1, separating the building's interior and exterior objects is difficult. Therefore, we only filter out obvious non-exterior building objects. In this way, the sampled point cloud from the filtered building objects still contains interior points. If the voxel-based method is used, then the building interiors will also be voxelized and reconstructed. This violates the goal of only extracting the building envelope. Furthermore, the main surface extraction method after voxelization is the marching-cube algorithm. Its output geometry is sometimes not ideal: when some intersection patterns are neighbors, the extracted surfaces may contain small holes and gaps.

3D Alpha shape

The alpha shape is a concept proposed by Edelsbrunner and Mücke (1994). During the past decades, it has gained significance in the computational geometry field and has been used in various studies. Given a point cloud, the alpha-shape algorithm can extract its outer boundaries. The 3D alpha shape can be intuitively described as follows. As shown in figure 2.16,

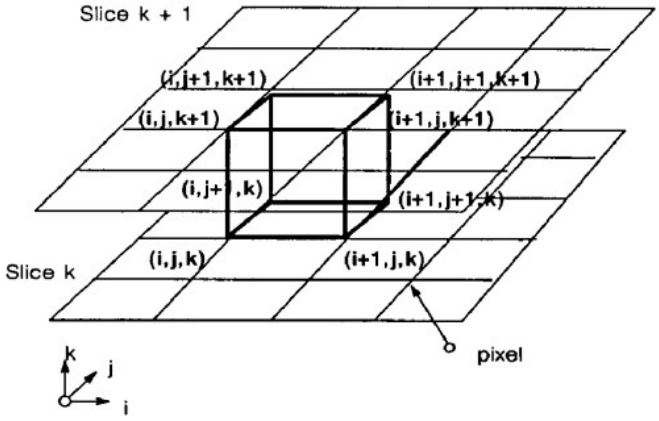

Figure 2.15.: 14 patterns of different intersection conditions (Lorensen and Cline 1987)

consider R^3 space is filled with foam, and the input points are solid points. Remove all the foam without touching the solid points with an imaginary spoon with a radius of α, and the remaining foam shape is a α-hull Edelsbrunner and Mücke (1994). Straighten all the curves of the α-hull, and the result is the alpha shape.

More formally, the alpha shape can be defined as follows. For a given finite point set

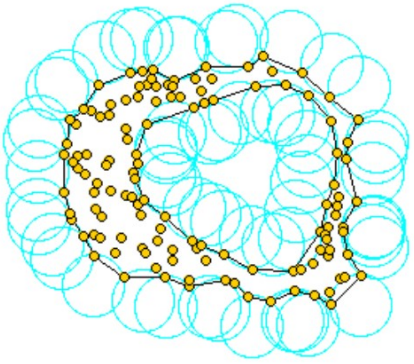

Figure 2.16.: Intuitive working principle of the 3D alpha shape, source.CGAL

S, firstly a α-ball is defined. A α-ball is an open ball with a radius of α ($0 < \alpha < \infty$). In special cases, a 0-ball is a point, and a ∞-ball is a half-space. For any given α-ball b, b is empty if $b \cap S = 0$. Then consider subsets $T \subseteq S$ with the $|T| = k + 1 (0 \leq k \leq 3)$ that define the k-simplex of σ_T that is the convex hull of T (Conv(T)). All k-simplices are constrained to be properly k-dimensional. For $0 \leq k \leq 2$, σ_T is considered α-exposed if there exists an empty α-ball b and $T = \delta b \cap S$. For any fixed α, $F_{k,\alpha}$ = all α-exposed k-simplices. The α-shape of S, denoted as φ_α, is the polytope that contains the boundaries of all the simplices in $F_{k,\alpha}$: the triangles in $F_{2,\alpha}$, the lines in $F_{1,\alpha}$, and the points in $F_{0,\alpha}$.

The interior and the exterior of the α-shape are determined using the following method.

For every α-exposed triangle, there exist two α balls, b_1 and b_2, so that $T \subseteq \delta b_1$ and $T \subseteq \delta b_2$. If both balls are empty, σ_T does not belong to the interior boundary of φ_α. If b_1 is empty and b_2 is not empty, σ_T is part of the φ_α's interior boundary.

The alpha shape algorithm includes two crucial steps. In the first step, for the given point set S, the Delaunay triangulation D of S is computed. Then, the interval associated with each simplex of D is checked. If the interval is no smaller than the α, then it belongs to the α-complex. After removing all the simplices that do not belong to the alpha complex, the domain covered by the alpha complex is the final alpha shape.

Apart from the initial definition, there also exist different types of 3D alpha shape variations. For instance, in some implementations, the alpha shape can be regularized and the singular faces are removed. Furthermore, a weighted alpha shape can be computed by assigning different weights to input points. Firstly, a regular triangulation is computed for all the input points. For two arbitrary points with centers of C_1 and C_2 and radius of r_1 and r_2, they are considered orthogonal if ${C_1C_2}^2 = {r_1}^2 + {r_2}^2$, and sub-orthogonal if ${C_1C_2}^2 = {r_1}^2 + {r_2}^2$. For all the simplices in the regular triangulation, they belong to the alpha complex if the following criteria are met: a sphere exists such that it is orthogonal to the weighted points associated with the simplex's vertices, and it is sub-orthogonal to all other weighted points.

Since the 3D shape's invention, it has been widely applied in many projects and studies for geometry reconstruction. For example, it can be used in tumor visualization (Al-Tamimi et al. 2015), tree modeling (Vauhkonen et al. 2009), and 3D printing (Zhu et al. 2019). More related to our research on building reconstruction, the 3D alpha shape is proposed to be a potential way to extract building envelope in the study of Noardo et al. (2020). The alpha shape is also a common method for extracting building boundaries out of LiDAR data (Santos et al. 2019).

Figure 2.17 shows one example of reconstruction results using different alpha values. The 3D alpha shape algorithm is potentially a good reconstruction method because of the following reasons. Firstly, it can extract the outer boundaries of input point sets, and this characteristic can be used for extracting only the building's exterior. Furthermore, the alpha value can be fine-tuned and changed to obtain building envelopes in different levels of detail. Despite the advantages alpha shape has on extracting building envelopes, it is also worth noting that inappropriate settings of alpha value may lead to reconstructed surfaces with holes and cavities.

Footprint projection and extrusion

In many studies, researchers first obtain building footprints and extrude the footprints to achieve building reconstruction. Poullis (2013) developed a framework that can reconstruct building envelopes for urban applications automatically. The core of this framework is to cluster the points that belong to the same building together, extract building footprints for each building, and construct 3D building envelopes by extruding the footprints.

Figure 2.19 shows reconstructed building envelopes on an urban scale. This method can produce watertight building envelopes, but the building envelopes are significantly simplified. Similarly, Peters et al. (2022) performed automatic 3D reconstruction of buildings for 10 million buildings using building footprint extrusion. In their studies, the building footprints

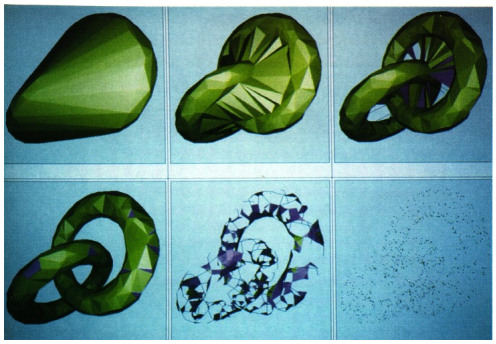

Figure 2.17.: Alpha shape reconstruction results using different alpha value(Edelsbrunner and Mücke 1994)

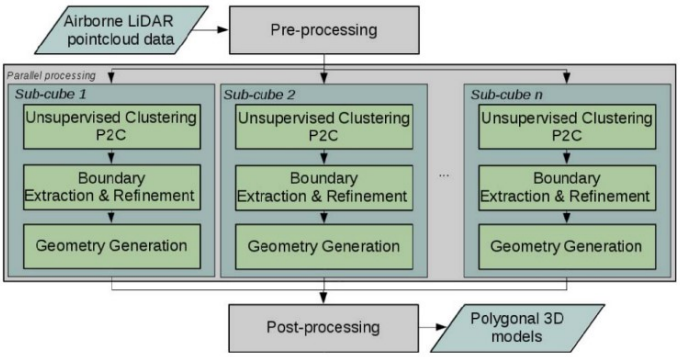

Figure 2.18.: Data processing pipeline of generating building envelopes using clustering algorithms (Poullis 2013)

are obtained from Dutch municipalities. Figure 2.20 shows their workflow. Using building footprints and height points from Actueel Hoogtebestand Nederland (Current Elevation of Netherlands) (AHN), firstly the roofs are detected using a region-growing algorithm. Then the boundary lines and the intersection lines are derived and used for footprint partitioning. Finally, the detected roof parts are extruded to obtain the 3D building mesh.

The footprint projection and extrusion method does not apply to this research because we aim to reconstruct building envelopes that can be used in various applications. For some applications, for instance, wind simulation or solar potential estimations the level of detail is enough, but for checking for building permits, the extruded models are detailed enough to be put into use.

Possion Surface reconstruction

Possion surface reconstruction is a surface reconstruction method proposed by Kazhdan et al. (2006). The Possion surface reconstruction works by using an implicit function framework. In the first step, it computes a 3D-indicator function X. In the second step, it extracts the reconstructed surface by extracting a suitable iso-surface. Figure 2.21 shows the general

Figure 2.19.: Generated building envelopes using clustering algorithms (Poullis 2013)

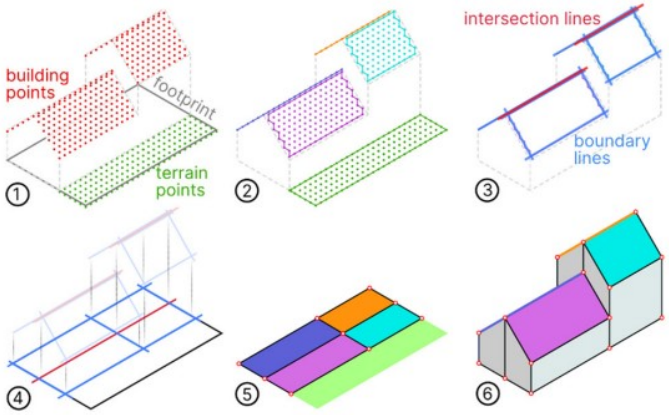

Figure 2.20.: Workflow of footprint partitioning and extrusion (Peters et al. 2022)

working principle of the Possion reconstruction algorithm. The key insight that differentiates the Possion surface reconstruction from other implicit function-based methods is that it points out that there are relationships between the input points and the indicator function. Furthermore, the indicator function is almost constant everywhere. Therefore, the oriented points can be considered as gradients of the indicator functions. In this way, the problem of computing the indicator function can be simplified into the problem of inverting the gradient operator: the optimal indication function X should be found that yields minimal $||\nabla X - \vec{V}||$, where $\vec{V}$ is the vector field defined by oriented points. This problem can be transferred into the classic Possion problem by solving the following equation:

$$\triangle X = \nabla \cdot \nabla X = \nabla \cdot \vec{V}$$

The Possion reconstruction method has the advantage of producing smooth surfaces from irregular point sets and is robust to noise. However, the Possion reconstruction also can not separate the building's interior and exterior. Using this method will result in a collection of

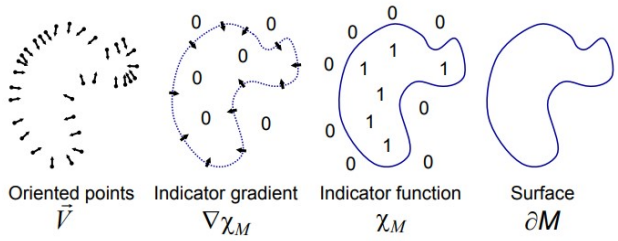

Figure 2.21.: Working principle of the Possion surface reconstruction algorithm (Kazhdan et al. 2006)

reconstructed exterior and interior surfaces. Therefore, this method is not suitable for this project.

3. Methodologies

In this chapter, the developed methodologies of this research are presented. The developed methodologies are developed based on the research objectives (section 1.2) and previous studies relating to this research subject in chapter 2. Figure 3.1 shows an overview of the developed workflow. Firstly, section 3.1 covers the main considerations when extracting point clouds from IFC models. Then section 3.2 explores the possibilities of simplifying the extracted point clouds to ease the following reconstruction process. section 3.3 describes the building envelope extraction process using the 3D alpha shape algorithm. In the end, section 3.4 explains the developed methodology for removing extracted envelope's redudant geometries.

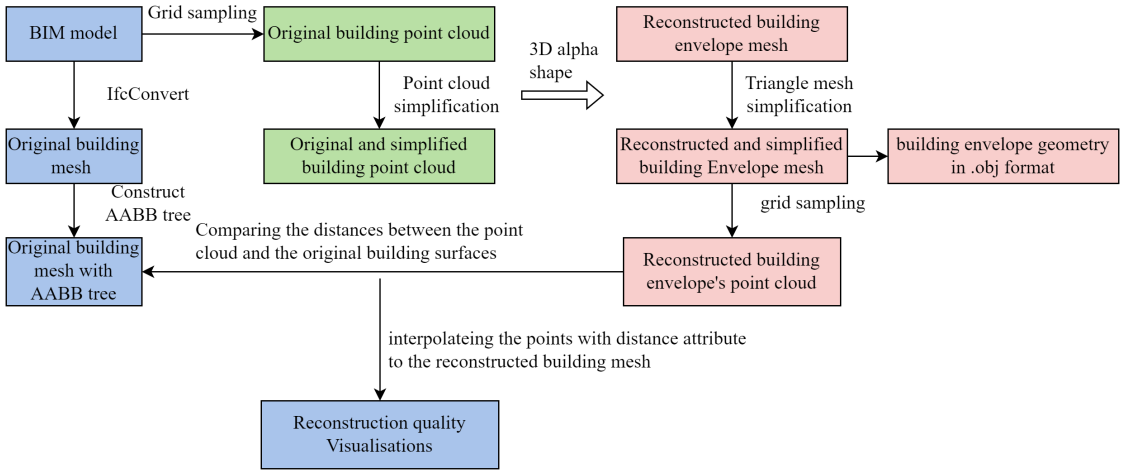

Figure 3.1.: Overview of the developed methodologies

3.1. Point cloud extraction

The first step of our developed methodology is to extract point clouds from IFC models. In this section, firstly, the possibilities of filtering irrelevant objects are explored and the subset of IFC data used for point cloud extraction is determined. Secondly, we describe the developed method for extracting point clouds from the determined IFC data subset.

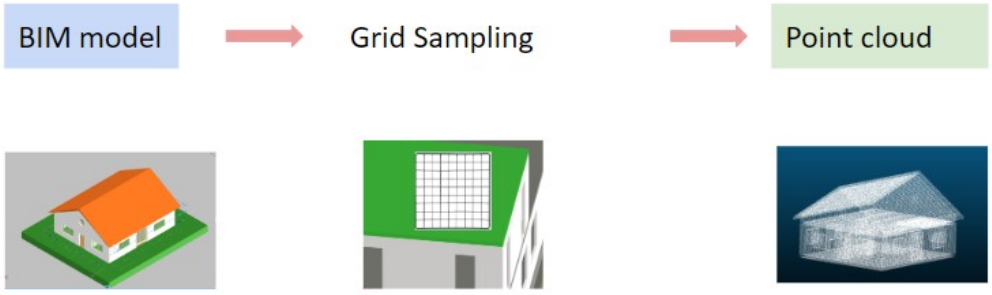

Figure 3.2.: Input and output of the point cloud extraction process

3.1.1. Filtering of IFC data

As aforementioned in subsection 2.1.1, the IFC data contains various types of detailed building information. There exists a subset of IFC data that is useless for building envelope extraction. Keeping these irrelevant IFC data may result in failures of point cloud extraction. For example, keeping *IfcProduct* that has no geometry when extracting point clouds is not feasible. The useless IFC data also slows down both the point cloud extraction and the envelope reconstruction process. In addition, these data may lead to artifacts in the reconstruction results. Given the two aforementioned reasons, before the point cloud extraction process, it is ideal to filter out as many irrelevant IFC data as possible. The filtering process took inspiration from the study conducted by Donkers et al. (2015), shown in figure 3.3.

First and foremost, the IFC objects without geometries need to be filtered out. This first

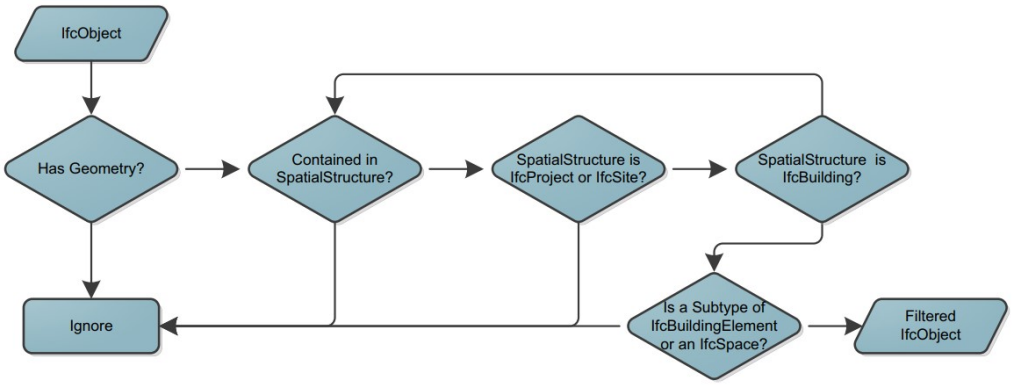

Figure 3.3.: The filtering process of IFC objects (Donkers et al. 2015)

filter guarantees that point clouds are only extracted from IFC objects that have geometries, and therefore no error occurs during the point cloud extraction process.

Secondly, there are two types of the IFC objects that have geometries. The first type is the physical objects, for instance, walls, roofs, and doors. The second type is the non-physical

objects, for instance, *IfcSpace* that describes a bounded area or volume. Keeping both the geometry of the physical objects and the non-physical objects leads to redundancy. In addition, objects with intangible geometries are usually unreliable (Vaart 2022). Therefore, it is desirable to remove all the non-physical IFC objects.

In addition, the physical objects that do not belong to buildings should be filtered out, since they do not contribute to the building envelope. Finally, the building's physical objects that clearly belong to the building interiors are removed. It is worth noting that only a subset of interior building objects that clearly belongs to the building interior is filtered out, for instance, furniture. Interior walls and floors are not removed, because it is difficult to differentiate them from the exterior walls and floors.

In conclusion, during the filtering process, objects that have no geometry, that are non-physical objects, and objects that do not belong to the building or clearly belong to the building interiors are filtered. This filtering process results in a subset of IFC data that only contain physical building objects, and with as little building interior data as possible. Figure 3.4 shows how the filtering process is achieved. Firstly, among all the sub-classes of *IfcObject*, only *IfcProduct* objects contain physical building objects. Therefore, we only keep the *IfcProduct* objects. Then among all the *IfcProduct* objects, only objects that contain physical building objects are kept. Finally, among all the physical building objects, the objects that do not meet the filtering criteria are deleted, for instance, *IfcFurniture* objects.

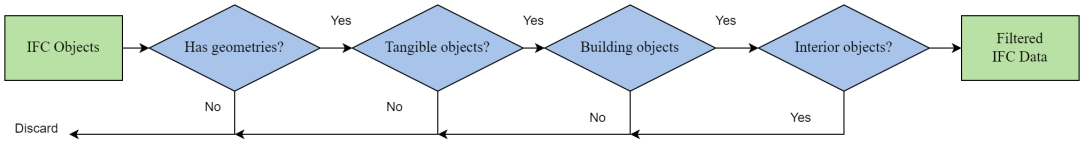

Figure 3.4.: The filtering process of IFC objects

3.1.2. Grid sampling

After obtaining the appropriate subset of IFC data, we need to extract point clouds from this subset. The step aims to extract the point cloud that is detailed enough to preserve building geometries. They are points data present in the original IFC data: vertices of different geometric objects. However, only extracting the vertices is not enough for preserving the building geometries. For instance, for a curved roof, only extracting the vertices can cause ambiguities in geometry reconstruction. Therefore, a certain type of surface sampling needs to be performed to obtain point clouds with enough details to capture the building geometries.

Commonly, there are two types of sampling methods: random sampling, and grid sampling. The random sampling method refers to the method that samples a number of points from surfaces randomly. It is not suitable for this study because it produces point clouds with various densities within every building surface. This can lead to problems when selecting the appropriate alpha value in the building envelope reconstruction process because different point cloud densities require different alpha values (see section 3.3 for more details). Grid sampling refers to extracting point clouds by applying a 2D grid on top of surfaces. It

is suitable for this research because it can produce point clouds that have the same density within every building surface. For instance, all extracted points from the same wall surface have approximately the same distance from each other, equal to the grid size. However, it is worth noting the point densities at the building connection part are not the same as the grid size.

After deciding on the sampling method, it is also important to choose the appropriate grid size because it decides the point density on building surfaces. A good choice of grid size should achieve a balance between the extracted point cloud's level of detail and its total number of points. The density of the generated building point clouds is of vital importance to the building envelope reconstruction results. The point clouds should preserve the detailed features of the building envelope, for instance, building overhangs and windows. At the same time, an overly dense point cloud can lead to slow performance in the shape reconstruction process. The minimum distance between points should be bigger than the minimum size of building objects. Since small windows can sometimes have a width that is smaller than 0.5m, it is better to only investigate grid sizes that are smaller than 0.5m. On the other hand, the chance of having exterior objects with scales smaller than 0.1m is small. In addition, from our experiments, it is observed that reconstruction from a point cloud sampled using a grid size smaller than 0.1m is big, and it can not produce reconstructed envelopes even for small and simple IFC models, for instance, FZK-Haus. Therefore, in this research, we should set the grid size range to 0.1m to 0.5m.

3.2. Point cloud simplification

After successfully extracting point clouds from IFC files, we notice that they can be huge: they usually contain millions of points. This may create processing difficulties for the following shape reconstruction algorithms, especially for big building models. Thus it is beneficial to reduce the size of the point clouds by using reasonable simplification measures. In this section, we present the main considerations for point cloud simplification.

Commonly, there are four types of point cloud simplification methods: random simplifying, grid simplifying, hierarchy simplifying, and Weighted Locally Optimal Projection (WLOP) simplifying. The random simplification method arbitrarily removes a subset of points. The main advantage of the random simplifying method is its speed. However, it is not suitable for our situation, because it damages the relatively uniform point densities within every building surface.

The grid simplification method simplifies input point clouds by applying a 3D grid on input point clouds. The 3D grid is constructed based on the point cloud's bounding box. For every cell of the grid, all points within this cell will be clustered into one representative point. The grid simplification method is also not suitable for our application for the following two reasons. Firstly, it is worth noting that the grid constructed in the grid simplification method is a 3D grid based on the building's bounding box, and the sampling grid constructed in section 3.1 is a 2D grid projected onto every building surface. Clustering points by the 3D grid cell may slightly damage the uniform point density within the surface created by 2D grids. Furthermore, if the 3D grid size is set to be too big, then it will cause too much loss of the building's original geometric information. If the grid is too dense, for instance, the same density as the aforementioned sampling grid, then it is not able to significantly simplify the

point cloud. Therefore, this method can not effectively reduce the point cloud size.

The hierarchical simplification method simplifies the input point clouds by clustering points together. More specifically, this method split the input point cloud into smaller subsets recursively and stops when pre-defined conditions are met, for instance, the number of remaining clusters is below a certain threshold. The hierarchical simplification method is not ideal for this research for similar reasons to the random simplification: it damages the uniform point density across every building surface.

WLOP simplification algorithm is a method to simplify point sets developed by Huang et al. (2009). For the input point cloud, the WLOP method defines another small set of projected points by minimizing a similarity-measure parameter between the projected point set and the original point set. It can remove noise and outliers from the input point cloud, and produce a point cloud with uniform density. It is ideal because it can produce evenly-distributed results. In the WLOP simplification method, the most important parameter is the spherical neighborhood radius. The spherical neighborhood radius (h) is used to constrain the range of the projection process. According to Huang et al. (2009), the ideal size should be calculated using the following formula:

$$h = 4\sqrt{d_{bb}/m}$$

where d_{bb} is the diagonal line length of the points' bounding box, and m is the number of the original points.

3.3. Building envelope extraction

After extracting and simplifying the extracted point cloud, the building envelope needs to be extracted from the point clouds. This section covers the developed method of extracting the building envelope from the sampled point cloud.

First and foremost, the appropriate geometry reconstruction method should be decided. As aforementioned in subsection 2.2.2, there are many point cloud-based geometry reconstruction techniques. Among them, the voxel-based method first performs voxelization and then extracts the geometries using the marching cube algorithm. The 3D Alpha shape extracts the input point cloud's outer boundary. The footprint projection and extrusion method first projects the input point cloud to a footprint and then extrudes them into a 3D building model. Possion surface reconstruction reconstructs surfaces by calculating an implicit field based on the input points. However, except for the alpha-shape method and the footprint projection and extrusion method, all other methods have one common fatal flaw: they can not only reconstruct the exterior shape of the point cloud. The alpha-shape method can produce building geometries with great detail, but the footprint projection and extrusion method may cause a loss of information, especially with buildings that have slanted walls or walls with irregular shapes. Therefore, in this research, we choose the 3D alpha shape as the reconstruction technique. Figure 3.5 shows the workflow of this process.

Secondly, When using the 3D alpha shape for building envelope reconstruction, choosing the appropriate alpha value is very important. As aforementioned in subsection 2.2.2, the alpha value is the α-ball's radius used in the 3D alpha shape algorithm. The starting point

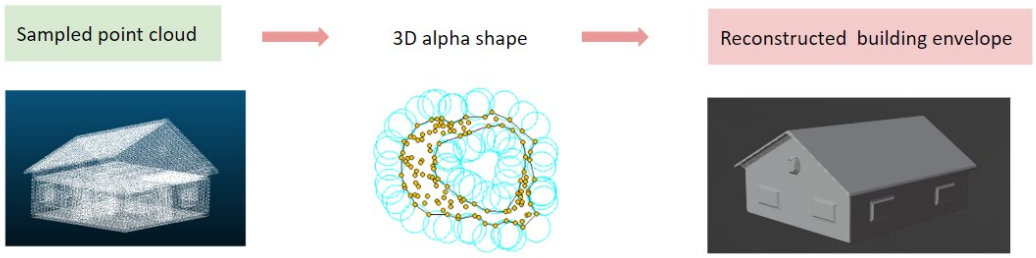

Figure 3.5.: Reconstructing building envelopes using alpha shape

of the 3D alpha shape algorithm is the R^3 space. As shown in figure 3.6, the alpha ball iteratively removes spaces while not touching any of the input point sets, thus gradually carving out the exterior shape of the input point cloud. A bigger alpha value decreases the reconstruction time but may cause the loss of geometry details. On the other hand, a smaller alpha value produces reconstruction results with more detail, but it is computationally expensive. Furthermore, a small alpha value can produce holes on the reconstructed surfaces. In this study, we choose the alpha value based on the following reasons. As shown in fig-

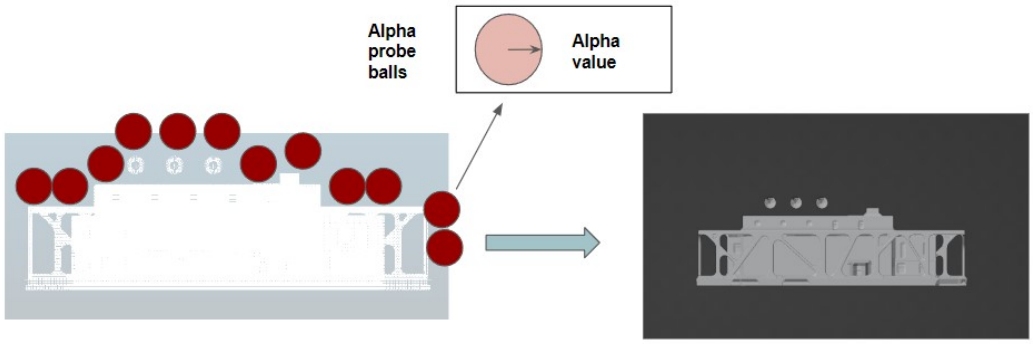

Figure 3.6.: The role of alpha value in 3D alpha shape algorithm

ure 3.7, since our point clouds are constructed by grid sampling (see section 3.1 for more details), it is important to keep the alpha value to no smaller than the grid size. Otherwise, the α-balls can easily get in between the points, and create holes or caves on the building's surface. In addition, in order to capture all the building's exterior features, the chosen alpha value should not be bigger than the smallest size of the building's exterior features. As aforementioned, the smallest size of the building's exterior features is 0.5m. Therefore, the upper range of the alpha value should be 0.5m.

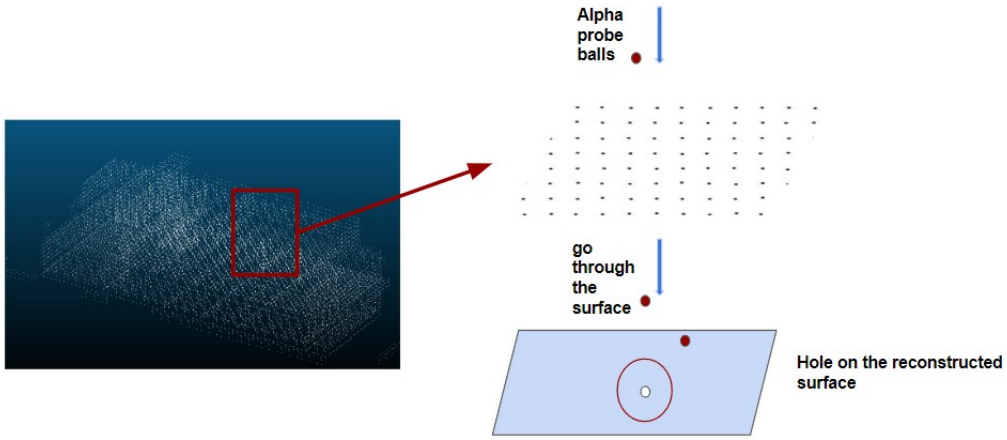

Figure 3.7.: The reason for setting the alpha value to be no smaller than the sampling grid size

3.4. Building envelope simplification

After extracting the building envelope, it is observed that the extracted geometries have a great number of redundant edges and vertices, making the results unnecessarily complex, and even bigger than the original IFC files. In addition, it is worth noticing that most of these edges and vertices do not contribute to preserving the building envelope's shape. Considering all the above reasons, it is necessary to remove the redundant geometries from the extracted building envelopes.

We choose to use the edge-collapse method (Dey et al. 1999) to perform simplification, because it is one of the most widely used mesh simplification techniques. This edge-collapse method simplifies the mesh by iteratively replacing the edge with vertices and then removing the two triangle faces that are adjacent to the edge (Dey et al. 1999). Figure 3.10 shows the process in more detail. At every iteration time, the edge with the lowest cost will be removed. The cost is a calculated indicator to measure how greatly removing the current edge affects the mesh's shape. A new vertex will be placed in a position calculated by the placement function. This process is repeated until the stop condition is met.

There are different versions of edge collapse methods. They vary mainly in the stop conditions, the cost function, and the placement function. It is necessary to choose the appropriate version for this research.

There are three types of stop predicates. Among them, the first type of stop predicate stops the simplification process when the number of edges present in the mesh is below a pre-set value. This method is not applicable to the simplification of building envelope meshes, because the size of building models varies greatly and therefore the number of edges present in the extracted building envelope mesh also varies greatly. The second type of stop predi-

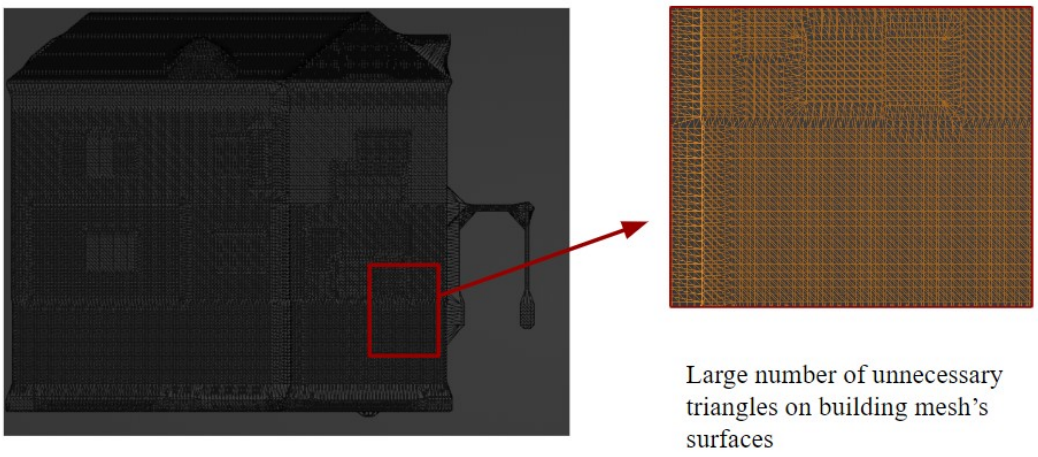

Figure 3.8.: Building envelopes with redundant geometries

cate stops the edge collapse process by checking the length of specific edges. During every iteration time, the edge that lies on the top of the priority queue is checked. If it is bigger than a threshold, then the simplification process stops. Since building envelope meshes have very long edges, for instance an edge of a wall, and also have very short edges, for instance an edge of a small window, this method is also not suitable. The third type of stop predicate stops when the ratio between the current number of edges and the original number of edges is below one pre-set percentage, and it is more suitable for this research compared to the other two stop conditions. As shown in figure 3.8, the extracted building envelope contains a high number of redundant edges and vertices. Therefore, it is reasonable to set a low stop percentage, for instance, 1% percent.

The method for calculating the cost and placement is also of great importance. For the edge-collapse algorithm, there are mainly two types of cost and placement strategies present. The first cost and placement strategy is the Lindstrom-Turk cost strategy, developed by Lindstrom and Turk (1998). This memory-less method does not compare the simplified mesh with the original mesh. At each iteration time, the algorithm finds the edge with the lowest cost from all the candidate edges and replaces it with a vertex. The placement of the vertex is calculated by three linearly-independent constraints. The constraints are selected incrementally based on their importance, and if the candidate constraint conflicts with existing constraints, it will be taken out of consideration. The most important constraints are to keep the outer boundary of the triangle mesh, followed by constraints that aim to keep the total mesh volume unchanged. The third important constraint helps to minimize the local volume and area changes and the last constraint tends to favor equilateral triangles over elongated triangles. Once three constraints are selected, we can determine the 3D position of the new vertex. The cost is calculated as the weighted sum of the local change of volume and area brought by the edge collapse process.

Another cost and placement strategy is the Garland-Heckbert cost and placement strategy

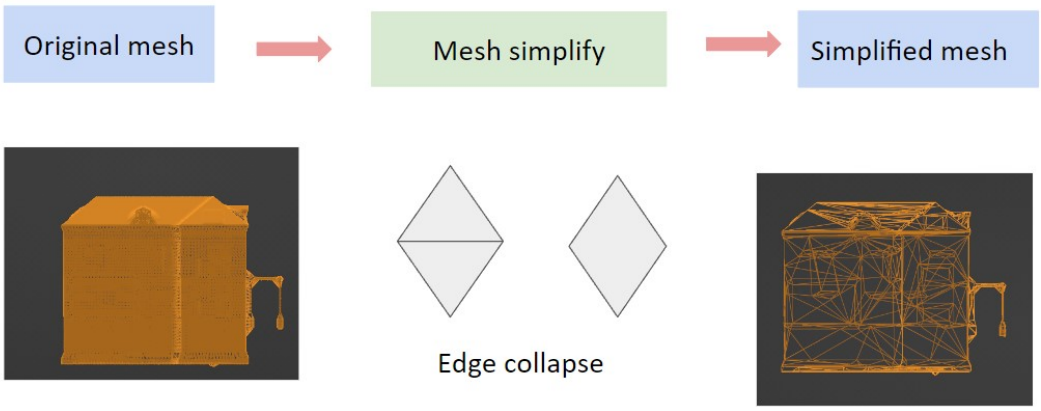

Figure 3.9.: Triangle mesh simplification using edge collapse

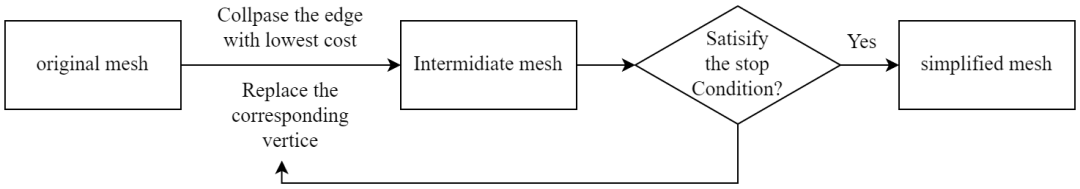

Figure 3.10.: The detailed workflow of edge collapse

developed by Garland and Heckbert (1997). It approximates the squared distance to the original mesh as the cost. The point that can minimize the distance error function will be chosen as the new vertex placement.

Our aim is to produce building envelopes with surfaces that are as close to the original surfaces as possible, therefore the Garland-Heckbert cost and placement strategy aligns better with the aim. However, the Garland-Heckbert cost strategy is not a memory-less method and the distance calculation process is very computationally expensive. We tested the Garland-Heckbert method and it can not produce results within a reasonable time frame. Therefore, we use the Garland-Heckbert cost and placement strategy.

4. Implementation Details

4.1. Used Datasets

In order to test the effectiveness of our developed building envelope extraction approach, we perform tests on a set of selected IFC models. In order to test the robustness of our developed approach, we aim to select buildings with varieties. For instance, buildings with different types of roofs, buildings with exterior stairs, and buildings with different levels of scale and complexity.Table 4.1 shows an overview of the used IFC models. A complete overview of these used IFC models can be found in Appendix B.

Model name	File size	Number of IFC objects
BIMcollab_ARC	25382 KB	1611
BIMcollab_STR	631 KB	241
Mauer_BmB	4042 KB	191
Smiley-West	5867KB	831
FZK-Haus	2511KB	96
Institute-Var-2	10678KB	814
BUREAUX	5156KB	755

Table 4.1.: Used Dataset

4.2. Used software

4.2.1. Programming language and used libraries

In this research project, the C++ language is used to develop the building envelope extraction tool. During the development process, the following C++ libraries are used:

- IfcOpenShell: IfcOpenShell is a library developed to help read and extract information from IFC models. In the sampling point cloud from IFC models phase, the IfcOpenShell library is used to read and parse the input IFC files. In addition, to obtain the shapes of building objects, we use the relevant functionalities in the helper class developed by Vaart (2022).

- Computational geometry algorithms library (CGAL): CGAL is a library that contains various types of geometric processing functionalities. In the building envelope reconstruction phase, we use the alpha shape class from CGAL for reconstruction. In addition, functions from CGAL are used during the point cloud simplification and mesh simplification steps. Finally, in the error analysis phase, the AABB tree class is used to find the closest point pairs between the reconstructed mesh and the original building mesh.

4.2.2. Used software

- Blender: Blender is a 3D computer graphics open-source software allowing the visualization and editing of 3D models. In our study, Blender is used to visualize and examine the extracted building envelopes.
- CloudCompare: CloudCompare is a free open-source software for point cloud visualization and processing. In our study, CloudCompare is used to visualize the extracted point clouds and sampling of the reconstructed envelope for further error analysis.
- IfcConvert: IfcConvert is a tool based on the IfcOpenShell library, and it can convert IFC files into various types of other formats. In our study, we use IfcConvert to convert the input IFC models into building meshes in OBJ format, therefore making the comparison between the reconstructed geometry and original geometries possible.
- Paraview: Paraview is an open-source 3D visualization software. In our study, we use Paraview for error visualization.
- Open IFC Viewer: Open IFC viewer is an open-source viewer developed for visualizing IFC files. In this research, the open IFC viewer is used for input IFC model inspection.

4.3. Implementations

This section covers the implementation details of our developed data processing pipelines based on the methodologies described in chapter 3. The implementations of point cloud extraction, point cloud simplification, building envelope reconstruction, and building envelope simplification respectively.

4.3.1. Point cloud extraction and simplification

The process of point cloud extraction can be divided into two steps. Firstly, the input IFC files are read and parsed by IfcOpenShell. Then all the *IfcProduct* objects that do not meet the filtering criteria described in section 3.1 are removed.

For all the remaining *IfcProduct* objects, we use the GetShape function from the helper class developed by Vaart (2022). This function takes each *IfcProduct* object as input and produces its shape in TopoDS_Shape. Then the TopoExp_Explorer is used to get the surfaces, stored in Topo_DS_Face format. Since sampling operation is not easily achievable on the TopoDS_Face, we first convert the extracted surface to b-rep format using the BrepTopAdaptor tool. In addition, to get the boundary information needed for constructing the grid, a 2D projection of

the original surface is extracted using BRepTopAdaptor_FClass2d. After obtaining the 2D projection, we use the BRepTools::UVBounds() tool to extract the boundary information.

After the surface extraction and transformation, a virtual grid is constructed using the 2D boundary information obtained. Then we project the grid onto the original 3D surface. If the grid points fell within the original 3D surface, then we extract the corresponding 3D points.

In the point cloud simplification step, the WLOP simplification implemented by CGAL is used. For the parameter settings, the require_uniform_sampling is set to false. The spherical neighborhood radius (h) is calculated using the formula mentioned in section 3.2.

4.3.2. Building envelope reconstruction and simplification

The building envelope is reconstructed by the 3D alpha shape class from CGAL. In order to output the reconstructed envelope in .obj format, every vertex is indexed. Then we collect the visible facets of the 3D alpha shape, and output all the vertices and visible facets to an OBJ file.

In the building envelope simplification phase, the edge collapse method developed by CGAL is utilized. The stop predicate, cost, and function strategies are passed as parameters. In addition, for this study, the Bounded_normal_change_filter is useful. As shown in figure 4.1, the edge collapse process can easily cause self-intersection issues even for relatively simple triangle meshes. Using the Bounded_normal_change_filter, during every iteration time, for a potential candidate edge, the filter examines all the faces that are adjacent to the two vertices of the edge, of whether a potential placement will flip the face normal of these faces or not. If the placement would flip one or more face normal of these faces, then we will discard this potential edge. By adding this filter, we avoid possible self-intersections in the resulting simplified mesh and better ensure their qualities.

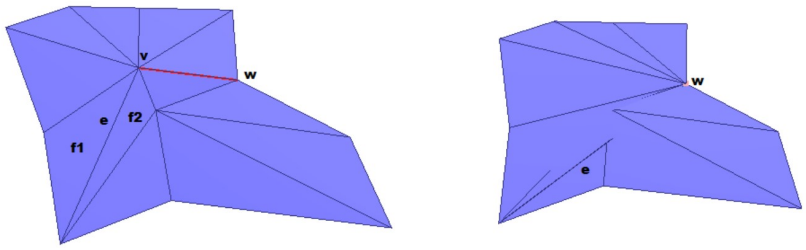

Figure 4.1.: Intersections caused by the edge collapse mesh simplification, source.CGAL

5. Results and Discussion

This chapter is divided into two sections: results and discussion. Firstly, the result section presents the results from different steps and the final extracted envelopes. Secondly, the discussion section analyzes the obtained results from different aspects.

5.1. Results

In this section, first example results along the data processing pipeline are presented to better illustrate the effects of each step. Secondly, the final extracted building envelopes are presented.

5.1.1. Intermediate results

After the point cloud extraction step, the extracted point clouds are shown in figure 5.1. From the examples, it is observed that the building geometries are well preserved in the extracted point clouds, including shapes of roofs, walls, windows, and other exterior structures for instance pillars. As shown in figure 5.2, it is also worth noting that the extracted point cloud has consistent point density within every building surface. This lays a good foundation for the building envelope reconstruction.

After the point cloud extraction, it is also potentially beneficial to simplify the point cloud to improve the reconstruction speed. Figure 5.3 shows some examples of point clouds before and after WLOP simplification. From the tested dataset, there is no apparent geometry distortion visible, but the actual effects of the simplification can only be inspected after using the simplified point cloud to reconstruct building envelopes (see subsection 5.2.2 for more details).

After extracting and potentially also simplifying point clouds, the building envelopes are reconstructed using the 3D alpha shape algorithm and simplified using the edge collapse technique. Figure 5.4 shows one example result to demonstrate the effects of the simplification. From visual interpretation, the triangle mesh simplification reduces the redundant triangles, and the shape of the building meshes is kept rather successfully.

5.1.2. Final results

In this section, the final extracted building envelopes are shown in figure 5.5. Observations from different views are provided. Comparing the reconstructed building envelopes and

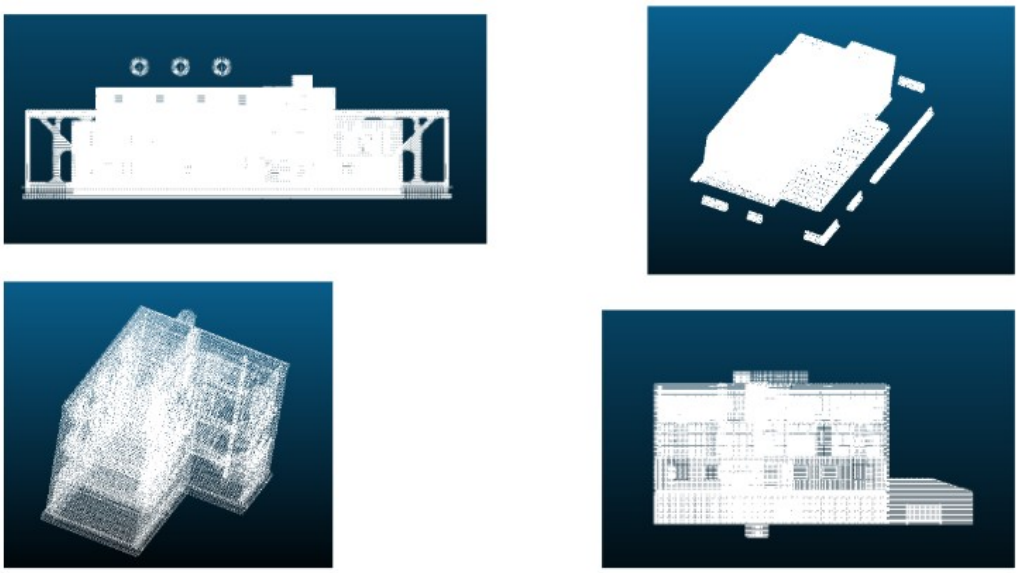

Figure 5.1.: Extracted point cloud from IFC files (samples)

the original IFC model (shown in 5.6), by visual interpretation, the developed methodology can extract building envelopes rather successfully. A full visual overview of the extracted envelopes can be found in Appendix C.

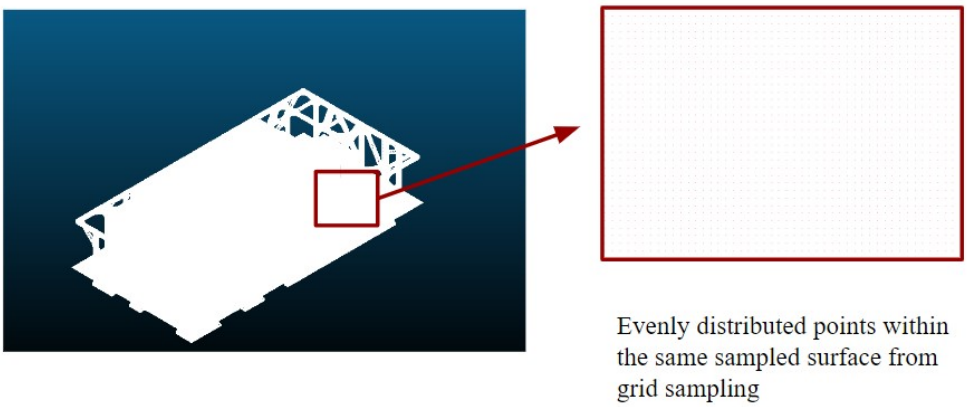

Figure 5.2.: Evenly distributed points within the same sampling surface

5.2. Discussions

5.2.1. Quality assessment

From section 5.1, it is clear that our method can extract building envelopes from IFC models successfully. In most models, by visual interpretation, the reconstructed building envelope resembles the original building's exteriors with only minor deviations, and the delicate details of the exterior envelopes are preserved. However, in order to analyze the quality of the extracted building envelopes, it is necessary to evaluate them quantitatively. As described in subsection 2.1.3, common evaluation aspects of reconstructed geometries are: geometric accuracy, topological accuracy, simplicity, and reconstruction speeds. Since our developed methodologies do not preserve the topology information, in this section, we cover three main indicators for the building envelope's quality assessment: geometric accuracy, geometric simplicity, and time efficiency.

Geometric Accuracy

The first and also the most important indicator is the accuracy. It is the most significant indicator because an extracted building envelope will be unreliable and therefore potentially useless if it does not resemble the original building exterior enough, no matter how simple they are and how fast can users extract them.

In this research, the geometric accuracy is measured by the deviations between the reconstructed surfaces and the original surfaces. More specifically, as shown in fig 5.7, for every sampled point from the reconstructed surfaces, its closest point in the original surfaces is found, and the squared distance between these two points is calculated. These calculated squared distances are viewed as reconstruction errors.

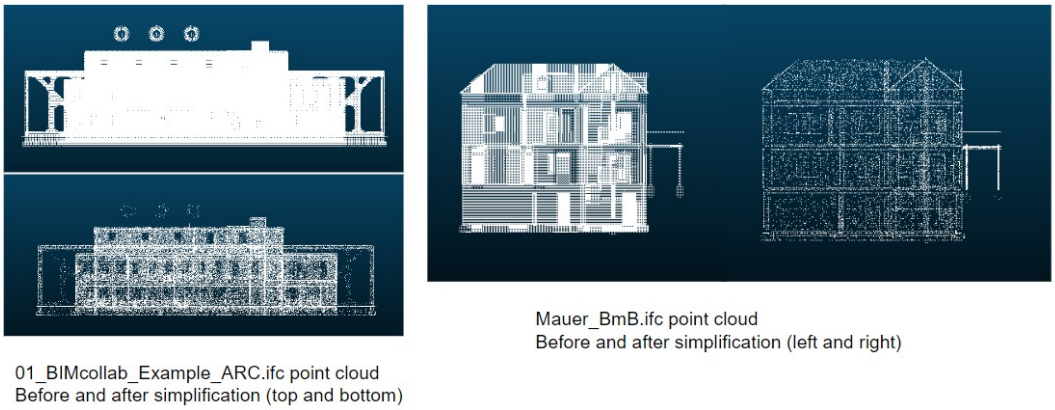

Figure 5.3.: Example of building point clouds before and after WLOP simplification

In order to grasp the characteristics of the reconstruction error distribution, it is beneficial to calculate its common statistics. Therefore, as shown in table 5.1, the mean, standard deviation, and percentage of extreme points that have error values between 2.50-5.00cm, 5.00-10.00cm, and bigger than 10.00cm are calculated. Figure 5.8 and figure 5.9 show the calculated statistics visually.

For all the tested IFC models, the mean reconstruction errors are within 2cm, and 85.7%

Model Name	Mean	SD	2.50-5.00cm	5.00-10.00cm	bigger than 10.00cm
BIMcollab ARC	0.52cm	1.46cm	5.23%	2.35%	0.27%
BIMcollab STR	1.71cm	9.02cm	4.87%	2.73%	3.50%
Mauer BmB	0.35cm	1.66cm	1.36%	0.38%	1.16%
Smiley-West	0.61cm	1.59cm	7.26%	2.74%	0.11%
FZK-Haus	0.49cm	1.66cm	3.28%	3.67%	0.21%
Institute-Var-2	1.19cm	2.86cm	7.20%	4.41%	4.22%
BUREAUX	0.32cm	1.19cm	4.22%	0.84%	0.28%

Table 5.1.: Statistics of the error distribution for all tested buildings

of the tested models have average reconstruction errors that are smaller than 1.20cm. These are very small values, especially compared to the magnitude of buildings. The small mean reconstruction errors for the tested building models indicate high reconstruction accuracy. In addition, among the tested building models, it is observed that building envelopes extracted from buildings with relatively simpler exteriors have lower average reconstruction errors. The term building with simple exteriors indicates exteriors with only walls, planar roofs without holes, and a small number of windows, doors, and other small-scale exterior objects, for instance, the Mauer BmB model and the BUREAUX model. On the contrary, building envelopes extracted from buildings with relatively complex exteriors have higher average reconstruction errors. The term building with complex exteriors refers to exteriors

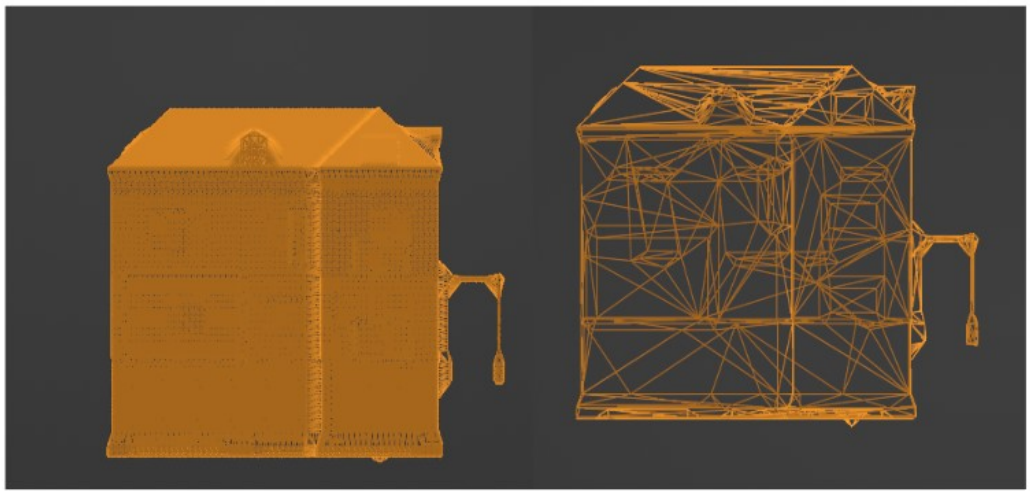

Figure 5.4.: Example results from mesh simplification,(a): building mesh before simplification,(b):building mesh after simplification

with complex roof structures and a big number of small-scale objects, for instance, pillars, doors, and windows. Figure 5.10 shows two examples of buildings with complex exteriors. This is caused by the key working principle of the alpha shape algorithm: it can not capture geometries that are smaller than the radius of the α-ball. Therefore in complex buildings, the reconstruction errors for small-scale objects are bigger.

The standard deviations indicate how dispersed the reconstruction errors are from the mean value. For all the tested IFC models, the standard deviations are at least 2 times as big as the mean value. More specifically, 42.86% of the tested models have standard deviations that are 2-3 times as big as the mean value. 42.86% of the tested models have standard deviations that are 3-5 times as big as the mean value. Most extremely, the BIMcollab STR model's reconstruction error distribution has a standard deviation is 5.3 times as big as its mean value. These relatively big standard deviations reflect that the reconstruction errors are very spread out, and therefore the mean value can not effectively present the whole distribution. However, it is also worth noting that even though the standard deviations are relatively big compared to the corresponding mean values, they are still small compared to the usual scale of building objects: all the standard deviation values are within 10.00cm, and the scale of building objects are usually greater than 0.5m. Therefore, it is still safe to say that the building envelope reconstruction has high geometric accuracy.

Finally, the percentages of points that have extreme reconstruction errors are calculated. These percentages indicate the percentage of reconstructed surfaces that have big deviations from the original surfaces. These points are points with error values between 2.50-5.00cm, 5.00-10.00cm, and bigger than 10.00cm. For the total percentage of points with extreme values (points with an error value that is bigger than 2.50cm), from figure 5.9 it is clear that

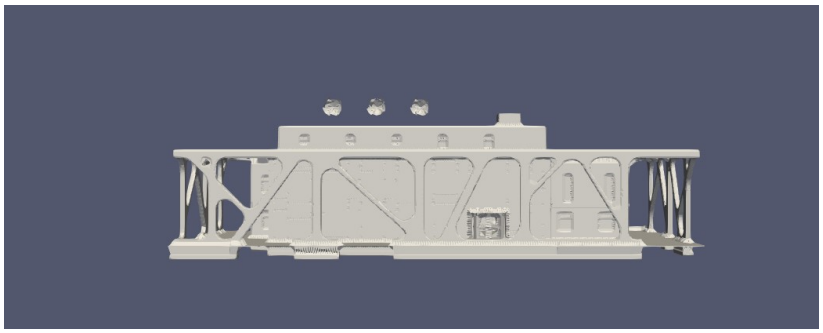

(a) front view

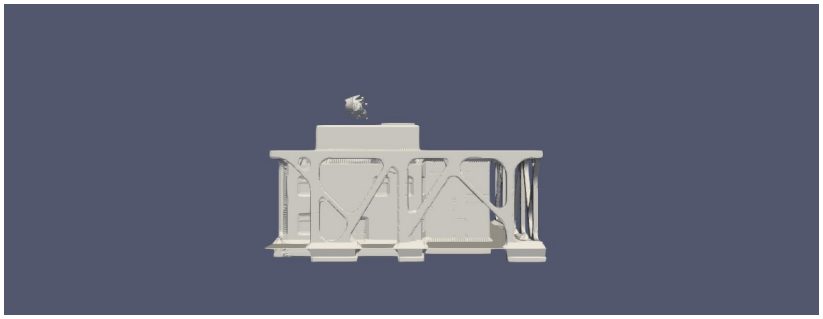

(b) Left view

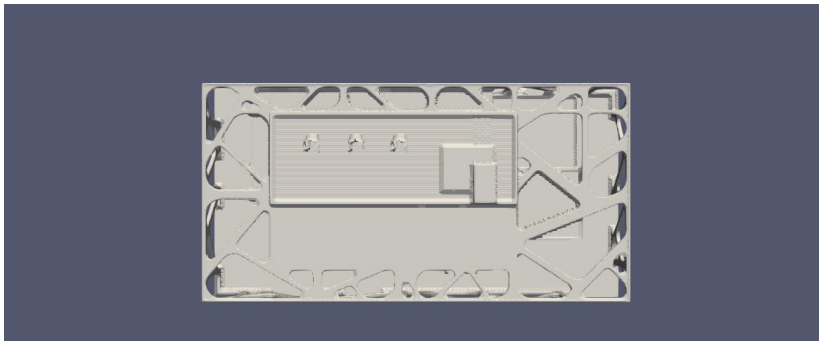

(c) Top view

Figure 5.5.: Extracted building envelope of the BIMcollab_ARC model

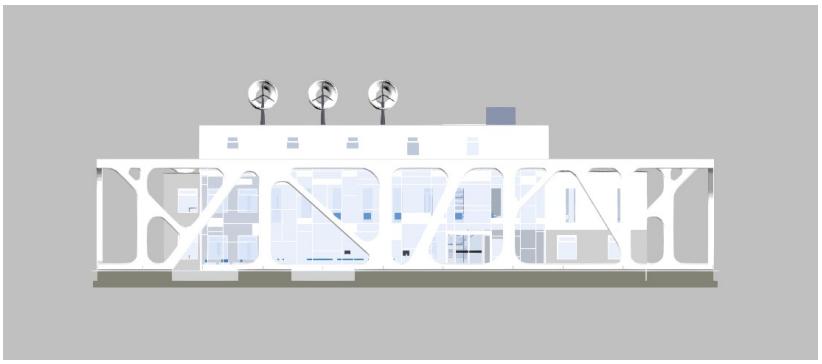

(a) front view

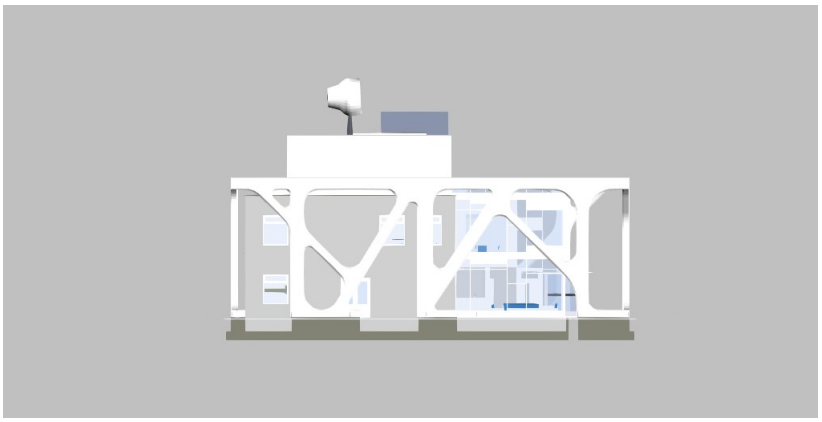

(b) Left view

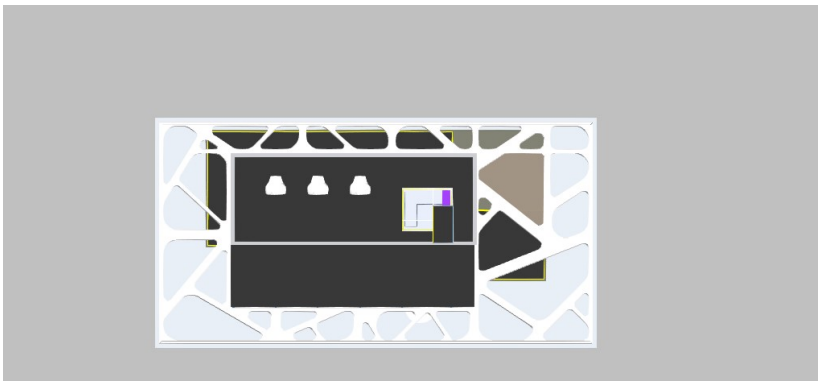

(c) Top view

Figure 5.6.: original IFC model of the BIMcollab_ARC model

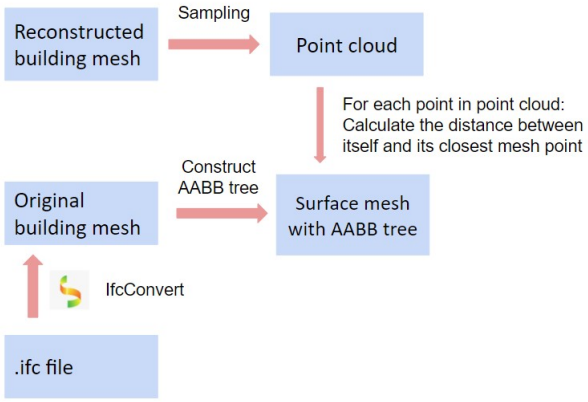

Figure 5.7.: The workflow of measuring the geometric accuracy

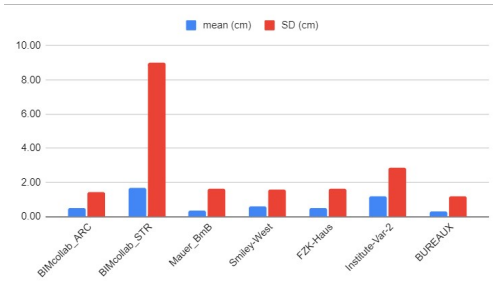

Figure 5.8.: Mean and SD of the reconstruction errors

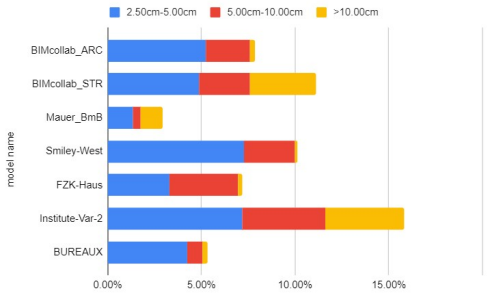

Figure 5.9.: Percentage of inaccurate points in the reconstruction result

71.42% of the tested models have less than 10% of extreme points, and the rest of the 28.57% of the tested models have 10% to 15% extreme points. For the percentage of points with error values that is bigger than 10.00cm, it is observed that 57.14% of the tested models have less than 0.5% of this type of extreme points and all of the tested models have less than 5% of this type of extreme points. This also indicates the overall high geometric accuracy of the extracted envelopes.

These calculated statistics describe different aspects of the reconstruction error distribution, however, they can not give information about where exactly the relatively big errors occur. Therefore, as shown in 5.11, the reconstruction errors are visualized in 3D space, with different colors indicating different error values (cooler colors indicate smaller values and warmer colors indicate bigger values). Error visualizations for all the tested building models can be found in Appendix D.

First and foremost, from these visualizations, it is observed that all buildings' walls and roofs are reconstructed with very high geometric accuracy. In the visualizations, for all buildings, the walls and roofs are colored dark blue, indicating a deviation of smaller than 0.001m from the original surfaces. This indicates the walls and roofs of the extracted building envelopes are reconstructed very accurately. The windows and doors have bigger recon-

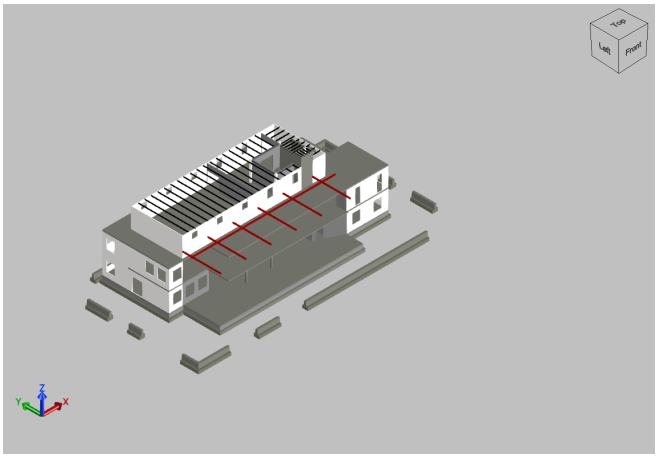

(a) BIMcollab STR model with complex roof structure

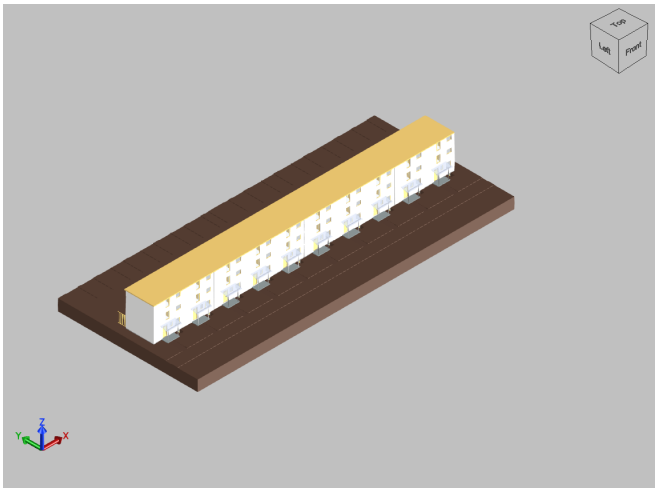

(b) Smiley-West model with large number of windows

Figure 5.10.: Examples of buildings with complex exteriors

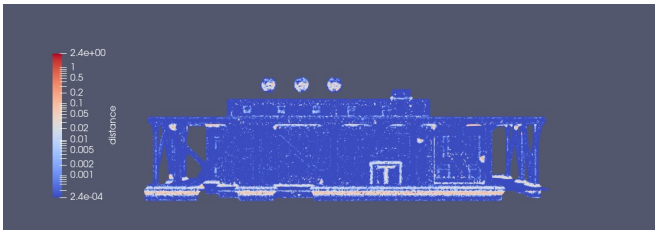

(a) BIMcollab ARC model, front view

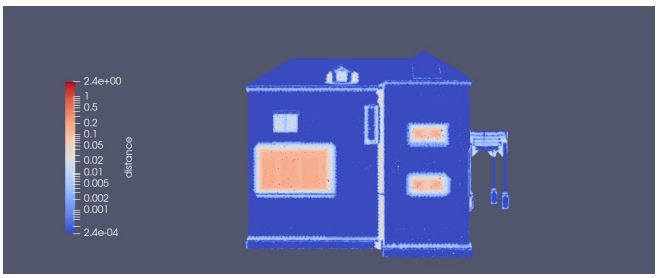

(b) Mauer BmB model, front view

Figure 5.11.: Reconstruction error visualization

structed errors. For the tested models, the windows and doors are colored pink, indicating a deviation of approximately 0.1m from 0.3m from the original surfaces. It is worth noting that the big errors (approximately 1m) in the BIMcollab STR model are not caused by windows but by failure to extract openings. In addition, the connection parts between separate building elements, for instance, walls and roofs, also have a reconstruction error of approximately 0.05m to 0.1m. Lastly, small-scale exterior objects, for instance, the exterior spiral staircase in the BUREAUX model and antennas in the BIMcollab ARC model have relatively big reconstruction errors of 0.1m to 0.2m. This is because roofs and walls usually have regular shapes. In all the tested buildings, walls are rectangular shapes and their straight-line boundaries can be easily captured by the 3D alpha shape algorithm. The same reasoning applies to buildings with planar or slanted roofs. For buildings with curved roofs, for instance, the Institute-Var-2 model is also composed of planar surfaces with a scale much bigger than the alpha value, therefore their geometries can also be captured successfully. The big reconstruction errors from windows and doors are caused by the fact that the windows' and doors' surfaces are very close to the wall surfaces or to each other. Figure 5.13 shows an example. Many windows and doors have distances of only 0.1m from walls, which is approximately the smallest possible grid size. Since the alpha value should be slightly bigger than the grid size, it is natural that the window and door surfaces can not be accurately extracted, since the distances between them and the wall they are located are smaller than the alpha value. The same reasoning applies to small-scale exterior objects, for instance, spiral staircases.

One limitation of the calculated reconstruction error is that it is an absolute value and not a signed value. Therefore, we can not know whether the reconstructed building envelope is bigger or smaller than the original building. For instance, given the reconstruction error of the window to be 0.2m, merely from the calculated reconstruction error it is impossible to know whether the windows are lower or higher than the wall surfaces that it locates in. This is of particular importance for building permit checking: if the extracted

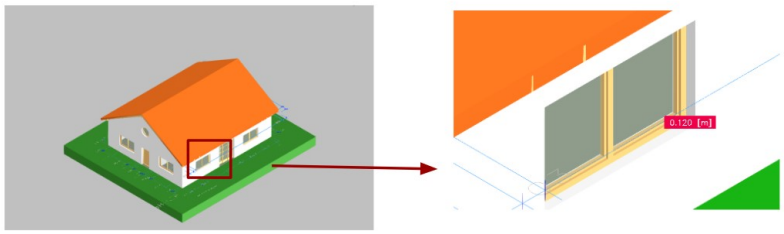

Figure 5.12.: Distances between window surfaces

building envelopes are smaller than the original model, then it is not ideal to use them for the maximum height checking, because it may lead to false results. After visualizing and comparing the reconstructed building envelope and the original models, it is observed that all the extracted building envelopes' windows and doors are slightly extruded from their original places. Figure 5.13 shows one example, with the red color indicating the extracted building envelope surfaces, and the grey color indicating the original building surfaces. This is expected because principally, the alpha-shape algorithm starts from the 3D R^3 space and gradually removes unnecessary spaces using the α-balls. Since the radius of the α-balls is set slightly larger than the point cloud densities on surfaces, the unnecessary spaces can not be fully removed in places with these small-scale geometries.

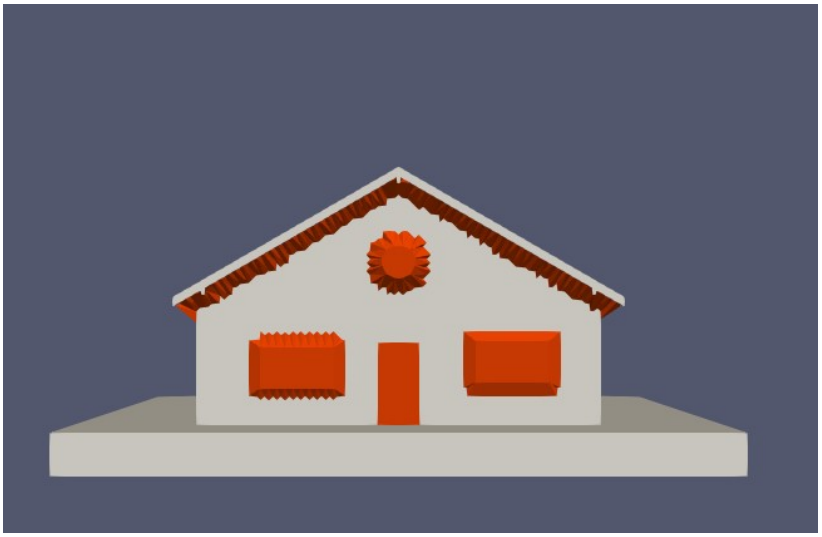

Figure 5.13.: Extruded reconstructed windows and doors, using FZK-Haus as an example

Geometric Simplicity

Apart from the geometric accuracy, the building envelope's simplicity is also very important, especially under the circumstances of processing big building models or processing a large number of buildings, for instance, processing on a city scale. In order to evaluate the

simplicity of the extracted building envelopes, the number of vertices and edges within the input IFC models and the extracted building envelopes are compared. Since the file sizes depend heavily on the encoding, the input and output file sizes are not compared.

Table 5.2 shows the differences between the input and output vertices. It is observed that for all the tested building models, extracting the building envelope removed more than 90% of vertices. This shows that the developed approach can simplify the number of vertices significantly.

Table 5.3 shows the differences between the input and output faces. It shows that 85.71%

model name	Input vertices	Output vertices	Reduced percentage
BIMcollab ARC	1361836	7437	99.45%
BIMcollab STR	26464	2275	91.40%
Mauer BmB	113736	381	99.67%
Smiley-West	660400	1500	99.77%
FZK-Haus	81204	217	99.73%
Institute-Var-2	167396	1210	99.28%
BUREAUX	211572	1261	99.40%

Table 5.2.: Input and output of the number of vertices

of the tested models have reduced the number of faces, but one of them has increased the number of faces, due to the fact that the extracted building envelopes have triangulated faces.

In conclusion, regarding the number of vertices, the extracted building envelope is much

model name	Input faces	Output faces	Reduced percentage
BIMcollab ARC	155384	4260	97.26%
BIMcollab STR	2916	4574	-56.86%
Mauer BmB	15820	684	95.68 %
Smiley-West	73898	3064	95.85%
FZK-Haus	8470	430	94.92%
Institute-Var-2	19033	2424	87.26%
BUREAUX	26647	2481	90.69%

Table 5.3.: Input and output of the number of faces

simpler than the original IFC models. Regarding the number of faces, 85.7% of the tested models also have reduced the number of faces significantly. One tested model has more output faces than input faces, but it is due to the fact that the output envelope is triangulated and the input IFC model is not.

Time efficiency

Lastly, it is of great necessity to check whether the developed approach can extract building envelopes quickly. Therefore, the amounts of time spent on point cloud extraction and

building envelope reconstruction are documented respectively. The amounts of time spent on point cloud simplification and building envelope simplification are not documented because they are usually relatively quick. Figure 5.14 shows the point cloud generation and building envelope extraction time for each testing model.

It is observed that for all tested models, we can extract the building envelopes within 140s.

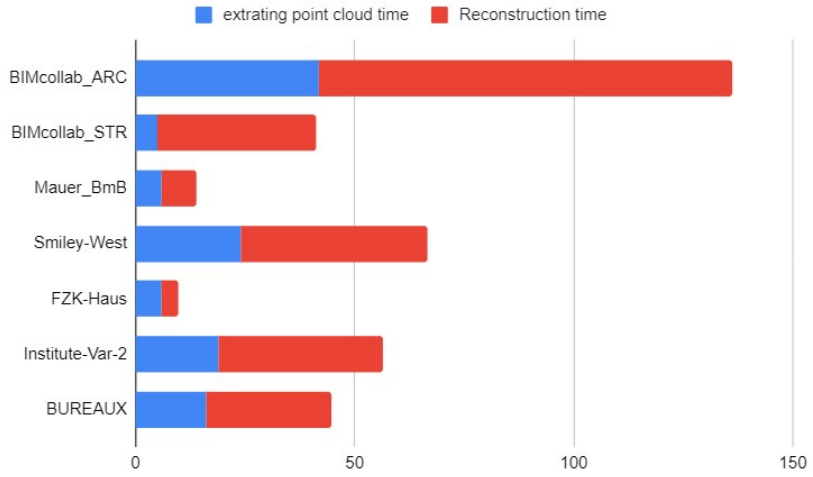

Figure 5.14.: Processing time of the data processing pipeline

This shows that for all tested models, the building envelopes can be extracted efficiently. It is observed that buildings with higher levels of complexity, for instance, BIMcollab ARC model, take a longer extraction time. In addition, for each building, reconstructing the building envelope takes more time than extracting the point cloud. It is expected since the point cloud extraction only needs to grid sample all the qualified surfaces, but the 3D alpha shape reconstruction process needs to first construct Delaunay triangulation and then remove all the simplices with intervals smaller than the alpha value. Even though for all the tested models the time efficiency is good, our developed approach is unable to extract building envelopes of big and complex building models, for instance, the Witte de Withstraat model.

5.2.2. Parameters

As described in chapter 3 and chapter 4, there are many parameters present along the developed data processing pipeline. More specifically, during the point cloud extraction step, we need to decide on the appropriate size for the sampling grid. After obtaining the point cloud, the percentage of retained points during point cloud simplification needed to be chosen. When reconstructing the building envelopes, we should choose the appropriate alpha value for the alpha shape reconstruction algorithm. Finally, the percentage of retained edges in the building envelope needs to be specified. In this section, we discuss how the changes in these parameters affect the final reconstruction results, and thus decide on the set of parameter settings that leads to the best reconstruction results.

Cell size of the sampling grid

As described in section 3.1, the cell size of the sampling grid is a very important parameter. It decides whether the building's geometry is well preserved in the extracted point cloud. In this section, we test grid sizes ranging from 0.1m to 0.5m on a subset of IFC models. The effects of changing grid size are indicated by the most important quality indicator: geometric accuracy.

Table 5.4 shows the statistics of the error distributions from the test results. Figure 5.15 and figure 5.16 show these statistics visually. For all the tested results, the mean values are within 2.00cm. This indicates that for all the tested grid sizes, the overall geometric accuracy is high. For the Smiley-West-10 model, the cell size shows a positive correlation with the average value of the reconstruction errors: a smaller grid size leads to a smaller mean value. For the other tested models, such correlations do not exist.

For all the tested results, the standard deviations of the reconstruction errors are within

Model Name	cell size	Mean	SD	2.50-5.00cm	5.00-10.00cm	bigger than 10.00cm
Smiley-West-10	0.5m	1.36cm	4.61cm	7.93%	2.99%	3.24%
Smiley-West-10	0.3m	0.83cm	2.45cm	7.73%	3.44%	1.02%
Smiley-West-10	0.1m	0.61cm	1.59cm	7.31%	2.73%	0.10%
FZK-Haus	0.5m	0.42cm	1.39cm	2.20%	3.09%	0.09%
FZK-Haus	0.3m	0.50cm	1.64cm	3.12%	3.67%	0.17%
FZK-Haus	0.1m	0.49cm	1.66cm	3.28%	3.67%	0.21%
Institute-Var-2	0.5m	1.17cm	3.39cm	3.55%	5.64%	3.16%
Institute-Var-2	0.3m	1.27cm	3.29cm	3.51%	3.96%	5.38%
Institute-Var-2	0.1m	1.19cm	2.86cm	7.20%	4.38%	4.25%

Table 5.4.: Statistics of the error distribution, using different cell size

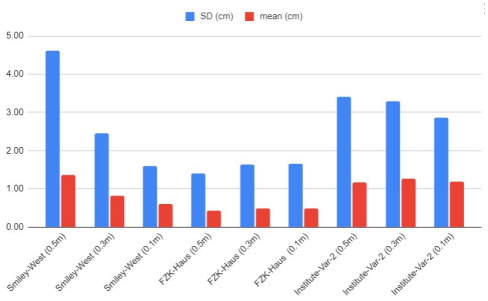

Figure 5.15.: Mean and SD of the reconstruction errors, using different cell size

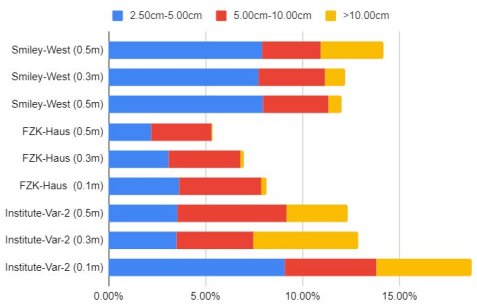

Figure 5.16.: Percentage of inaccurate points in the reconstruction result, using different cell size

5.00cm. The standard deviations are 2-4 times bigger than the corresponding mean value, indicating a spread-out distribution. 66.67% of models' SD decreases as the re-sampling

grid size gets smaller. Figure 5.16 shows the percentage of extremely inaccurate points in the reconstruction results. There is no apparent correlation between the grid size and the percentage of extreme points either. In conclusion, there are no obvious correlations between these statistics and the grid size.

For reconstruction error visualizations, figure 5.17 to figure 5.19 shows one example result: the extracted envelope using point clouds generated from different grid sizes, using the Institute-Var-2 model as input. From the error distributions, it is observed that for all the tested grid sizes, the majority parts of big surfaces, for instance, roofs and walls are reconstructed fairly well. At least 99% percent of these surfaces are indicated by dark blue, which means the deviations between the reconstructed surfaces and the original surfaces are below 0.01cm. However, using different sampling grid sizes, the reconstruction accuracy differs greatly in building parts that have a smaller scale (for instance, windows and doors), and where the geometries change drastically, such as the edge where a wall meets a roof. It is clear that with the increase in the grid size, these small-scale geometries also become more distorted from their original surfaces. It is observed that using a grid size of 0.1m results in smaller reconstruction errors on the small-scale exterior objects, for instance, windows, doors, and balconies. In addition, using a grid size of 0.1m is also beneficial for preserving the geometric details of the buildings.

Percentage of retained points during point cloud simplification

As aforementioned in chapter 3, it is worth investigating the possibility of downsizing the point cloud to speed up the reconstruction process, under the premise of not significantly damaging the quality of the results. In this section, we test the retained percentage of the input points ranging from 50% to 5%.

Table 5.5 shows the statistics of the error distributions from the test results. Figure 5.20 and figure 5.21 show these statistics visually. For all the tested results, the mean values are within 3.00cm. This indicates that after simplifications, the overall geometric accuracy is still high. The correlations between the retained percentage of points and the mean error value are not clear. The standard deviations are also relatively big compared to the mean values, especially when the retained percentage is reduced to 10% and 5% for the FZK-Haus model: the standard deviation is more than 10 times bigger than the mean value, indicating a very dispersed distribution. For the FZK-Haus model, the standard deviation increases drastically when the retained percentage decreases. However, for the other tested models, such correlation is not observed. From figure 5.21, it is clear that there is no apparent correlation between the retained percentage and the percentage of extreme points either.

The spatial distribution of the geometric errors is also examined. Figure 5.22 to figure 5.24 shows one example result. From these results, it is observed that even though the majority part of the building is accurately reconstructed, obvious distortions are observed when using a low retained percentage.

Furthermore, it is observed that simplifying point clouds leads to holes and artifacts in the reconstruction results. Figure 5.25 shows one example of this phenomenon. In conclusion, we advise against point cloud simplification when the computer power permits reconstruction. Otherwise, we advise keeping a minimum of 50% percent of the original points.

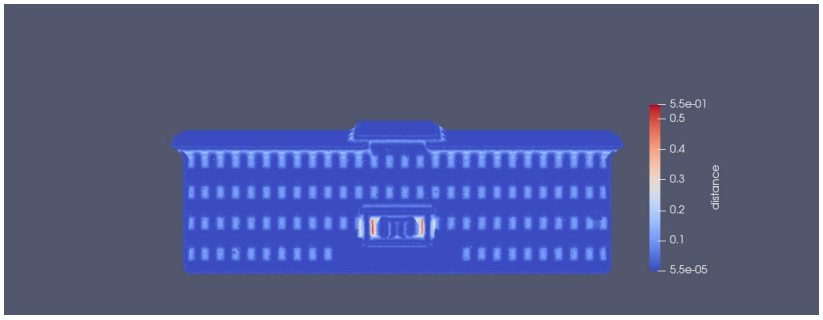

(a) grid size:0.5m

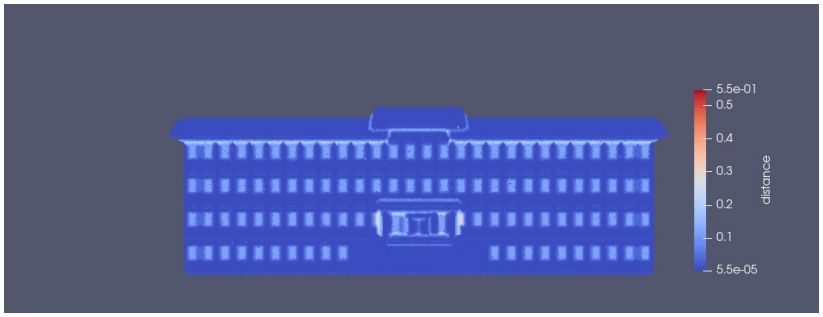

(b) grid size:0.3m

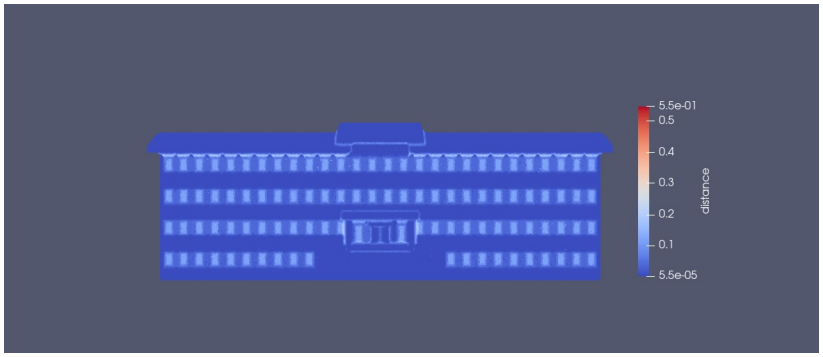

(c) grid size:0.1m

Figure 5.17.: Reconstruction error distribution, Institute-Var-2 model, front view

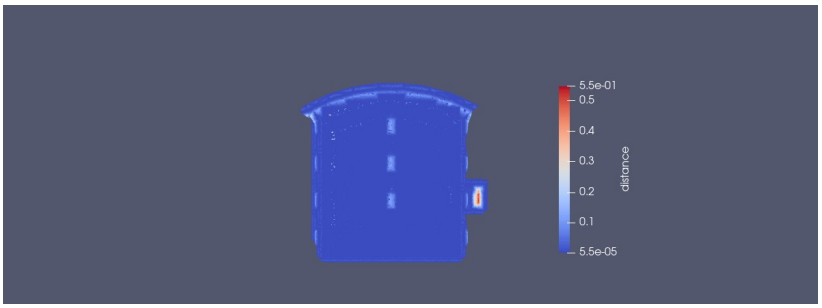

(a) grid size:0.5m

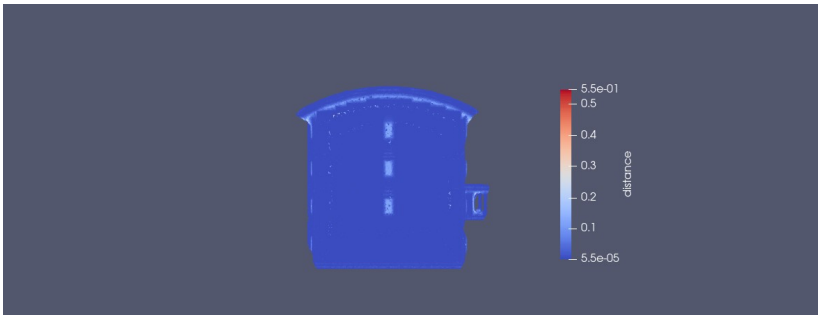

(b) grid size:0.3m

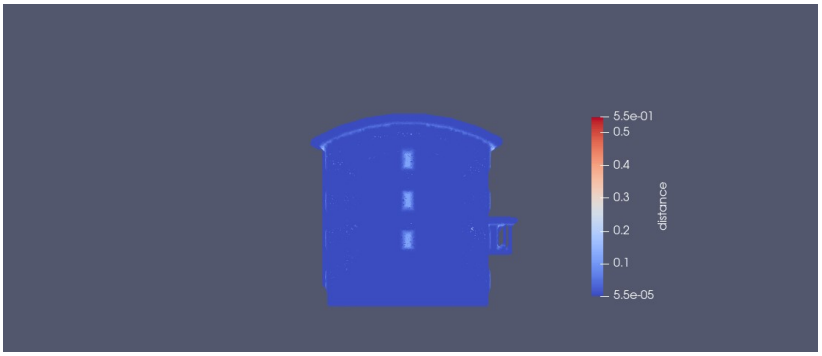

(c) grid size:0.1m

Figure 5.18.: Reconstruction error distribution, Institute-Var-2 model, left view

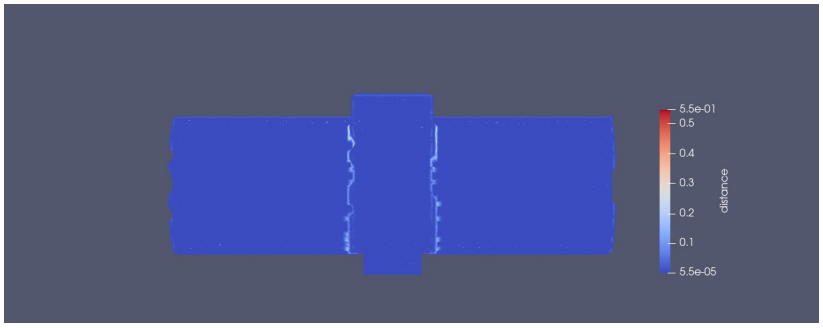

(a) grid size:0.5m

(b) grid size:0.3m

(c) grid size:0.1m

Figure 5.19.: Reconstruction error distribution, Institute-Var-2 model, left view

model name	mean (cm)	SD (cm)	2.50cm-5.00cm	5.00cm-10.00cm	bigger than 10.00cm
Smiley-West (50%)	0.58	1.56	6.91%	2.56%	0.10%
Smiley-West (10%)	0.79	1.89	5.61%	2.68%	0.71%
Smiley-West (5%)	0.69	1.78	3.96%	1.67%	0.72%
FZK-Haus (50%)	0.46	1.61	2.97%	3.45%	0.18%
FZK-Haus (10%)	1.95	13.04	3.17%	2.63%	2.08%
FZK-Haus (5%)	2.58	15.89	2.70%	2.16%	2.74%
Institute-Var-2 (50%)	1.03	2.71	4.33%	4.13%	3.93%
Institute-Var-2 (10%)	0.99	2.66	5.13%	3.43%	1.11%
Institute-Var-2 (5%)	1.00	2.76	4.64%	2.40%	0.97%

Table 5.5.: Statistics of the error distribution, using different retained percentages of points

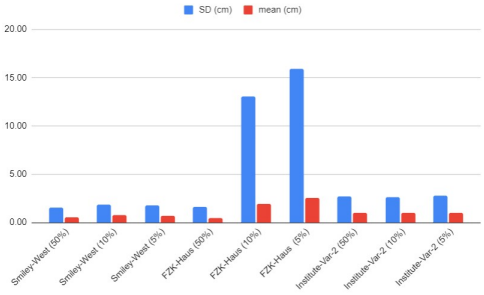

Figure 5.20.: Mean and SD of the reconstruction errors, using different retained percentages of points

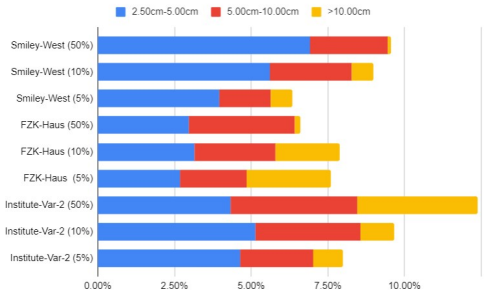

Figure 5.21.: Percentage of inaccurate points in the reconstruction result, using different retained percentages of points

Alpha value of the alpha shape reconstruction algorithm

The alpha value is the main control parameter for the building envelope reconstruction process. Since the alpha value should be slightly bigger than the grid size, after deciding the grid size to be 0.1m, the alpha value's testing range is set to be from 0.2m to 0.5m.

Table 5.6 shows the statistics of the testing results, and figure 5.26 and figure 5.27 demonstrate these calculated statistics visually. It is observed that for all the tested alpha values, the average reconstruction error is within 2.00cm, indicating high overall accuracy. For all the tested models, it is clear that there is a positive correlation between the alpha value and the reconstruction errors. The standard deviations are all much bigger than the average value, indicating rich variability of the reconstruction errors. All the standard deviations are within 4.00cm. For every tested IFC model, the standard deviation decreases with the decrease of the alpha value. From figure 5.27, it is also clear that the total percentage of the extreme points has a positive correlation with the alpha value.

As for reconstruction error visualizations, figure 5.28 to figure 5.30 show one example result. From the error distributions, it is observed that for all the alpha values, the major-

(a) Retained percentage: 50%

(b) Retained percentage: 10%

(c) [Retained percentage: 5%

Figure 5.22.: Reconstruction error distribution using different retained percentages of points, FZK-Haus model, front view

(a) Retained percentage: 50%

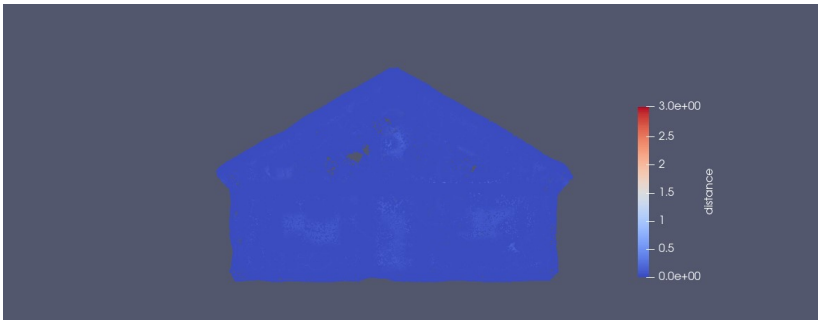

(b) Retained percentage: 10%

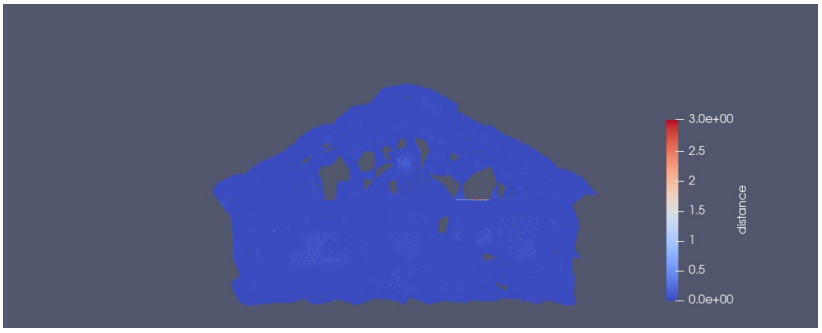

(c) [Retained percentage: 5%

Figure 5.23.: Reconstruction error distribution using different retained percentages of points, FZK-Haus model, left view

(a) Retained percentage: 50%

(b) Retained percentage: 10%

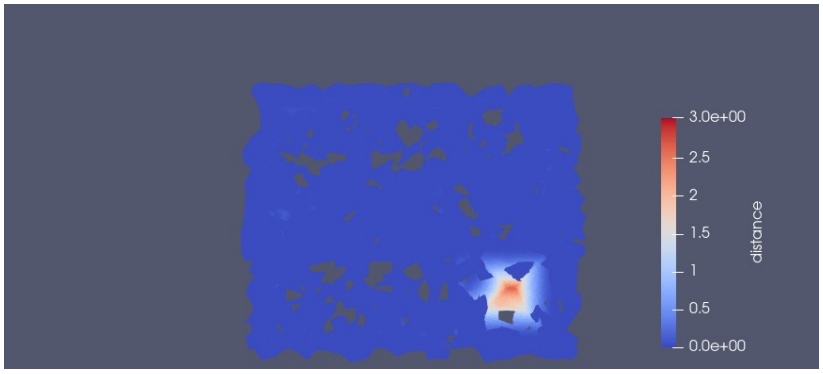

(c) [Retained percentage: 5%

Figure 5.24.: Reconstruction error distribution using different retained percentages of points, FZK-Haus model, top view

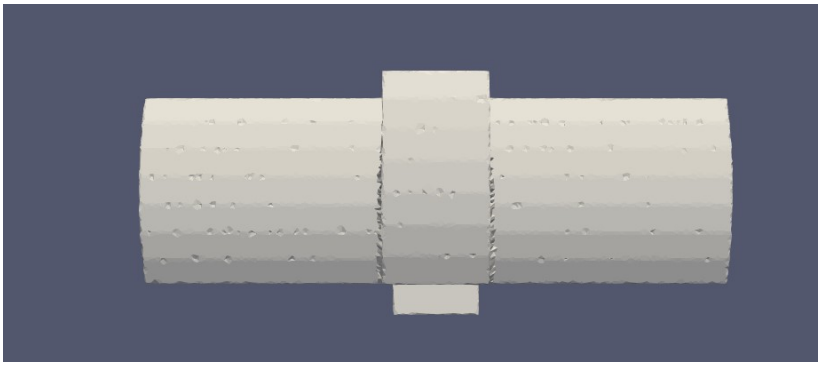

(a) Institute-Var-2 model (50%)

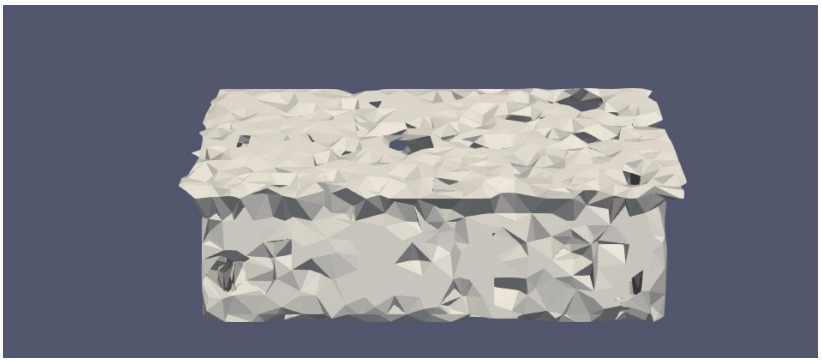

(b) FZK-Haus model (10%)

Figure 5.25.: Examples of holes and artifacts caused by point cloud simplification

Model Name	alpha value	Mean	SD	2.50-5.00cm	5.00-10.00cm	bigger than 10.00cm
Smiley-West-10	0.2m	0.61cm	1.69cm	7.26%	2.73%	0.12%
Smiley-West-10	0.35m	0.87cm	2.47cm	8.13%	3.71%	0.95%
Smiley-West-10	0.5m	1.45cm	4.39cm	7.91%	4.40%	3.34%
FZK-Haus	0.2m	0.49cm	1.66cm	3.30%	3.64%	0.21%
FZK-Haus	0.35m	0.57cm	1.80cm	3.68%	4.51%	0.27%
FZK-Haus	0.5m	0.69cm	2.03cm	3.99%	5.28%	0.64%
Institute-Var-2	0.2m	1.19cm	2.86cm	7.19%	4.44%	4.22%
Institute-Var-2	0.35m	1.40cm	3.28cm	8.57%	4.92%	5.18%
Institute-Var-2	0.5m	1.70cm	4.09cm	8.27%	4.84%	6.74%

Table 5.6.: Statistics of the error distribution, using different alpha values

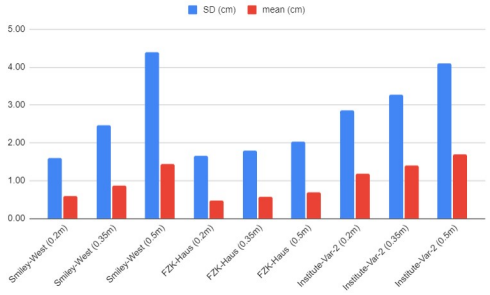

Figure 5.26.: Mean and SD of the reconstruction errors, using different alpha values

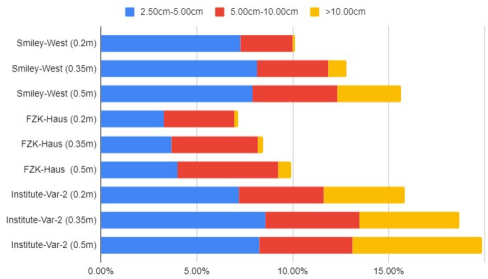

Figure 5.27.: Percentage of inaccurate points in the reconstruction result, using different alpha values

ity parts of the big surfaces are reconstructed very accurately. Almost all of these surfaces are indicated by dark blue, which means the deviations between the reconstructed surfaces and the original surfaces are below 0.01cm. However, using different alpha values, the reconstruction accuracy differs greatly in building parts that have smaller-scale details, for instance, windows and doors. A smaller alpha value leads to smaller errors in these parts.

In conclusion, for the grid size of 0.1m, it is observed that using an alpha size of 0.2m results in the most accurate reconstruction results. This also to a degree proves that it is correct to set the alpha value to only slightly bigger than the grid size.

Percentage of retained edges during mesh simplification

As aforementioned, after reconstructing building envelopes, it is essential to move unnecessary edges and vertices from the reconstructed building mesh. In this process, we should decide on the appropriate percentage of retained edges. An appropriate value should downsize the building mesh while not significantly changing the reconstructed geometries. We tested the percentage of retained edges ranging from 1% to 0.5%, and analyze the results similarly to the aforementioned parameters.

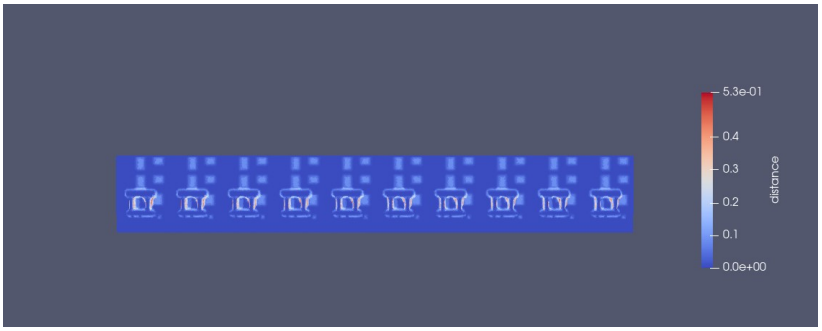

(a) alpha value:0.5m

(b) alpha value:0.35m

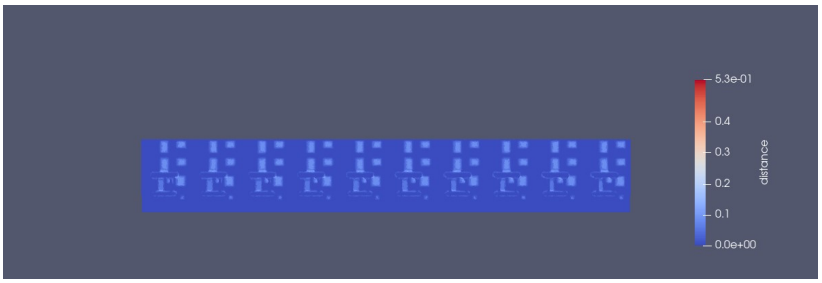

(c) alpha value:0.2m

Figure 5.28.: Reconstruction error distribution, Smiley-West model, front view

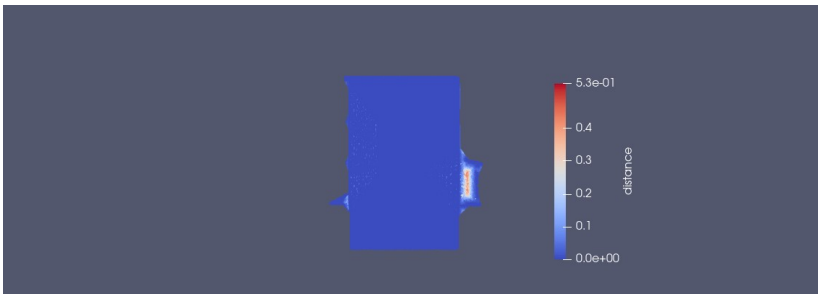

(a) alpha value:0.5m

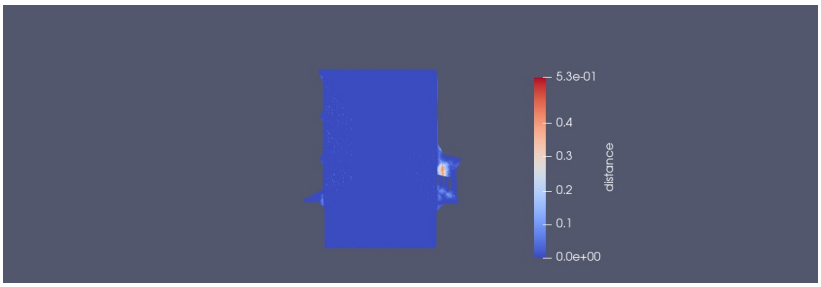

(b) alpha value:0.35m

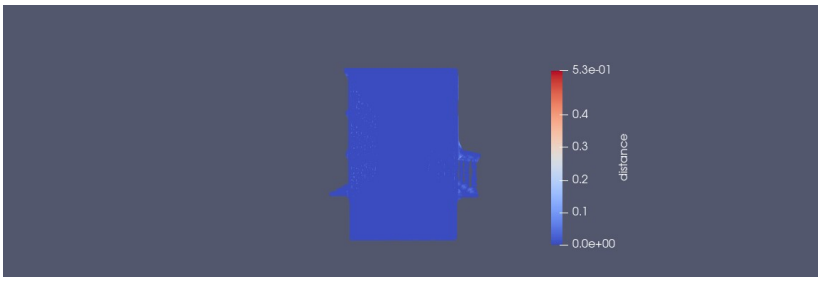

(c) alpha value:0.2m

Figure 5.29.: Reconstruction error distribution, Smiley-West model, left view

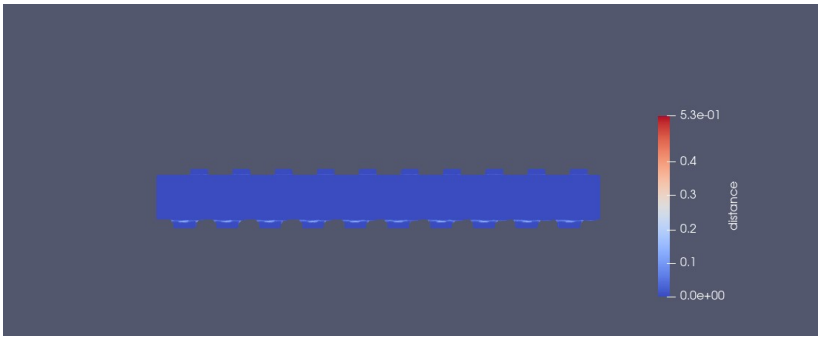

(a) alpha value:0.5m

(b) alpha value:0.35m

(c) alpha value:0.2m

Figure 5.30.: Reconstruction error distribution, Smiley-West model, left view

Table 5.7 and figure 5.31 to figure 5.32 shows calculated statistics of the result's error distribution. It is observed that for every test, the mean error value is within 1.20cm and the standard deviation value is within 1.70cm, indicating an overall small value but spread-out distribution. The percentage of extreme points that have an error of bigger than 10.00cm is all within 5% for all the tested building models. These all indicate that the tested results have good overall geometric accuracy. For every model, the mean value, the SD value, and the percentage of extreme points do not change significantly with the changes in the percentage of retained edges.

To further examine the effects of the retained percentage of edges on the geometric ac-

Model Name	Retained percentage	Mean	SD	2.50-5.00cm	5.00-10.00cm	bigger than 10.00cm
Smiley-West-10	10%	0.61cm	1.60cm	7.28%	2.74%	0.11%
Smiley-West-10	1%	0.60cm	1.60cm	7.18%	2.61%	0.13%
Smiley-West-10	0.5%	0.69cm	1.96cm	7.38%	2.07%	1.04%
FZK-Haus	10%	0.49cm	1.66cm	3.28%	3.68%	0.21%
FZK-Haus	1%	0.48m	1.66cm	3.21%	3.64%	0.21%
FZK-Haus	0.5%	0.50cm	1.86cm	3.31%	3.35%	0.49%
Institute-Var-2	10%	1.19cm	2.86cm	7.18%	4.41%	4.23%
Institute-Var-2	1%	1.14cm	2.80cm	7.21%	4.25%	4.14%
Institute-Var-2	0.5%	1.13cm	2.76cm	8.19%	4.34%	3.88%

Table 5.7.: Statistics of the error distribution, using different retained edge percentages

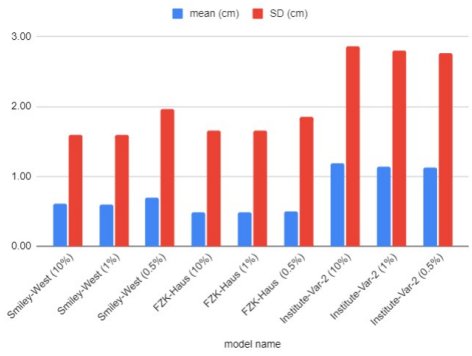

Figure 5.31.: Mean and SD of the reconstruction errors, using different retained edge percentages

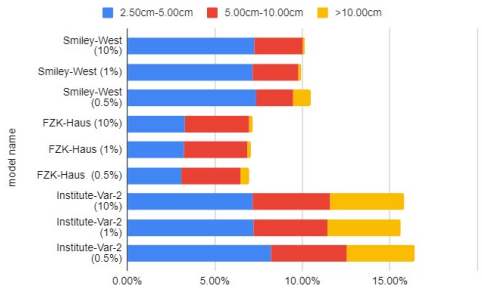

Figure 5.32.: Percentage of inaccurate points in the reconstruction result, using different retained edge percentages

curacies, the spatial distributions of the geometric errors are visualized. Figure 5.33 to figure 5.35 show one example. From the spatial distributions, it is observed that for walls and roofs, mesh simplification does not affect their geometric accuracies. However, using a smaller retained percentage of edges leads to slightly bigger errors on windows and doors.

5.2.3. Limitations

There are four main limitations to the current method. Firstly, it is not able to extract building envelopes from big IFC models. Secondly, the extracted building envelopes have several flaws. In addition, the quality of the extracted building envelope depends heavily on the fine-tuning of a large number of parameters. Lastly, since the geometric information is reconstructed and not mapped, geometric errors are inevitable. In this section, these limitations are explained in detail.

Firstly, the reconstruction method failed to extract the building envelope from big and complex IFC models. Figure 5.36 shows examples of models that the developed approach can not extract building envelopes. This may limit the real-world use of this tool since many BIM models in the AEC industry are relatively complex and contain thousands of building objects.

Secondly, extracted building envelopes using this method have several flaws. Firstly, the developed approach only extracts the geometries. The extracted geometries are stored in a triangle mesh format and are not segmented into meaningful building elements, for instance, walls or roofs. Then consequentially, the semantic information of the building elements, for example, whether a surface belongs to a wall or a roof, is not extracted. In addition, the building topology indicates the relationships between different building components, are not preserved.

Another issue present is that the accuracy of the extracted building envelopes depends heavily on the appropriate settings of a set of parameters, for instance, the cell size of the sampling grid and the alpha value. Fine-tuning these parameters can be time-consuming, and obtaining the optimal results can be challenging.

Lastly, even though most parts of the building envelopes have high reconstruction accuracy, it still introduces various types of geometry distortion. This is the main limitation the developed approach has compared to direct geometry mapping methods.

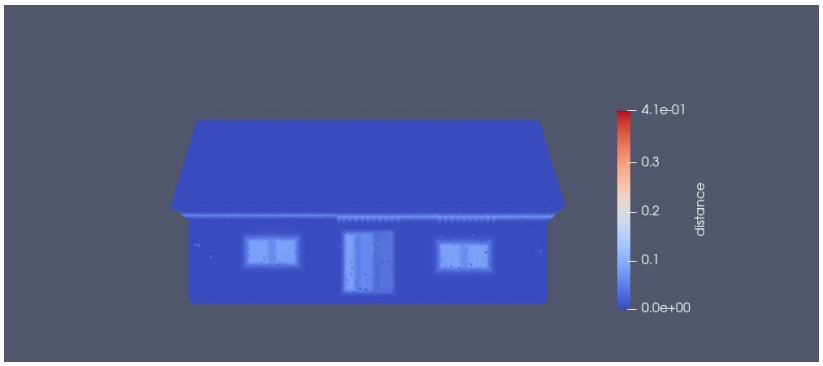

(a) Retained percentage of edges: 10%

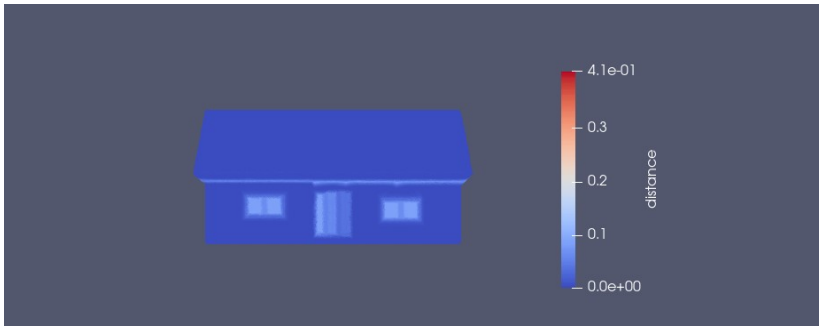

(b) Retained percentage of edges: 1%

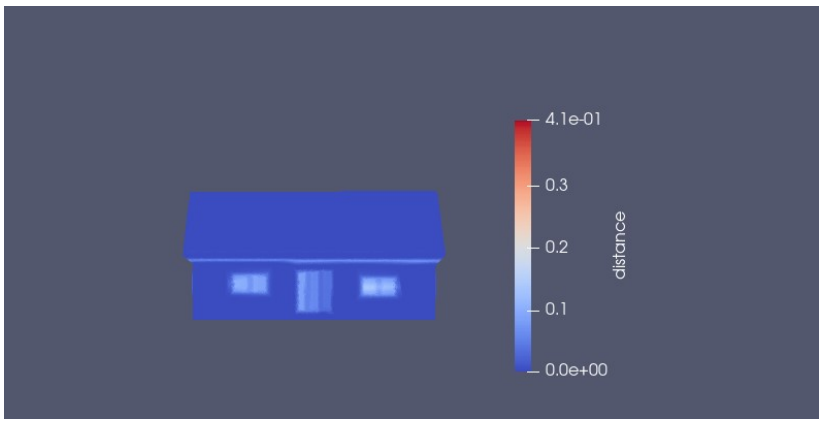

(c) [Retained percentage of edges: 0.5%

Figure 5.33.: Reconstruction error distribution using different retained percentages of edges, FZK-Haus model, front view

(a) Retained percentage of edges: 10%

(b) Retained percentage of edges: 1%

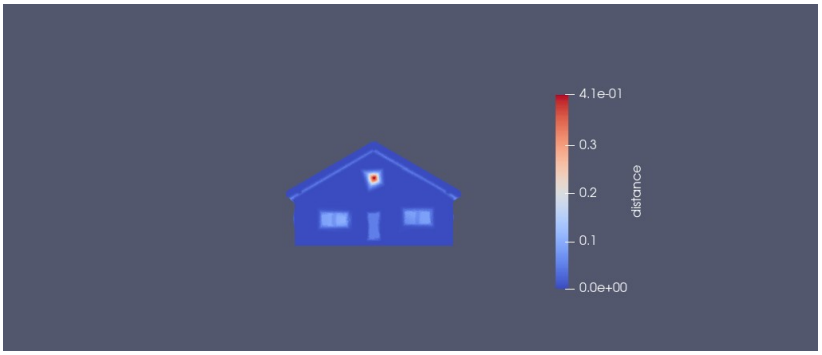

(c) [Retained percentage of edges: 0.5%

Figure 5.34.: Reconstruction error distribution using different retained percentages of edges, FZK-Haus model, left view

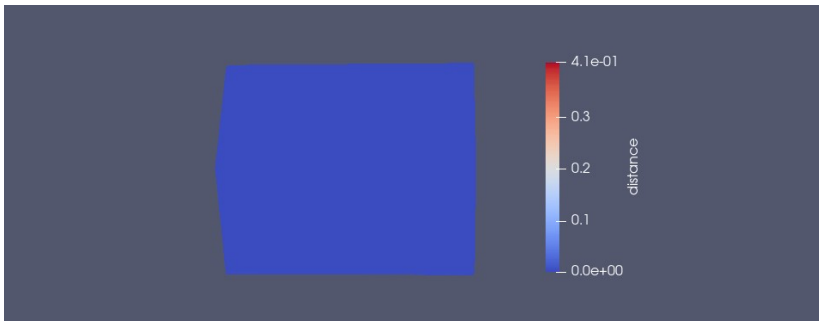

(a) Retained percentage of edges: 10%

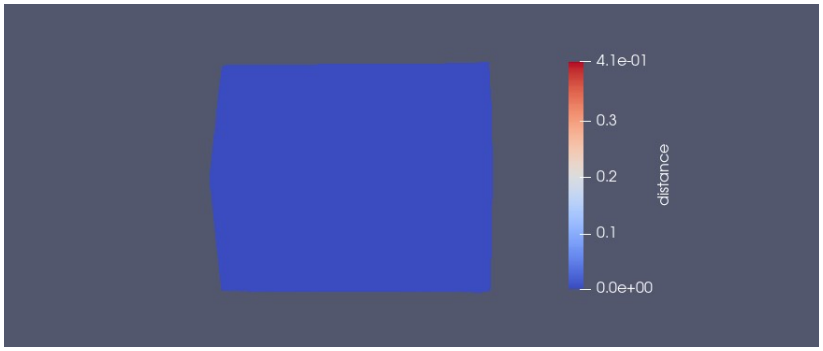

(b) Retained percentage of edges: 1%

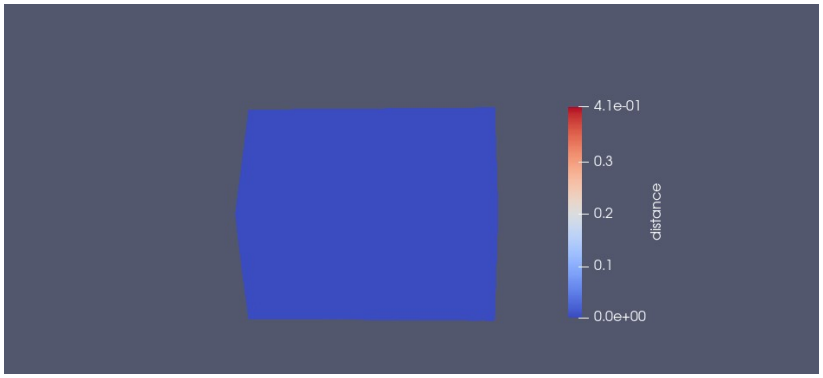

(c) [Retained percentage of edges: 0.5%

Figure 5.35.: Reconstruction error distribution using different retained percentages of edges, FZK-Haus model, left view

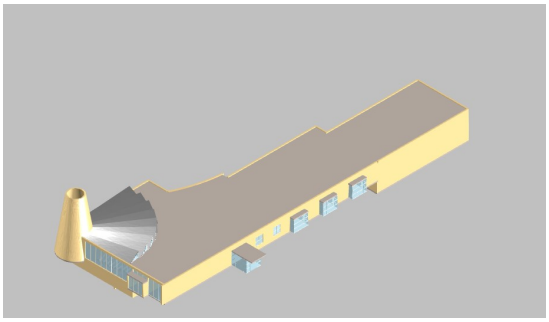

(a) CUVO model

(b) Witte de Withstraat model

Figure 5.36.: Examples of big and complex IFC models

6. Conclusions and future work

6.1. Conclusions

In this study, we developed a reconstruction method that can extract accurate building envelopes from BIM models. The developed approach is based on the aforementioned main research question:

- How can we extract building envelopes from different types of BIM both accurately and efficiently?

To effectively answer the main research questions, the following sub-questions need to be answered.

- How to extract a point cloud from a BIM model that is suitable for building envelope reconstruction?

A point cloud suitable for building envelope reconstruction needs to meet two criteria: firstly it should preserve the building exterior's geometric details. secondly, it should not be too big for the reconstruction algorithm. To meet these two criteria, the following design decisions are made during the point cloud extraction process. Firstly, to reduce the point cloud's size, irrelevant IFC data are filtered. Secondly, for all the remaining building objects' surfaces, point clouds are extracted by grid sampling. To what degree the building exterior's geometric details are preserved is controlled by the grid size parameter. It is advised that the grid size should be no bigger than the scale of the smallest building exterior objects, therefore usually 0.5m to 0.1m. However, the exact grid size should be decided after examining the input IFC model's characteristics. A building with simpler exteriors can choose a bigger sampling grid size, and a building with more complex exteriors should choose a smaller sampling grid size.

This approach can successfully extract the building point cloud with well-preserved building geometries. In addition, within every building surface, the point cloud is evenly distributed.

- From the extracted point cloud, how can we develop a building envelope extraction method, that can reconstruct the building envelope both accurately and efficiently?

To develop an appropriate building envelope extraction method, common geometry reconstruction methods, for instance, voxelization and Possion surface reconstruction are thoroughly surveyed. The 3D alpha shape algorithm is chosen because it is the only algorithm that can extract the point cloud's outer boundary with great detail.

During the reconstruction process, to guarantee the accuracy of the reconstructed result,

we test and decided on the appropriate alpha value. The alpha value range should be no smaller than the sampling grid size, and no bigger than the size of the smallest building objects. It is also worth noting that, it is beneficial to set the alpha value not too bigger than the grid size, if the computational power permits, to make the maximum use of the point set's geometric information.

- How to measure the quality of the extracted building envelope?

After the literature study, it is concluded that the common quality indicators for reconstructed geometries are: geometric accuracy, topological accuracy, simplicity, and processing speeds. Since our developed methodologies do not preserve the topology information, the qualities of the extracted building envelopes are measured by their geometric accuracy, simplicity, and time efficiency.

To measure the geometric accuracy of the extracted building envelopes, we re-sampled the reconstructed building mesh to a point set and convert the original IFC model to a mesh. For each point in the point set, we measure the squared distance between itself and its closet point in the original building mesh. These distances are viewed as reconstruction errors. After obtaining the reconstruction error distribution, we calculate statistical indicators, for instance, the average value and standard deviations of the errors, thus gaining insight into the overall geometric accuracy. In addition, the error distribution is visualized spatially to check where in the buildings big reconstruction errors occur. The simplicity of the extracted building envelopes is measured by comparing their number of vertices and their number of edges to the original IFC model. And the time efficiency of the extraction process is measured by the processing time.

The overall geometric accuracy of the extracted building envelopes is very high. For all the tested models, the mean reconstruction errors are within 2cm. Walls and roofs are reconstructed with errors smaller than 0.001cm, but windows and doors usually have reconstruction errors of approximately 0.1m to 0.3m. The low geometry accuracy of windows and doors is caused by the fact that they are very close to the wall surfaces, and it is difficult for the 3D alpha-shape algorithm to capture such small surface differences. In addition, some other exterior small-scale objects also deviate about 0.1m to 0.3m from the original surfaces. This is also caused by the fact that the alpha shape can not capture such small-scale details.

- What are the factors that influence the reconstructed building envelope's quality?

The quality of the extracted building envelope is affected by two aspects: the parameter settings of the developed approach, and the characteristics of the input IFC models.

The parameter settings affect the extracted building envelope's quality greatly. At the point cloud extraction step, the size of the sampling grid determines whether the building geometries are well preserved. A too-big grid size leads to missing geometric details in the extracted point cloud, but a too-small grid size results in a too-big point cloud and causes difficulties in the reconstruction phase. During the point cloud simplification phase, it is also important to control the percentage of retained points. It is worth noting that we generally advise against taking the point cloud simplification step because it damages the extracted building envelope greatly. During the building envelope reconstruction process, the alpha value is also of vital importance. A too-big alpha value causes distortions or even complete neglect of small-scale exterior objects. A too-small alpha value causes small holes and cavities on the reconstructed surfaces. The final parameter is the percentage of retained edges in the building envelope mesh simplification process. A too-big retained percentage may lead

to a still complex building envelope, whereas a too-small retained percentage may lead to a simple but distorted result. Therefore, it is of vital importance to monitor and fine-tune the aforementioned parameters to obtain a high-quality result.

Secondly, it is affected by the characteristics of the input IFC models. Buildings with simple structures are easier to have accurate reconstruction results whereas complex buildings may have problems with their irregular parts, for instance, exterior stairs or antennas.

In conclusion, in this study, the building envelope can be extracted with high geometric accuracy and efficiently for various types of small buildings, but still with limitations. It can not process big IFC models. In addition, the building's topological and semantic information is not preserved. The quality of the extracted building envelope depends heavily on parameter settings. Lastly, the reconstruction process always brings errors compared to the direct mapping methods.

6.2. Future works

Based on the limitations present on our results, these future directions may be worth exploring:

- **Improving the processing capacity**: It will be beneficial to improve the capacity of the building envelope extraction tool. Currently, our tool works for small or medium IFC models. But it does not have the capacity to handle large IFC models and failed to produce results within a reasonable time frame. In the future, research can be made to make reconstructions for large models possible.
- **Geometry segmentation**: In this study, we only extract the geometry of the building envelope, and it is stored as triangle meshes in OBJ format. Even though the extracted geometries are of high accuracy, they can not be used directly in many use cases. Therefore, it will be highly beneficial to segment the triangle mesh into meaningful building parts, for instance, walls, roofs, and windows.
- **Semantic information reconstruction**: Throughout our processing pipeline, the semantics of the building object is lost. In the future, it will be beneficial to preserve the semantics of the building surfaces, possibly by retrieving the semantic information by evaluating the relative positions of the building elements after the aforementioned geometry segmentation process.
- **topological information reconstruction**: Throughout our processing pipeline, the building topology is lost. Further research can be done on reconstructing the building's topological information, for instance, how building elements are connected to each other.
- **Converting building envelope to CityGML format**: In this study, we only extract the geometry of the building envelope, and it is stored as triangle meshes in OBJ format. Further research can be done on converting the obtained building envelope from OBJ format to CityGML format, making the results more useful for users in the GIS industry.

A. Reproducibility self-assessment

A.1. Marks for each of the criteria

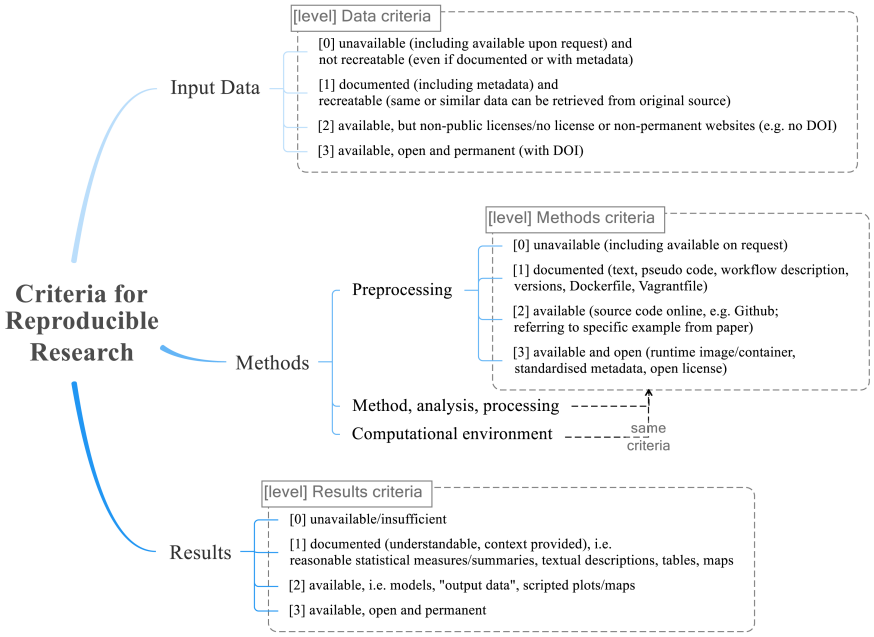

Figure A.1.: Reproducibility criteria to be assessed.

Criteria	Score	Reflections
preprocessing	3	Source code openly available on GitHub
methods	3	source code openly available on GitHub
computational environment	3	source code openly available on GitHub
computational environment	2	Models, ”output data”, scripted plots/data are available

Table A.1.: Re-productivity assessment

B. Used Datasets

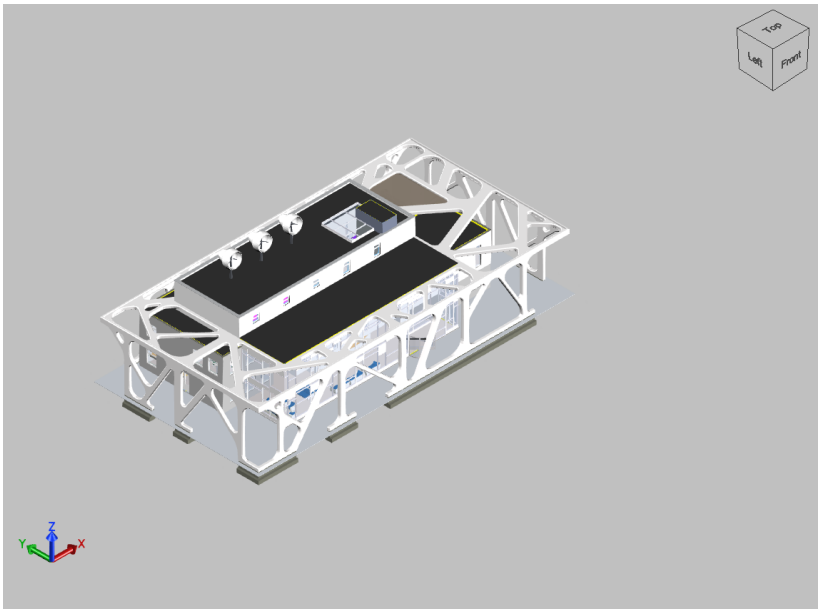

Figure B.1.: BIMcollab ARC model

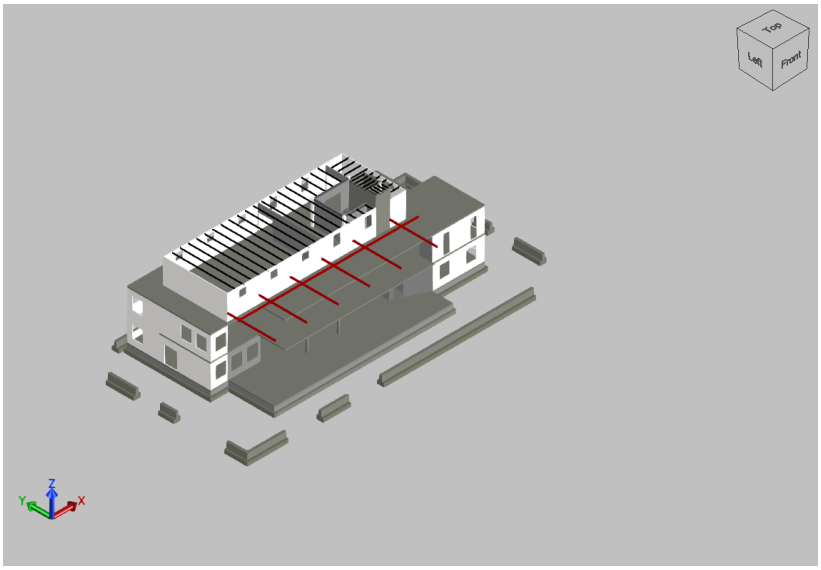

Figure B.2.: BIMcollab STR model

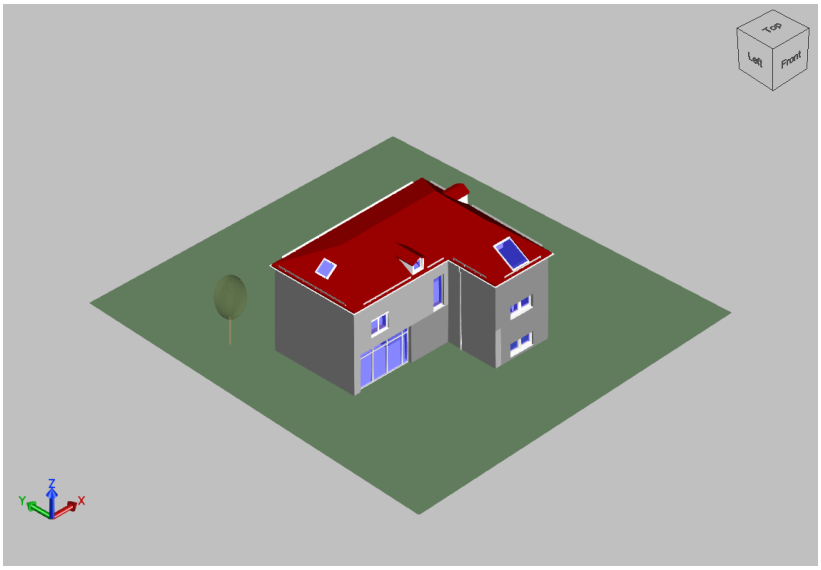

Figure B.3.: Mauer BmB model

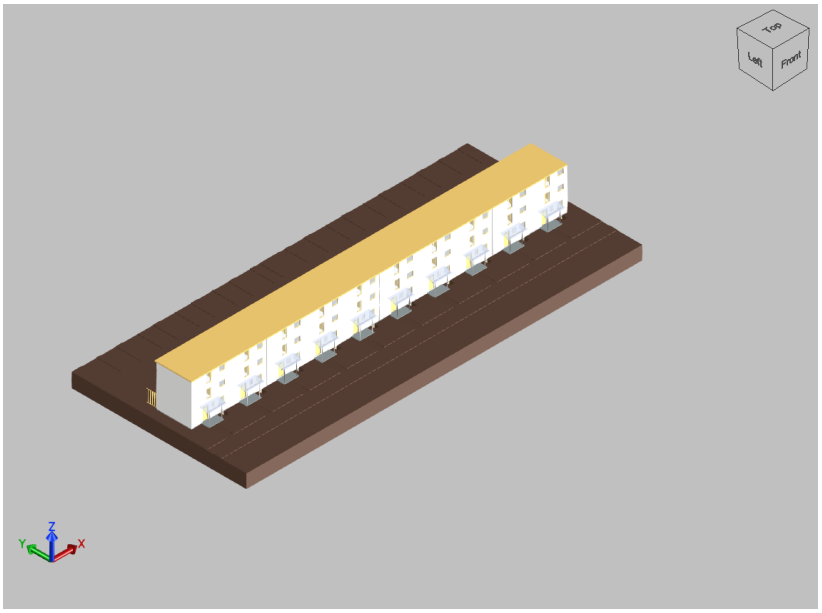

Figure B.4.: Smiley West model

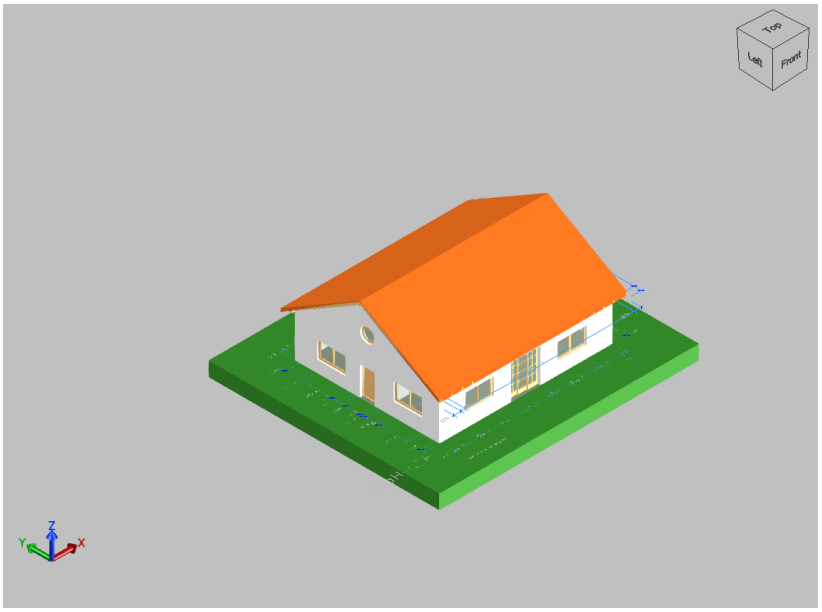

Figure B.5.: FZK-Haus model

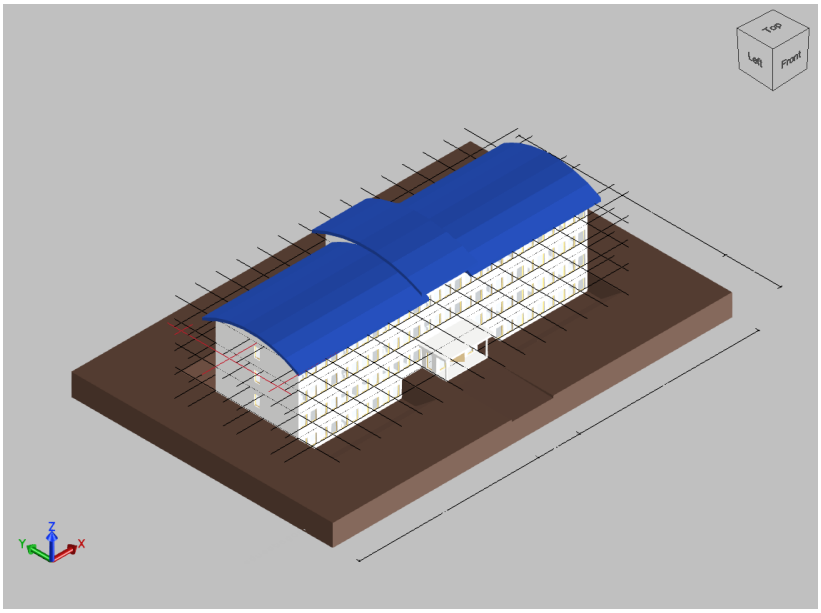

Figure B.6.: Institute-Var-2 model

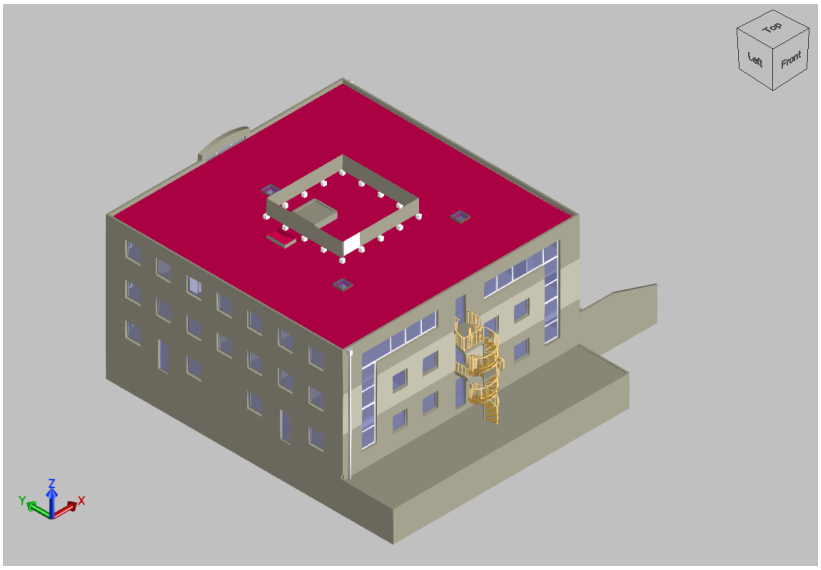

Figure B.7.: BUREAUX model

C. Results

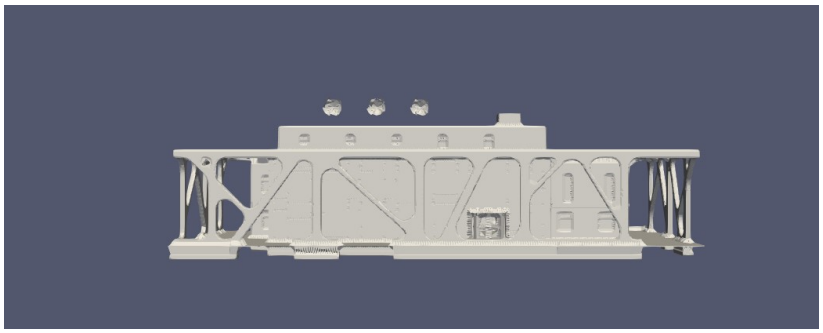

(a) front view

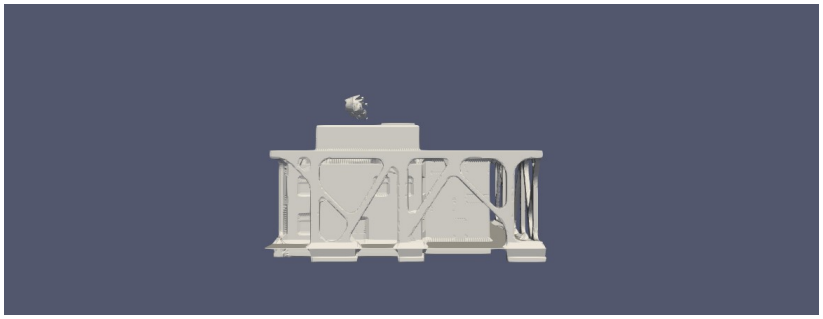

(b) Left view

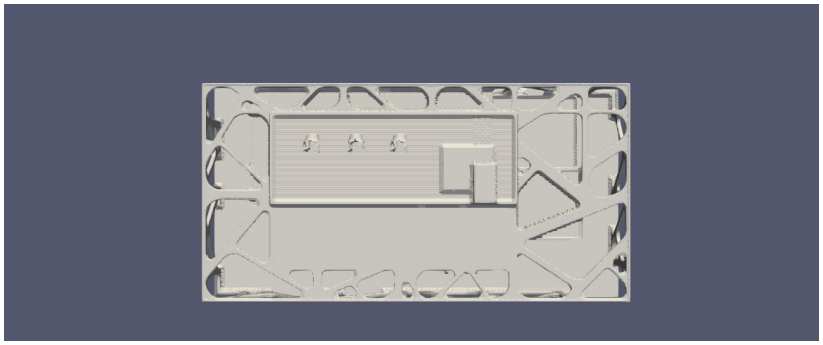

(c) Top view

Figure C.1.: Extracted building envelope of the BIMcollab_ARC model

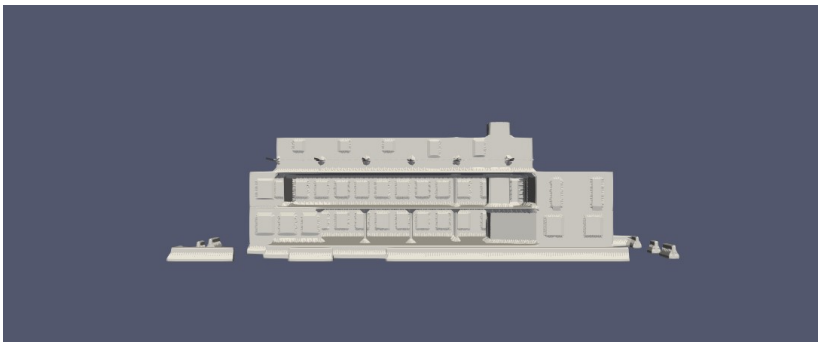

(a) front view

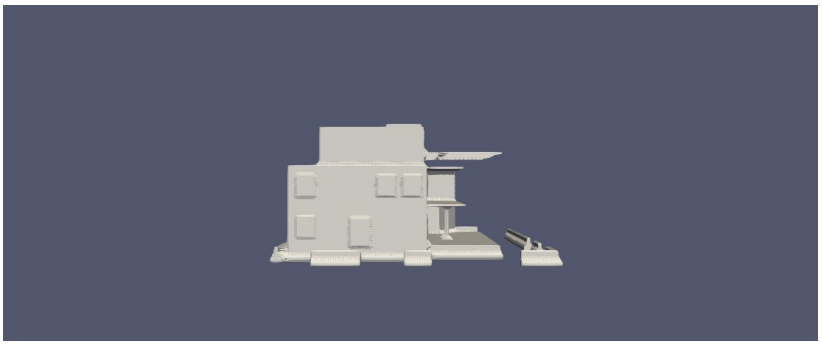

(b) Left view

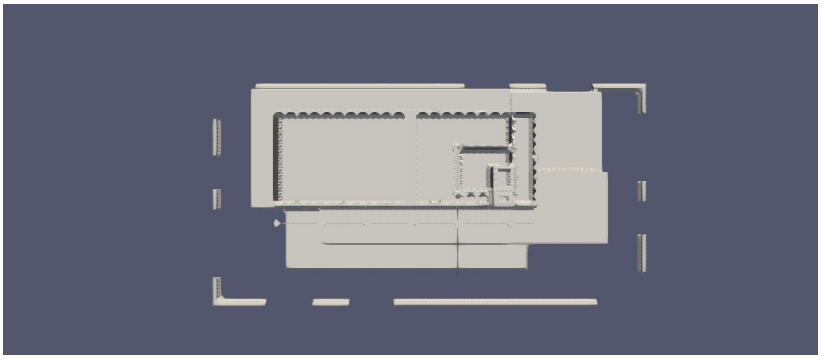

(c) Top view

Figure C.2.: Extracted building envelope of the BIMcollab STR model

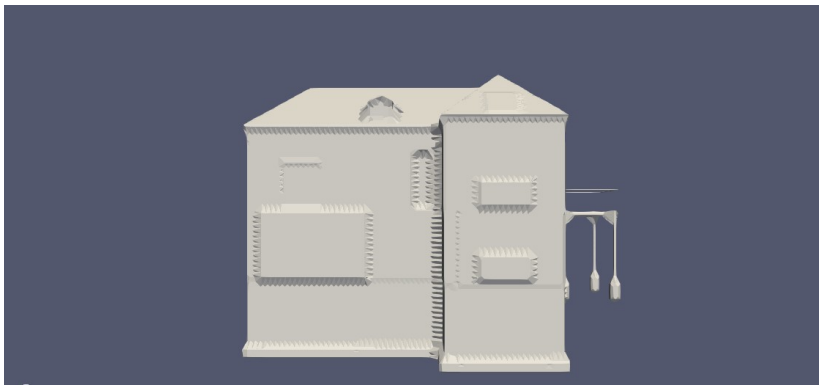

(a) front view

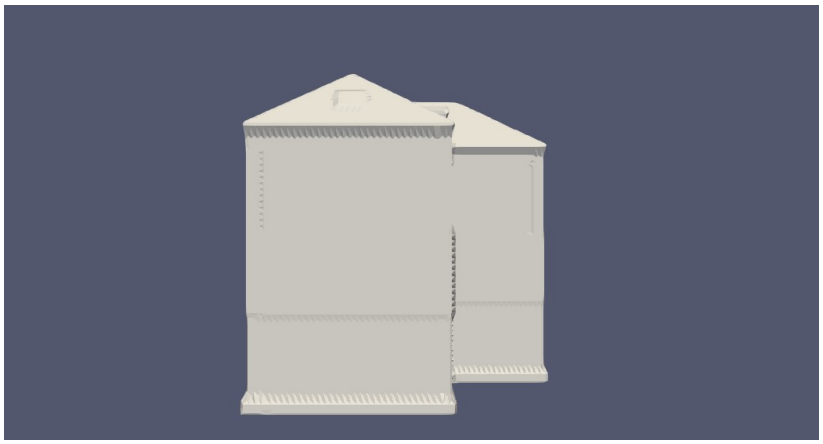

(b) Left view

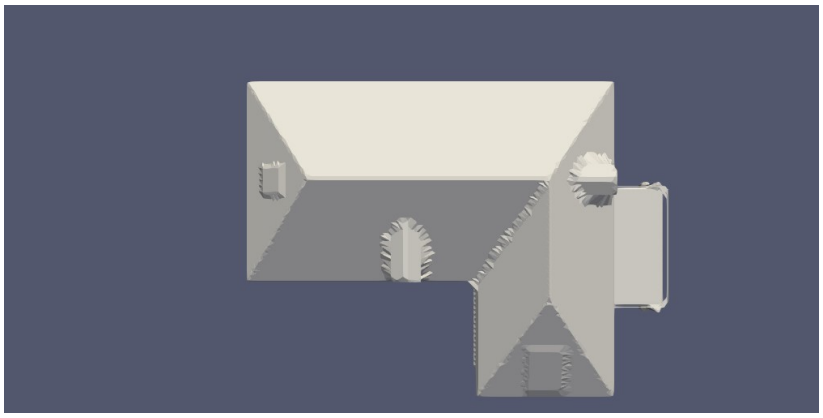

(c) Top view

Figure C.3.: Extracted building envelope of the Mauer BmB model

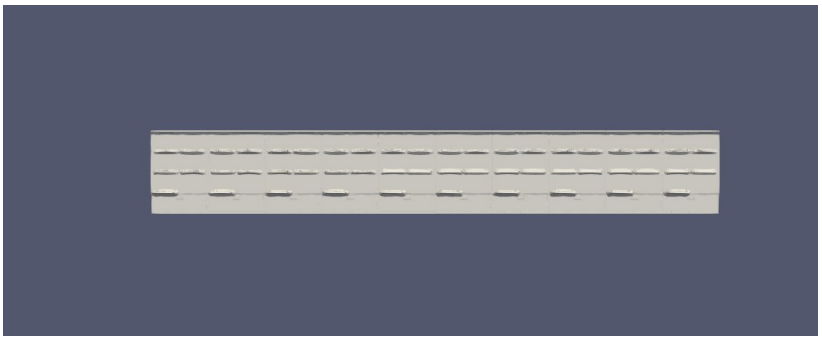

(a) front view

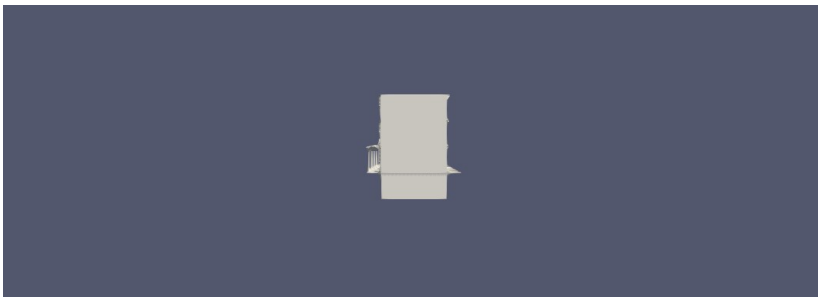

(b) Left view

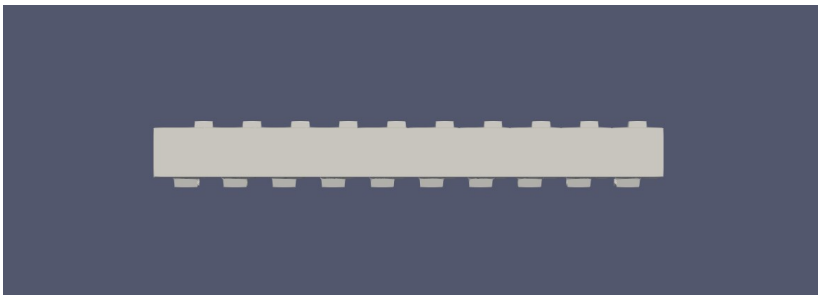

(c) Top view

Figure C.4.: Extracted building envelope of the Smiley-West model

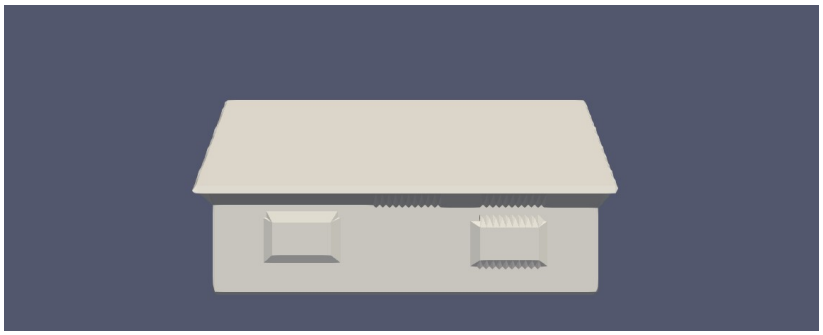

(a) front view

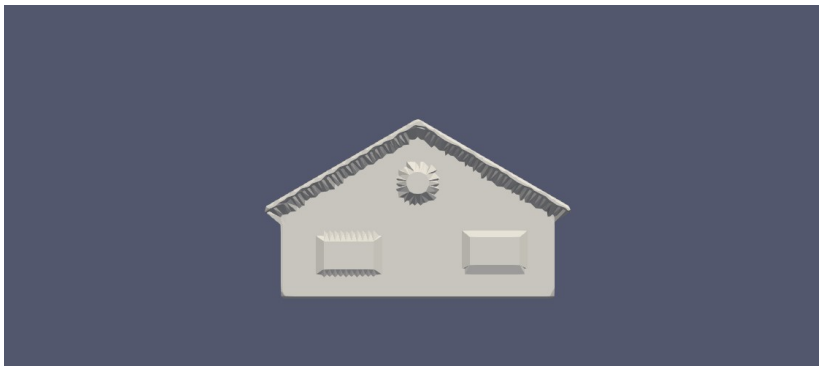

(b) Left view

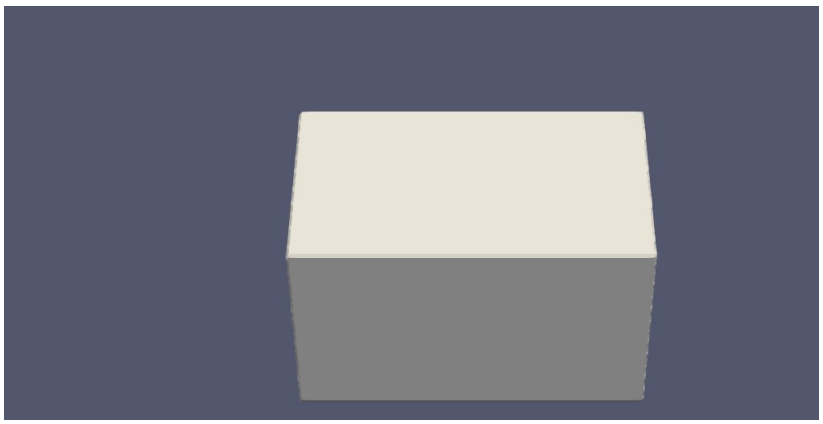

(c) Top view

Figure C.5.: Extracted building envelope of the FZK haus model

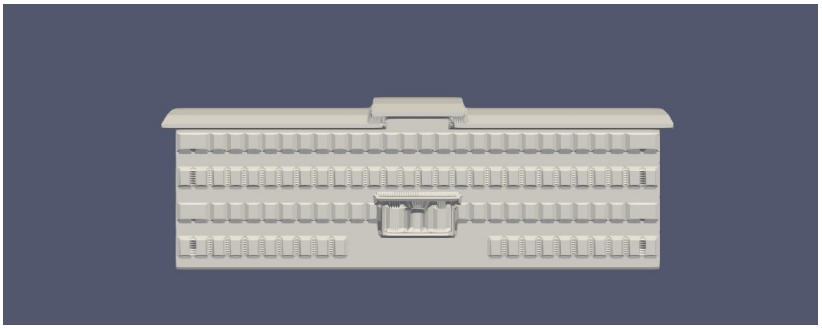

(a) front view

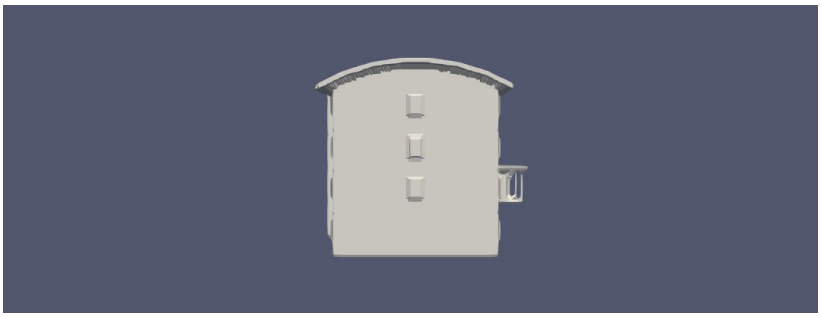

(b) Left view

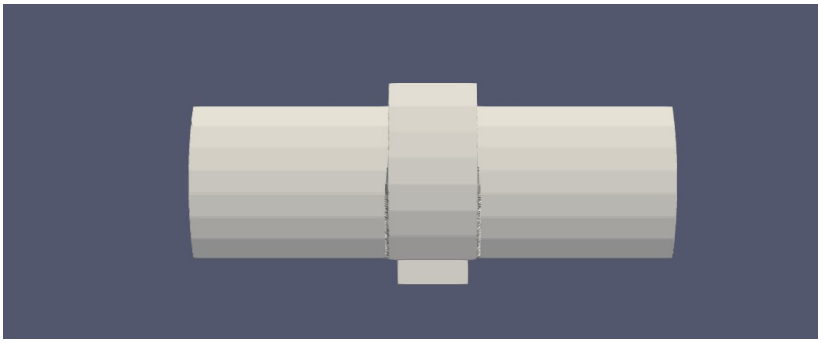

(c) Top view

Figure C.6.: Extracted building envelope of the Institute-Var-2 model

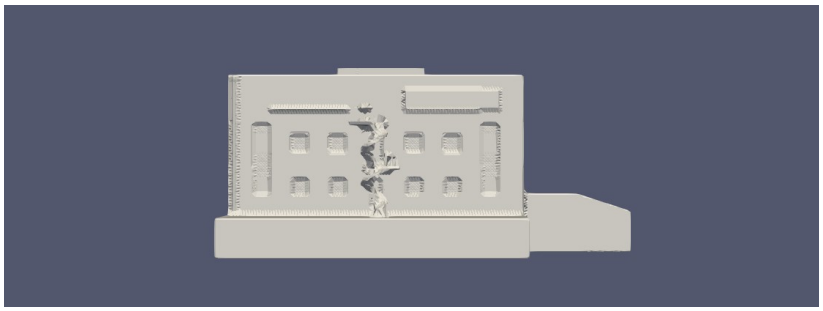

(a) front view

(b) Left view

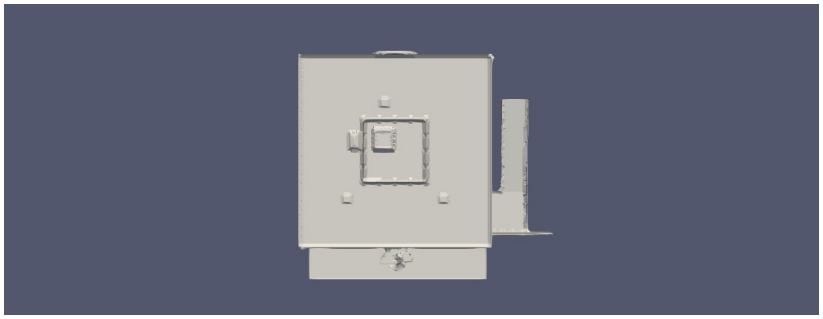

(c) Top view

Figure C.7.: Extracted building envelope of the Institute-Var-2 model

D. Reconstruction errors

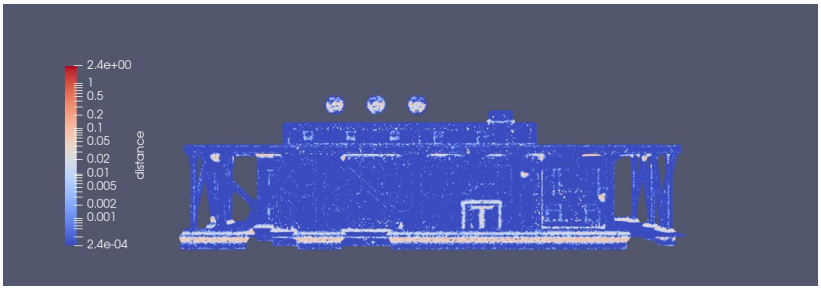

(a) front view

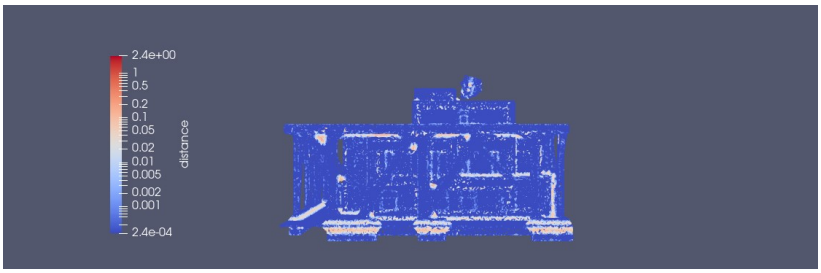

(b) Left view

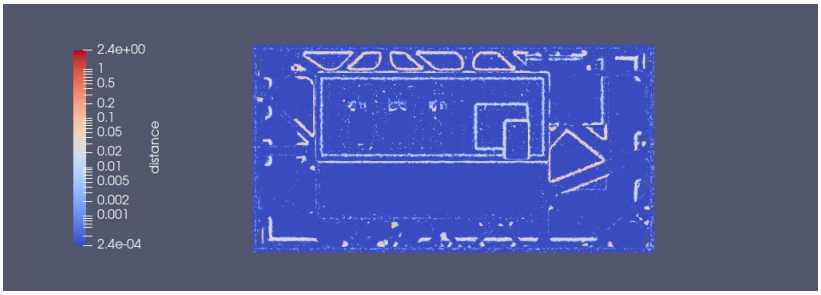

(c) Top view

Figure D.1.: Reconstruction errors of the BIMcollab ARC model

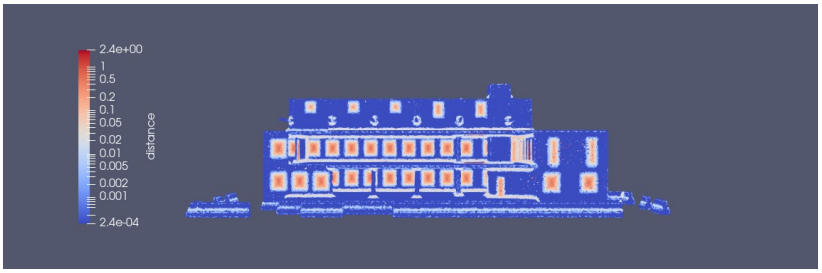

(a) front view

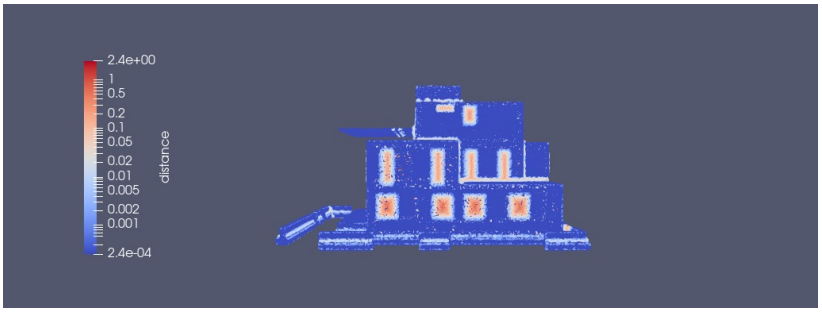

(b) Left view

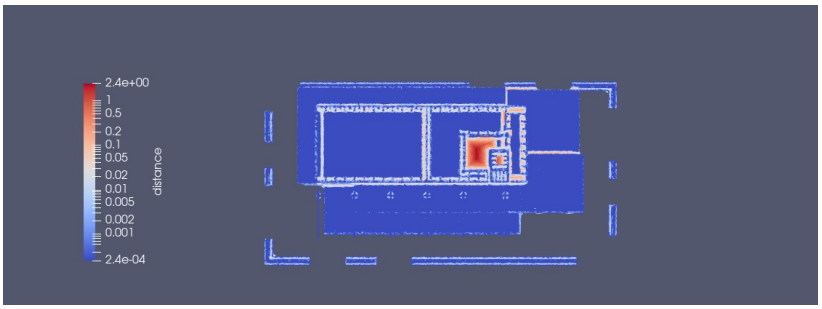

(c) Top view

Figure D.2.: Reconstruction errors of the BIMcollab STR model

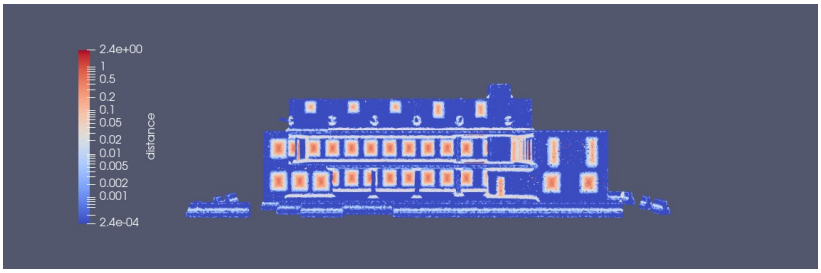

(a) front view

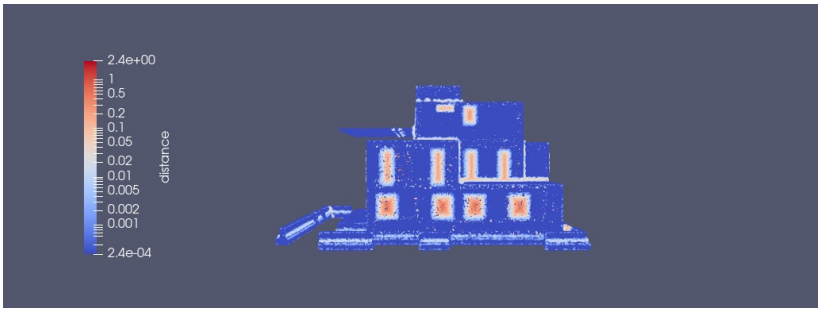

(b) Left view

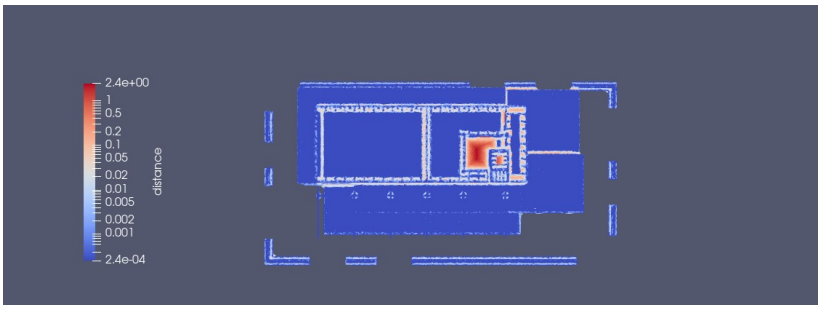

(c) Top view

Figure D.3.: Reconstruction errors of the Mauer BmB model

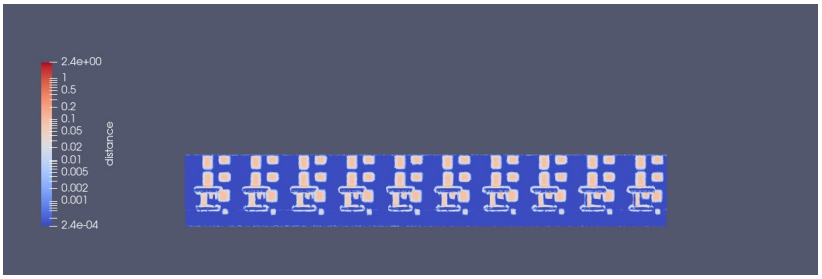

(a) front view

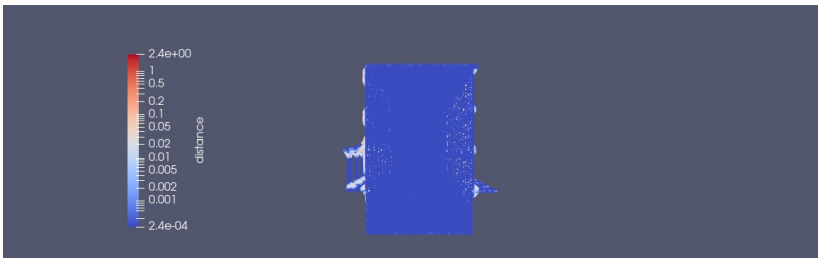

(b) Left view

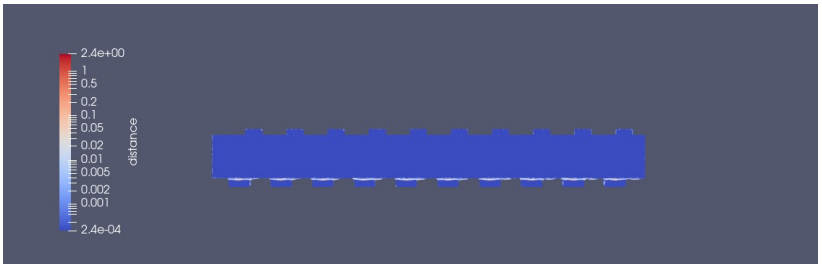

(c) Top view

Figure D.4.: Reconstruction errors of the Smiley-West model

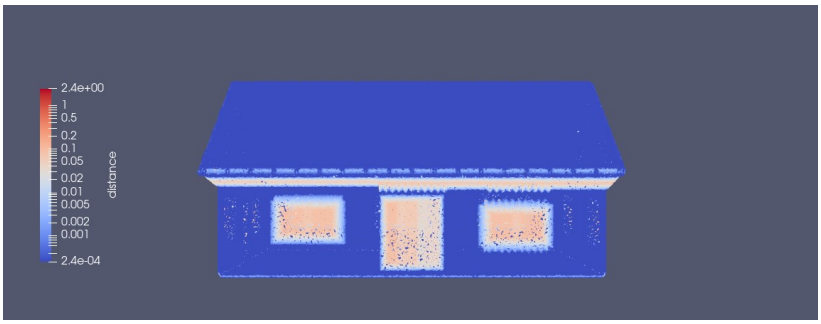

(a) front view

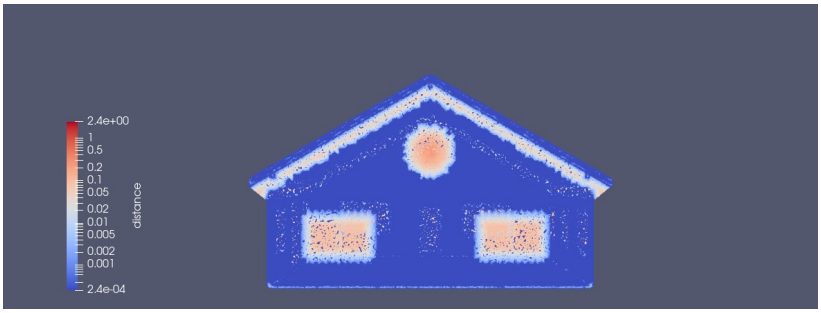

(b) Left view

(c) Top view

Figure D.5.: Reconstruction errors of the FZK-Haus model

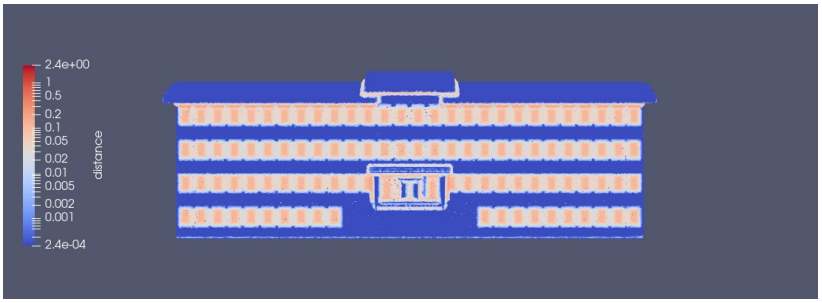

(a) front view

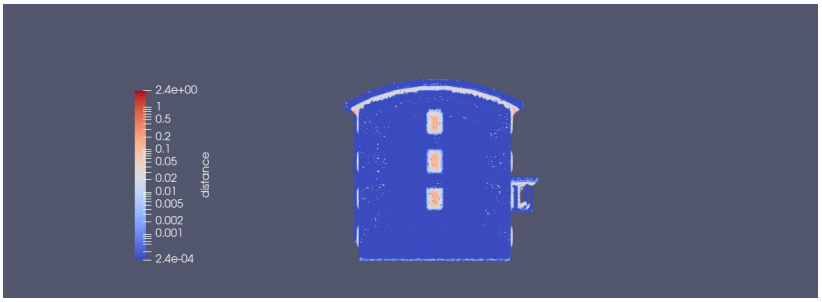

(b) Left view

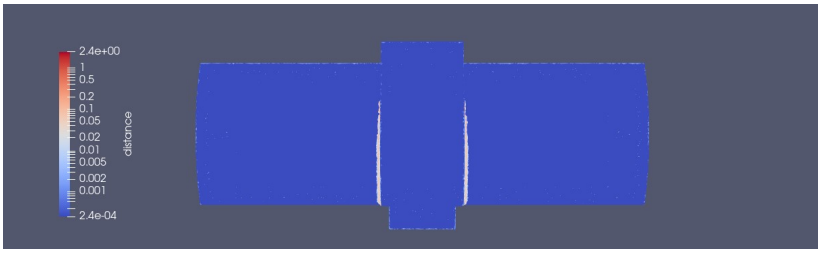

(c) Top view

Figure D.6.: Reconstruction errors of the Institute-Var-2 model

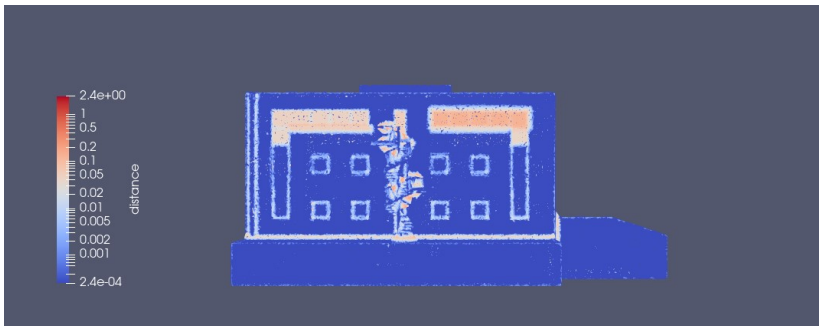

(a) front view

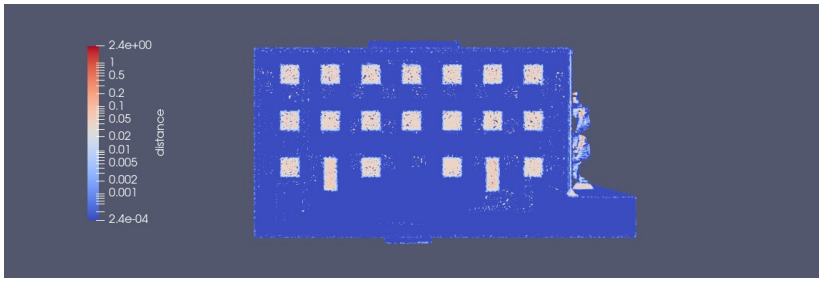

(b) Left view

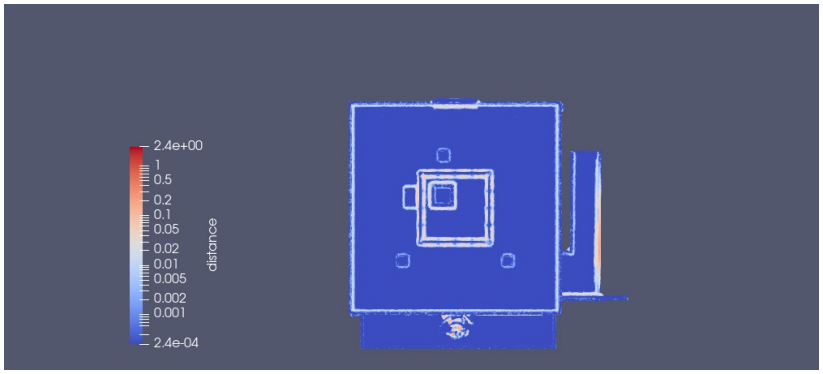

(c) Top view

Figure D.7.: Reconstruction errors of the BUREAUX model

Bibliography

Allegrini, Jonas et al. (Dec. 2015). "A review of modelling approaches and tools for the simulation of district-scale energy systems". In: *Renewable and Sustainable Energy Reviews* 52, pp. 1391–1404. DOI: 10.1016/j.rser.2015.07.123.

André Borrmann, Markus König (Sept. 2018). *Building Information Modeling: Technology Foundations and Industry Practice*. Springer-Verlag GmbH. 584 pp. ISBN: 3319928627. URL: https://www.ebook.de/de/product/34302331/building_information_modeling.html.

Aspert, N., D. Santa-Cruz, and T. Ebrahimi (2002). "MESH: measuring errors between surfaces using the Hausdorff distance". In: *Proceedings. IEEE International Conference on Multimedia and Expo*. IEEE. DOI: 10.1109/icme.2002.1035879.

Azhar, Salman, Malik Khalfan, and Tayyab Maqsood (2012). "Building information modeling (BIM): now and beyond". In: *Australasian Journal of Construction Economics and Building, The* 12.4, pp. 15–28.

Benner, J and Geiger, A and Leinemann, K (2005). "Flexible generation of semantic 3D building models". In: *Proc of the 1st Intern. Workshop on Next Generation 3D City Models, Gröger/Kolbe (Eds.), Bonn*, pp. 17–22.

Berger, Matthew et al. (Mar. 2016). "A Survey of Surface Reconstruction from Point Clouds". In: *Computer Graphics Forum* 36.1, pp. 301–329. DOI: 10.1111/cgf.12802.

Biljecki, Filip et al. (Dec. 2015). "Applications of 3D City Models: State of the Art Review". In: *ISPRS International Journal of Geo-Information* 4.4, pp. 2842–2889. DOI: 10.3390/ijgi4042842.

Brock, Linda (2005). *Designing the exterior wall: An architectural guide to the vertical envelope*. John Wiley & Sons.

Choi, Yosoon, Jangwon Suh, and Sung-Min Kim (May 2019). "GIS-Based Solar Radiation Mapping, Site Evaluation, and Potential Assessment: A Review". In: *Applied Sciences* 9.9, p. 1960. DOI: 10.3390/app9091960.

Crawley, Drury B. et al. (Apr. 2001). "EnergyPlus: creating a new-generation building energy simulation program". In: *Energy and Buildings* 33.4, pp. 319–331. DOI: 10.1016/s0378-7788(00)00114-6.

Deng, Yichuan, Jack C.P. Cheng, and Chimay Anumba (July 2016). "Mapping between BIM and 3D GIS in different levels of detail using schema mediation and instance comparison". In: *Automation in Construction* 67, pp. 1–21. DOI: 10.1016/j.autcon.2016.03.006.

Dey, Tamal et al. (1999). "Topology preserving edge contraction". In: *Publications de l'Institut Mathématique* 66.

Donkers, Sjors et al. (Sept. 2015). "Automatic conversion of IFC datasets to geometrically and semantically correct CityGML LOD3 buildings". In: *Transactions in GIS* 20.4, pp. 547–569. DOI: 10.1111/tgis.12162.

Doty, Steve and Turner, Wayne C (2004). *Energy management handbook*. Crc Press.

Du, Shenglan (2019). "Accurate, Detailed and Automatic Tree Modelling from Point Clouds". MA thesis. Delft University of Technology. URL: http://resolver.tudelft.nl/uuid:675ee438-3dc9-43c8-a7a7-f3b8807c583f.

Eastman, Chuck et al. (2011). *BIM Handbook A Guide to Building Information Modeling for Owners, Managers, Designers, Engineers and Contractors. A Guide to Building Information Modeling for Owners, Managers, Designers, Engineers and Contractors*. Wiley Sons, Incorporated, John, p. 640. ISBN: 9781118021675. URL: https://ebookcentral-proquest-com.tudelft.idm.oclc.org/lib/delft/detail.action?docID=698898.

Edelsbrunner, Herbert and Ernst P. Mücke (Jan. 1994). "Three-dimensional alpha shapes". In: *ACM Transactions on Graphics* 13.1, pp. 43–72. DOI: 10.1145/174462.156635.

Elberink, Sander Oude and George Vosselman (Mar. 2011). "Quality analysis on 3D building models reconstructed from airborne laser scanning data". In: *ISPRS Journal of Photogrammetry and Remote Sensing* 66.2, pp. 157–165. DOI: 10.1016/j.isprsjprs.2010.09.009.

Epstein, Erika (2012). *Implementing Successful Building Information Modeling*. Artech House Publishers. ISBN: 9781608071395. URL: https://ebookcentral-proquest-com.tudelft.idm.oclc.org/lib/delft/detail.action?docID=979850.

Fan, Hongchao, Liqiu Meng, and Mathias Jahnke (2009). "Generalization of 3D Buildings Modelled by CityGML". In: *Advances in GIScience*. Springer Berlin Heidelberg, pp. 387–405. DOI: 10.1007/978-3-642-00318-9_20.

Freitas, S. et al. (Jan. 2015). "Modelling solar potential in the urban environment: State-of-the-art review". In: *Renewable and Sustainable Energy Reviews* 41, pp. 915–931. DOI: 10.1016/j.rser.2014.08.060.

Gao, Hao, Christian Koch, and Yupeng Wu (Mar. 2019). "Building information modelling based building energy modelling: A review". In: *Applied Energy* 238, pp. 320–343. DOI: 10.1016/j.apenergy.2019.01.032.

Garland, Michael and Paul Heckbert (1997). "Surface simplification using quadric error metrics". In: *Proceedings of the 24th annual conference on Computer graphics and interactive techniques*, pp. 209–216.

Gharehbaghi, Koorosh (Feb. 2016). "On-Site Engineering Information Systems (EIS) for Building and Construction Projects". In: *IJCE* 4. DOI: 10.13189/cea.2016.040102.

Hamilton, Ian, HarryKennard, and Oliver Rapf (2021). *2021 Global Status Report for Buildings and Construction*. Tech. rep. UN Environment Programme.

Huang, Hui et al. (Dec. 2009). "Consolidation of unorganized point clouds for surface reconstruction". In: *ACM Transactions on Graphics* 28.5, pp. 1–7. DOI: 10.1145/1618452.1618522.

Jaud, Štefan et al. (Oct. 2020). "Georeferencing in the context of building information modelling". In: *Automation in Construction* 118, p. 103211. DOI: 10.1016/j.autcon.2020.103211.

Karydakis, Panagiotis (2018). "Simplification Visualization of BIM models through Hololens". MA thesis. Delft University of Technology. URL: http://resolver.tudelft.nl/uuid:748e5ed7-4a0d-4396-904b-64244ac0e56e.

Kazhdan, Michael, Matthew Bolitho, and Hugues Hoppe (2006). "Poisson surface reconstruction". In: *Proceedings of the fourth Eurographics symposium on Geometry processing*. Vol. 7, p. 0.

Li, Ziwei et al. (Apr. 2020). "A review of operational energy consumption calculation method for urban buildings". In: *Building Simulation* 13.4, pp. 739–751. DOI: 10.1007/s12273-020-0619-0.

Lindstrom, P. and G. Turk (1998). "Fast and memory efficient polygonal simplification". In: *Proceedings Visualization '98 (Cat. No.98CB36276)*. IEEE. DOI: 10.1109/visual.1998.745314.

Lorensen, William E. and Harvey E. Cline (Aug. 1987). "Marching cubes: A high resolution 3D surface construction algorithm". In: *ACM SIGGRAPH Computer Graphics* 21.4, pp. 163–169. DOI: 10.1145/37402.37422.

Noardo, F. et al. (Sept. 2020). "GEOBIM FOR DIGITAL BUILDING PERMIT PROCESS: LEARNING FROM A CASE STUDY IN ROTTERDAM". In: *ISPRS Annals of the Photogrammetry, Remote Sensing and Spatial Information Sciences* VI-4/W1-2020, pp. 151–158. DOI: 10.5194/isprs-annals-vi-4-w1-2020-151-2020.

Ohori, Ken Arroyo et al. (Aug. 2018). "Processing BIM and GIS Models in Practice: Experiences and Recommendations from a GeoBIM Project in The Netherlands". In: *ISPRS International Journal of Geo-Information* 7.8, p. 311. DOI: 10.3390/ijgi7080311.

Okba, EM (2005). "Building envelope design as a passive cooling technique". In: *Proceedings from the*. Vol. 490.

Peters, Ravi et al. (Mar. 2022). "Automated 3D Reconstruction of LoD2 and LoD1 Models for All 10 Million Buildings of the Netherlands". In: *Photogrammetric Engineering &amp Remote Sensing* 88.3, pp. 165–170. DOI: 10.14358/pers.21-00032r2.

Poullis, C. (Nov. 2013). "A Framework for Automatic Modeling from Point Cloud Data". In: *IEEE Transactions on Pattern Analysis and Machine Intelligence* 35.11, pp. 2563–2575. DOI: 10.1109/tpami.2013.64.

Prusti, Maarit (2022). "How could BIM support the digital building permit process in the Netherlands?" MA thesis. Delft University of Technology. URL: http://resolver.tudelft.nl/uuid:33b125b5-d902-4432-9043-2ceb10f2e53e.

Rasmussen, Mads Holten et al. (Nov. 2020). "BOT: The building topology ontology of the W3C linked building data group". In: *Semantic Web* 12.1. Ed. by Krzysztof Janowicz, pp. 143–161. DOI: 10.3233/sw-200385.

Sadineni, Suresh B., Srikanth Madala, and Robert F. Boehm (Oct. 2011). "Passive building energy savings: A review of building envelope components". In: *Renewable and Sustainable Energy Reviews* 15.8, pp. 3617–3631. DOI: 10.1016/j.rser.2011.07.014.

Santos, Renato Cesar dos, Mauricio Galo, and Andre Caceres Carrilho (Aug. 2019). "Extraction of Building Roof Boundaries From LiDAR Data Using an Adaptive Alpha-Shape Algorithm". In: *IEEE Geoscience and Remote Sensing Letters* 16.8, pp. 1289–1293. DOI: 10.1109/lgrs.2019.2894098.

Singh, S. P., K. Jain, and V. R. Mandla (Aug. 2013). "VIRTUAL 3D CITY MODELING: TECHNIQUES AND APPLICATIONS". In: *The International Archives of the Photogrammetry, Remote Sensing and Spatial Information Sciences* XL-2/W2, pp. 73–91. DOI: 10.5194/isprsarchives-xl-2-w2-73-2013.

Syed, Asif (2012). *Advanced building technologies for sustainability*. Vol. 3. John Wiley & Sons.

Al-Tamimi, Mohammed Sabbih Hamoud, Ghazali Sulong, and Ibrahim Lutfi Shuaib (July 2015). "Alpha shape theory for 3D visualization and volumetric measurement of brain tumor progression using magnetic resonance images". In: *Magnetic Resonance Imaging* 33.6, pp. 787–803. DOI: 10.1016/j.mri.2015.03.008.

Vaart, Jasper van der (2022). "Automatic building feature detection and reconstruction in IFC models". MA thesis. Delft University of Technology. URL: http://resolver.tudelft.nl/uuid:db6edbfc-5310-47db-b2c7-3d8e2b62de0f.

Vauhkonen, Jari et al. (2009). "Identification of Scandinavian commercial species of individual trees from airborne laser scanning data using alpha shape metrics". In: *Forest Science* 55.1, pp. 37–47.

Wang, Chao, Yong K. Cho, and Changwan Kim (Aug. 2015). "Automatic BIM component extraction from point clouds of existing buildings for sustainability applications". In: *Automation in Construction* 56, pp. 1–13. DOI: 10.1016/j.autcon.2015.04.001.

Xu, Yusheng, Xiaohua Tong, and Uwe Stilla (June 2021). "Voxel-based representation of 3D point clouds: Methods, applications, and its potential use in the construction industry". In: *Automation in Construction* 126, p. 103675. DOI: 10.1016/j.autcon.2021.103675.

Zhu, Xiaoqiang et al. (May 2019). "Alpha-shape based 3D printable manifold modeling". In: *Tenth International Conference on Graphics and Image Processing (ICGIP 2018)*. Ed. by Hui Yu et al. SPIE. DOI: 10.1117/12.2524212.

Colophon

This document was typeset using LaTeX, using the KOMA-Script class `scrbook`. The main font is Palatino.